DESIGN AND CONSTRUCTION OF AN AUTONOMOUS MOBILE SECURITY DEVICE

A thesis

submitted in partial fulfilment

of the requirements for the degree

of

Master of Science in Physics and Electronic Engineering

at the

University of Waikato

by

Daniel James Loughnane

2001

ABSTRACT

A Mobile Autonomous Robotic Vehicle for Indoor Navigation, or MARVIN, has been developed for operation as a security device in an indoor environment. The resulting design is a wheeled robot standing one metre in height, which will eventually navigate the environs of an office block without the need for human intervention. The navigation system consists of infrared sensors for obstacle detection and odometers to determine the heading and distance travelled. The device is powerful enough to negotiate such obstacles as fire doors and can manoeuvre within a space of less than one metre. MARVIN will provide a platform for future mechatronics research at the University of Waikato.

PREFACE

The aim of this project is to design and construct a large autonomous mobile security device, suitable for operation in an office or warehouse environment. This aim requires both mechanical and electronic design skills, combined with the ability to assemble the two to construct the final mechatronic device.

This thesis is presented in the following manner:

- **Chapter One** provides an introduction to the requirements of the project and outlines what previous work has been conducted in this field.
- **Chapter Two** outlines the hardware requirements of the security device. This chapter discusses the mobility considerations for the robot and discusses the design of the drive train. The design and construction methods used in assembling the chassis are also detailed.
- **Chapter Three** discusses the electronic requirements of the project. The circuitry of the microcontroller and driving electronics are explained, as are the design considerations for such electronics.
- **Chapter Four** details the sensors employed by the security device for navigational purposes. The systems implemented for obstacle detection are discussed and several alternative methods offered.
- **Chapter Five** outlines effective procedures for the modelling of a DC motor. The parameters of the motors used on the security device are analysed, as are the physical characteristics of the device. The algorithms for simple control of the device are detailed with an explanation of the requirements and limitations of the control system.
- **Chapter Six** summarises the abilities of the design and discusses the future developments that could be made to improve its performance.

ACKNOWLEDGEMENTS

I would like to gratefully acknowledge the following people for their support and encouragement throughout the design and construction of the autonomous mobile security device.

Thanks to Dr Dale Carnegie for giving me the opportunity to undertake graduate studies and for his continued support and direction. The technical staff at the Department of Physics and Electronic Engineering have been a great help. I would like to especially thank Bruce Rhodes and Scotty Forbes for their advice and good humour, which have help to make this project even more enjoyable.

I wish to thank my fellow graduate students for their assistance and my friends for providing relief from work. Special thanks go to Sara for her patience and tolerance and also for giving me the motivation to succeed.

Finally I would like to thank my family for their support and encouragement throughout my studies.

TABLE OF CONTENTS

LIST OF FIGURES

LIST OF TABLES

1. INTRODUCTION

This thesis project is aimed at the design, construction and development of a large autonomous robotic vehicle that would be suitable for use as a security device. The robot is to be known as a Mobile Autonomous Robotic Vehicle for Indoor Navigation, or MARVIN. It is required to be large enough to support future attachments or accessories.

There are several features of a robotic security device, which make it an attractive option for warehouses and office blocks. For example:

- Robots don't get bored during long hours of surveillance, which can lead to reduced human vigilance.
- Robots don't participate in "inside jobs", where the security of the building is breached due to co-operation of the security guards in the crime.
- Robots don't get tempted to steal any valuable inventory that may be stored in the building.

1.1 BACKGROUND

The world's first autonomous security robot, ROBART I, was developed in 1982 by the United States Naval Post-Graduate School and is shown in Figure 1-1. This robot simply navigated its environment by following a reflective patrol path and as such, had no sense of absolute location. It returned periodically to a recharging station by homing in on an infrared beacon. Two further prototypes have been constructed since ROBART I, with ROBART III, developed in 1992 to operate in urban warfare situations, the more recent.

Figure 1-1: ROBART I

The United States of America has many institutes that have extensive robotics research programs and competitions for large mobile robots. Military research into the development of the Mobile Detection Assessment and Response System (MDARS) has been ongoing since 1989, with the goal to provide multiple mobile platforms that perform random patrols within assigned areas of warehouses and storage sites. These robots have been developed to detect and report anomalies such as flooding, fire or intruders.

The MDARS executes a predetermined set of commands until completion, and then sits idle, awaiting a further set of instructions via R/F communication. The system is designed to have several MDARS operating co-operatively, surveying a large environment. The robots navigate their surroundings by using a network of passive landmarks in the form of reflective strips that are mounted to the walls and shelving of the warehouse. The location of the reflective strips is encoded in the control program of the robot and used as a parameter in the navigational calculations of the controller. Two examples of MDARS prototypes are shown in Figures 1-2 and 1-3 below:

Figure 1-2: Early prototype of MDARS interior robot.

Figure 1-3: MDARS exterior prototype still under development

There has been little development of autonomous mobile robots in New Zealand. The University of Canterbury has developed a large Automated Guided Vehicle (AGV) that follows a buried wire around the warehouse floor and as such is not strictly autonomous due to the exterior control feedback provided by the wire.

The Microelectronics Group at The University of Waikato has been developing small, autonomous, mobile robots that operate in a well-defined environment for a number of years. The "Micromouse", shown in Figure 1-4, is a small wheeled robot originally designed to race inside a maze, and has been the basis for most of this research since 1993.

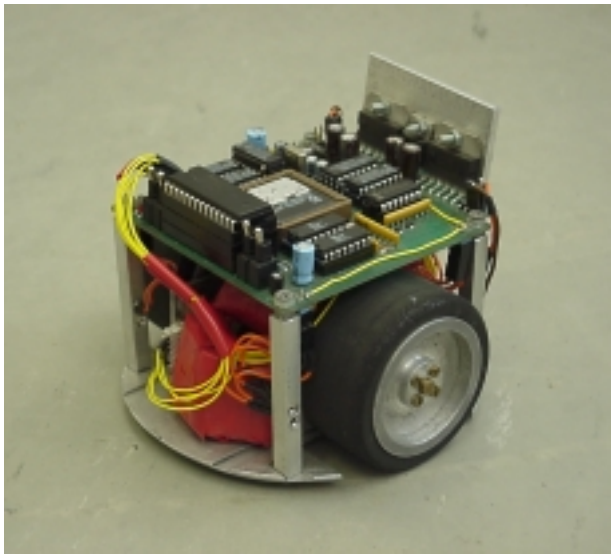

Figure 1-4: One of the micromice developed at the University of Waikato

The working environment for the micromouse is well controlled and the mechanics of the robot have been designed to operate within fine margins, so that optimal performance is achieved under race conditions. These projects have been very successful, with early developments winning the Australasian Micromouse Competition. Unfortunately, the micromouse platform offers relatively limited scope for further development. MARVIN is the largest robotic project undertaken at the university and as such poses many different design considerations and possibilities.

1.2 PROJECT OBJECTIVES

The security device is to be designed to patrol the halls and rooms of an office block or warehouse after hours. The potential development of such a project is enormous due to the size of the device, its possible operating environments, and the possible modifications that can be made to its design. It is the task of this thesis to design and construct the chassis and frame for the robot, together with the locomotion and simple collision avoidance procedures.

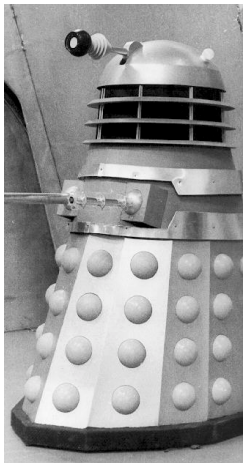

Figure 1-5: Early large-scale security device

To be fully autonomous, the device must be capable of operating independent of external control. This requires that all control theory and navigation be computed onboard the vehicle and that it must carry its own power supply. The robot must be large enough to open fire doors without difficulty and also be able to support a payload of over thirty kilograms to allow further additions and modifications to be made without major reconstruction of the chassis. It has to be able to negotiate its environment safely, yet with reasonable speed and accuracy for the duration of its operating hours without human intervention.

The office block or warehouse environment is very difficult to define and subject to change from day to day. The device must be able to map its surroundings and make adjustments, as necessary, to avoid any new obstacles in its path or alterations in its immediate environment. The Laser Range-Finding System developed by a fellow graduate student, Shaun Hurd[7], is to be incorporated in the navigation system to enable more accurate mapping of the environment. This system incorporates the motherboard from a desktop PC, with a camera and laser assembly, which must be mounted to the chassis of the robot.

1.3 SPECIFICATIONS

The design of the robot must allow for the following features to be met. These specifications are slightly flexible, but all efforts should be made meet or exceed them wherever possible.

- **Speed:** The robot must move quickly enough to patrol its environment at a suitable speed. It is deemed that a speed of **1m/s** is sufficient to achieve this.
- **Height:** The height of the robot is required to enable it to operate such devices as a lift, when developments are added in the future. Added height also gives the robot a physical presence. A height of **1m** is considered appropriate for these tasks.
- **Weight:** The robot needs to be heavy enough to give any additional attachments a solid base from which to operate from. The robot is also required to negotiate fire doors, which will require substantial inertia. The weight of the robot is required to be at least **30kg** to achieve these goals.
- **Power Supply:** The robot must carry its own power supply, which will be required to last the duration of its patrol. The supply must be rechargeable and cost effective.
- **Manoeuvrability:** The robot is required to manoeuvre in the confines of an office or corridor. This may involve obstacle avoidance or direction reversal in spaces as small as **1m** diameter.
- **Power:** The motors are required to drive the weight of the robot and any additional payload at the speed specified above. The required payload for the robot is set at **30kg**.
- **Flexibility:** Due to the large scope for future additions and improvements to be made to the original robot design, the chassis must be flexible enough to ensure these developments can be made with relative ease.

1.4 DEVELOPMENT

The development process for the security device is to take the following path:

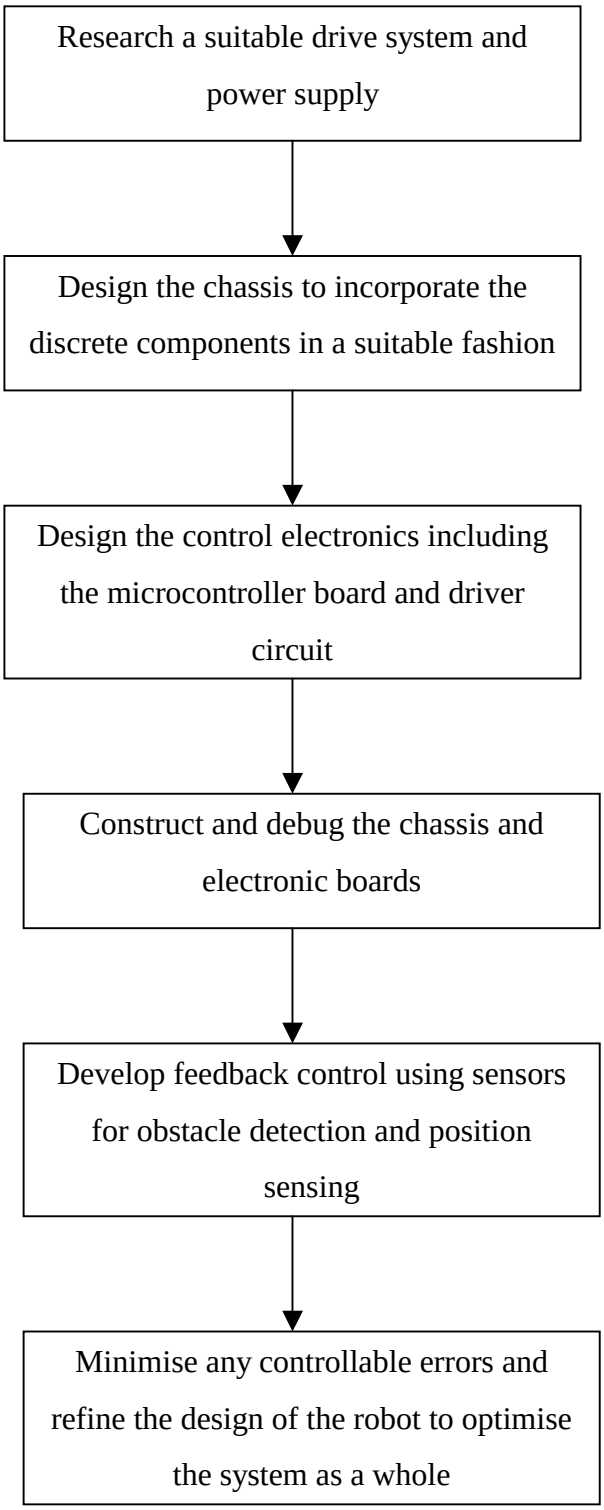

Figure 1-6: Flowchart of project development process

The development of MARVIN can be seen as the first step in a series of work to be conducted by the Physics and Electronic Engineering Department of the University of Waikato. The versatility of this robotic platform will be a major advantage over projects undertaken in the past and, although MARVIN is primarily designed as a large-scale security device, there are a number of tasks that could be undertaken by a robot based on a similar design strategy. Care must be taken therefore, to ensure that design decisions will not limit possible future developments.

2. HARDWARE

2.1 OVERVIEW

The hardware requirements for the large-scale security device can be met in a variety of ways. The design of MARVIN's chassis is dependent on the mobility configuration of the device and the components of the drive system that it needs to accommodate. The design of the hardware components will largely determine whether the device will meet the design specifications outlined in Section 1.3.

The mobility configuration will determine the physical characteristics of the device and how the individual components will be arranged on the chassis. The manoeuvrability and controllability of MARVIN is determined by the physical arrangement of the drive components in relation to the chassis and which steering system is employed.

The driving motors and gearing will determine the power supply requirements of the device. MARVIN's motors must be able to supply sufficient torque to the driving wheels to enable the payload and speed requirements to be met. A gear train will be implemented to reduce the performance expected of the motors and, consequently, the power requirements of the system.

The individual hardware components are to be assembled on a suitable chassis that will provide the device with strength and stability. The chassis will be employed in the future to accommodate additional appendages and developments intended for a mobile robotic platform. This will require a flexible design, which will enable these developments to be made and which is strong enough to support the future payload requirements.

2.2 DRIVE SYSTEM

2.2.1 Mobility Configuration

The drive train is a critical component of a mobile robot and must be accommodated for early in the chassis design. There are several factors that must be considered in order to select an appropriate drive train configuration for MARVIN:

- **Manoeuvrability** – the specifications state that the robot must be able to manoeuvre within a circle, one metre in diameter.
- **Controllability** – how difficult will the configuration be to control?
- **Traction** – the weight of MARVIN could be prone to wheel slippage if the driving wheels do not have sufficient downward force.
- **Stability** – as MARVIN is to be one metre tall, the stability of the system is vital.
- **Efficiency** – how much energy is wasted in manoeuvring the vehicle?
- **Maintenance** – is the system prone to excessive wear or maintenance?

Some realistic options for the mobility configuration of MARVIN are listed below:

- **The Tricycle**

  This method can either have a motor driving the rear wheels through a differential or simply driving the front wheel alone. Both instances require a motor to control the front wheel that pivots, enabling the robot to turn as shown in Figure 2-1A.

- **The Quad (Ackerman steering)**

  This arrangement can have two or four wheel steering (illustrated in Figure 2-1B), with the inside wheel at a slightly sharper angle than the outside in order to prevent slippage caused by its tighter turning circle. If a two wheel steering arrangement were implemented it would require a large motor for driving, a differential to transfer the power evenly to the driving wheels and another motor to control the steering. A four-wheel steering arrangement also requires a large driving motor coupled with a

differential but would require two motors to control the steering. Four wheel steering has a much tighter turning circle obtained from a similar sized chassis.

- **The Wheelchair (Differential drive)**

  This method has the two drive wheels on the centre axis of the robot with castors or skids at the front and rear to improve stability. The wheels are driven independently and turning achieved by driving them in opposite directions. This allows the device to turn 360 degrees around its centre shown in Figure 2-1C, below.

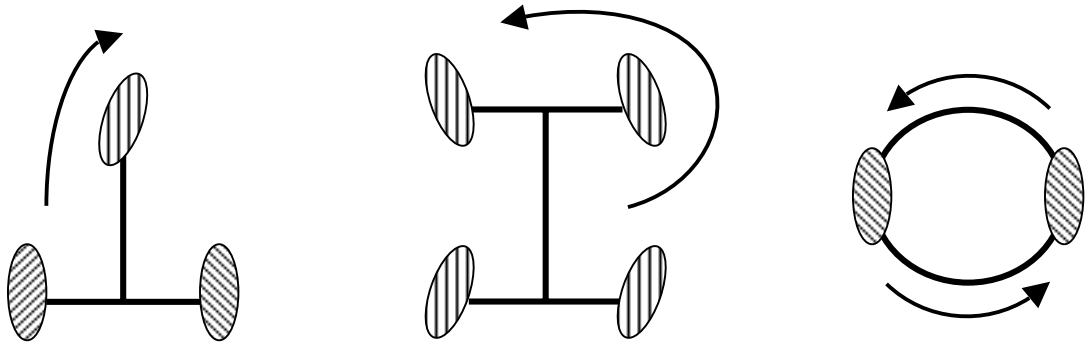

A: the tricycle **B: the quad (four wheel steer version)** **C: the wheelchair**

Figure 2-1: The three possible mobility configurations.

The wheelchair configuration is preferred to the quad and tricycle because of the tighter turning circle which is imperative as MARVIN will be required to perform 90 and 180 degree turns in the confines of an office block corridor. With the wheelchair configuration it is possible to design the chassis so that these turns can be executed on the spot.

Both the tricycle and quad arrangements are susceptible to slippage as the centre of gravity moves away from the driving wheels during acceleration and/or braking. They can also cause surface damage and introduce a large strain on the steering components if turning is executed while the mechatron is stationary. The control of a device that is implementing either of these systems can also be complicated if it is required that the device executes a three-point turn or travels in reverse. The differential drive system is much less complicated to control due to the simplified mechanics of the system.

The driving wheels of the device will support as much of the weight as possible, with castors being employed at the front and rear of the chassis to add stabilisation during acceleration and braking manoeuvres.

2.2.2 Drive-train

The security device has to have an overall height of one metre to provide future developments with a suitable basis from which to operate. As specified in the introduction (Section 1.3), the bare robot is to weigh at least 30kg and be able to travel at speeds of up to 1m/s. The driving motors must provide sufficient torque to the two driving wheels to allow MARVIN to manoeuvre within these defined parameters of operation. There are several factors that must be considered when choosing an appropriate drive system:

- **Capital cost**
- **Speed range**
- **Efficiency ratio** - what is the ratio of input power to output power? Wasted energy will generate heat and may introduce the need for a heat sink or fan.
- **Controllability** - what is the accuracy of the steady state operation of the drive system?
- **Braking** - are mechanical brakes required or will gravitational braking be sufficient?
- **Reliability**
- **Power to weight**
- **Power supply** - how large will the batteries need to be?

Due to the physical size of the robot, the driving wheels are required to be of a reasonable diameter. A large wheel diameter requires less torque from the driving motors, but the effect of the robot's inertia is increased and the braking force required is increased. If very narrow wheels are used, the amount of energy lost from the system due to friction is reduced, but the traction of the vehicle is reduced. When the drive train is designed, the wheels must be considered, as they are the only means for the energy from the motors to be translated into physical motion of the vehicle.

Regardless of the particular drive system, the energy produced by the motors has to be coupled to the driving wheels. There are a number of suitable configurations of motors and gear trains that would create an appropriate drive system for the device. In the wheel chair configuration, the drive wheels are mounted on the centre axis of the chassis and support a majority of the load weight, which could be up to 60kg (as outlined in the design specifications, Section 1.3). The following are the three main gearing arrangements applicable for this application:

The Spur Gear

This is one of the simplest gearing arrangements. The drive shaft from the motor is directly attached to a gearhead which, if the gearbox is a speed reducer, is meshed to a larger gear. Both gears are on the same plane of motion with the gears meshing parallel to each other. The speed reduction ratio is simply the ratio of teeth on the gear being driven to the number on the driving wheel. The axle of the driving wheel can be directly linked to the larger of the gears as shown in Figure 2-2.

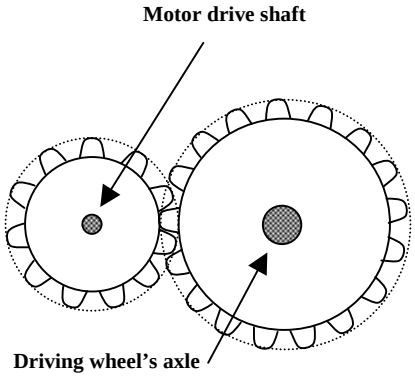

Figure 2-2: Spur gear arrangement

The Worm Gear

The worm gear consists of a helical gear, or worm, attached directly to the motor's drive shaft (in some cases the worm is cut into the shaft). The helical gear meshes with another larger gear producing a speed reducer as in the spur arrangement. The reduction ratio for the worm however, is the ratio of teeth on the driven wheel to the number of teeth per revolution on the driving worm. The major difference with the worm drive is that the direction of motion of the driven wheel is perpendicular to that of the motor shaft as shown to the left.

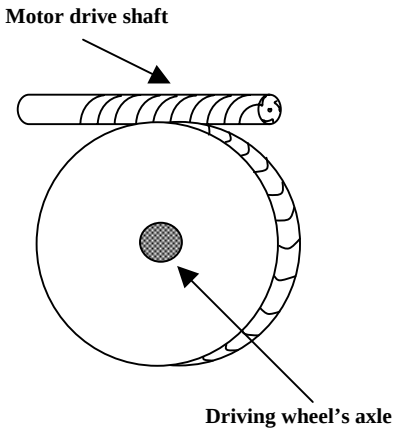

Figure 2-3: Worm gear arrangement

Belt Drive

The belt drive is the most inefficient of the methods considered for this application. Belts are constructed from rubber that can stretch when under stress and can slip when under extreme load. Toothed belts are available which are more resistant to slippage but stretch is still an issue. Chain drives operate on the same principle, with a metal chain running on sprockets, but these systems are prone to "slop", where the driving wheel can move a little even though the motor is stationary. The reduction ratios for such systems are calculated in the same way as for the spur gear. This arrangement is illustrated in Figure 2-4.

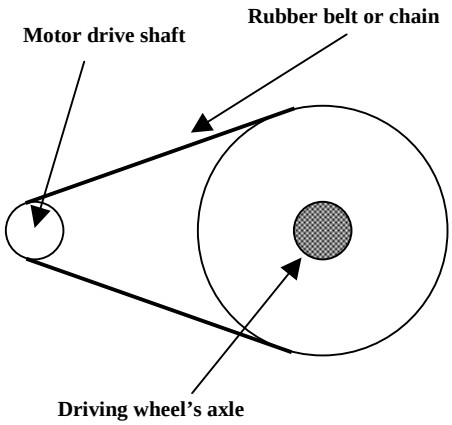

Figure 2-4: Belt drive arrangement

Many different arrangements of motors and gearboxes would prove suitable for MARVIN. Maxon Precision Motors Inc. manufacture DC motors of various sizes with gearheads that mount directly to the face of the motor for ease of assembly. They also incorporate an encoder unit or tachometer in the design of their motors that can be purchased and bolted directly to the back of the motor. Although this arrangement is very tidy and easy to assemble, the motors are very expensive. The required precision for this project does not justify the use of these motors.

Stepper motors can be controlled to move a set angle dependant on the input signal. These motors are often used in applications where precision is required and torque is not as much of an issue, for example, they are often used in PC floppy disc drives.

Permanent magnet DC motors provide greater torque than the stepper motor variation, with the brush type being more suited to this application. The power produced by such motors will be sufficient when passed through a suitable gearbox, to the driving wheels. Two large 24V DC motors have been acquired from an electric wheelchair and are powerful enough to carry the specified weight of the robot and allow for large future

payloads. The speed of the drive wheels is approximately walking pace, which is within the design specifications.

The motors are permanent magnet brush motors, with a worm gearbox mounted to the face of the motor. The shaft from the helical gear of the worm drive has a small spur gear mounted to it that is held in place with a key and grub-screw. The spur gear is configured in a planetary arrangement, not as the traditional spur gear arrangement outlined above. The physical workings of the gear system are very similar to that of a standard spur, but instead of the smaller gear mating to the outside of the larger as in Figure 2-2, it runs around the inside of the larger, ring gear as illustrated in Figure 2-5:

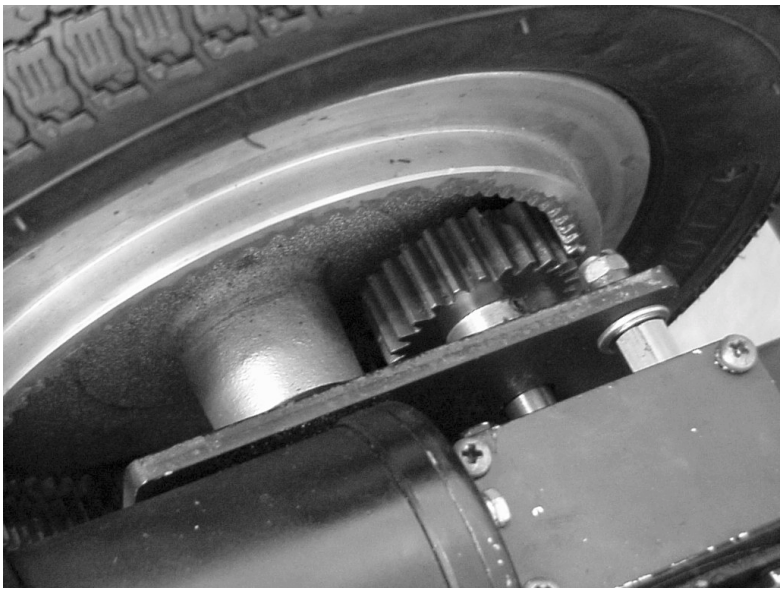

Figure 2-5: Planetary gearhead on the motor shaft driving the wheel

The worm has three teeth per revolution cut directly onto the motor shaft and drives a 51 tooth helical gear. This produces a reduction ratio of N_{worm} = 17:1 to the drive shaft, on which the 24 tooth planetary gear is mounted. This gear is mated directly to the wheel ring gear that has 75 teeth. The reduction ratio from the motor to the wheel is calculated using Equation [2-1] below:

$$N = \left(\frac{N_{wheel}}{N_{gearhead}} \right) * N_{worm} = \left(\frac{75}{24} \right) * 17$$

$$= 51.56 : 1 \qquad \textbf{Eqn. [2-1]}$$

where: N = reduction ratio

N_{wheel} = gearing ratio of wheel

$N_{gearhead}$ = gearing ratio of planetary gear head

N_{worm} = gearing ratio of worm drive

This shows that for every revolution of the driving wheel, the motor must turn 51.56 revolutions. Figure 2-6 shows the total arrangement of the gear train for the drive system:

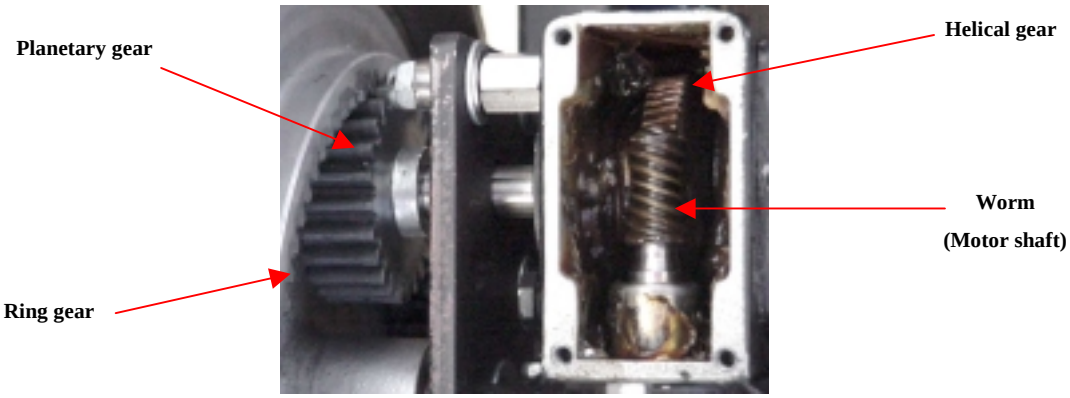

Figure 2-6: Close up view of gearbox and planetary gearhead

To allow for feedback control, odometers are attached to the back of the motors and are directly attached to the motor shaft. This was achieved by turning down a brass shaft on a metalwork lathe and tapping a thread into the back of the motor. The code-wheel of the shaft encoder is attached to the shaft with a grub-screw and experiences the same gearing as the motor, that is, *N*.

2.3 POWER SUPPLY

2.3.1 Battery Options

In order for the power supply of MARVIN to be portable, batteries must be used to supply the required power to the driving motors and control electronics. With so many different types available, choosing an appropriate arrangement for this application is an involved process. There are many different types of battery available on the market, each aimed a specific application:

- **Nickel Cadmium** (NiCd) – commonly used in cellular phones and power tools, these batteries can be deeply discharged repeatedly with no loss of performance and can be rapidly charged. The battery is prone to crystalline formation if not completely discharged before being replenished, giving the battery a "memory" which reduces the capacity considerably. The large voltage requirements of the security device would require a series of large batteries at significant cost.
- **Sealed Lead Acid** (SLA) – These are approximately half the price of comparative NiCd batteries, although they weigh a lot more due to the lead plates used in construction. Commonly known as a **gelcell** battery, they are popular in portable devices due to the absence of liquid acid, which can leak from the cells and the low maintenance requirements in comparison to the flooded lead acid variation. The SLA is not subject to memory but does have a very long charge time (8 to 16 hours) and must always be stored in the charged state to prevent the plates from forming a sulphate which can make recharging difficult or impossible.
- **Flooded Lead Acid** (FLA) – These are the more common variation of the SLA used primarily in automotive applications. The FLA must be stored upright to prevent acid leakage, but is by far the cheapest option and most suitable for this application where size and weight are not significant factors. The deep cycle variety of FLA can be repeatedly discharged and charged without degradation of performance.

The flooded lead acid battery is chosen above the others listed, as it is more readily available and the much less expensive option. The batteries can be easily secured to the chassis with a metal bracket and held in the upright position, making the gelcell variation unnecessary. There is a wide range of FLA batteries available on the market, each designed to perform a specific task.

The batteries supplying power to the driving motors and accessories of MARVIN need to provide relatively low current over a long period, with infrequent recharging. If a standard automotive lead acid battery (known as a starting battery) is heavily discharged and recharged repeatedly, premature failure is likely. This makes the starting battery unsuitable for the final design of the security device where reliability is a concern.

Deep cycle batteries are specifically designed to be run flat and recharged repeatedly without sacrificing their capacity. The material used in the construction of the battery is much denser than that used in a standard battery. Additionally, specially designed glass mats are placed between the lead plates to prevent the shedding of active material (lead) during charging and damage caused by vibrations. The disadvantage of these batteries is the added initial cost of purchase, with most variations over twice the price of a standard battery.

2.3.2 Battery Classification

For many years batteries have been rated in terms of "**Amp Hours**". This was a statement of the current that could be provided continuously by the battery for 20 hours. While this does give a vague indication of the capacity of the battery, it gives no indication of the battery's ability to power high load accessories. Battery manufacturers in New Zealand have adopted the SAE (Society of Automotive Engineers) standard, whereby a battery's capacity is rated in terms of **Cold Cranking Amps (CCA)** and **Reserve Capacity (RC)**.

The CCA of a battery gives a more accurate indication of its performance than simple Amp Hours. It is defined as the discharge load in amperes that a new, fully charged

battery can deliver at -18°C for 30 seconds whilst maintaining a minimum voltage of 1.2V per cell. The higher the CCA, the more powerful the battery.

The RC of a battery is expressed in minutes. It represents the time a new, fully charged battery will supply a constant load of 25A at 25°C without the voltage dropping below 10.5V for a 12V battery. This rating is more applicable to deep cycle batteries that are designed to power auxiliary items such as lights and motors, rather than high-load engine cranking.

2.3.3 Battery Selection

Ideally the power supply for the security device would be a deep cycle lead acid variety, but as the robot will only be required to run for short periods during development and testing, the deep cycle nature of the battery is not essential. Two standard 12V starting batteries have been connected in series to provide the required 24V at half the price of a deep cycle variation. The voltage levels of these batteries are to be regularly monitored to ensure they are never run flat and subsequently damaged. The batteries can be replaced at a later date (once the robot is required to operate for longer periods at a time) with a deep cycle variation due to the similarity in the external dimensions.

The maximum current drawn by the driving motors is found experimentally to be approximately 10A when travelling at its maximum speed. If the batteries are expected to run continuously for approximately two hours, the required RC value is 60 minutes. The batteries chosen to power the device during development have the following characteristics:

Manufacturer:	Champion Batteries
Model:	126HD Silver battery
RC:	55 minutes
CCA:	310 A

When powered by these batteries MARVIN can be expected to run for 110 minutes at full power before recharging would be necessary.

2.3.4 Recharging the Batteries

The batteries have been wired into two circuits, one to supply the power to the motors and control electronics and one for recharging the batteries. Panel mounted sockets have been installed in the chassis frame so that the batteries can be recharged without being removed or the terminals being accessed. These sockets are wired in parallel so that if both positive and negative rails of a 12 V power supply are used, the batteries will charge faster and more evenly than if a single 24V rail were used to charge both batteries in series. The wiring diagram below is colour coded to match the socket used on MARVIN.

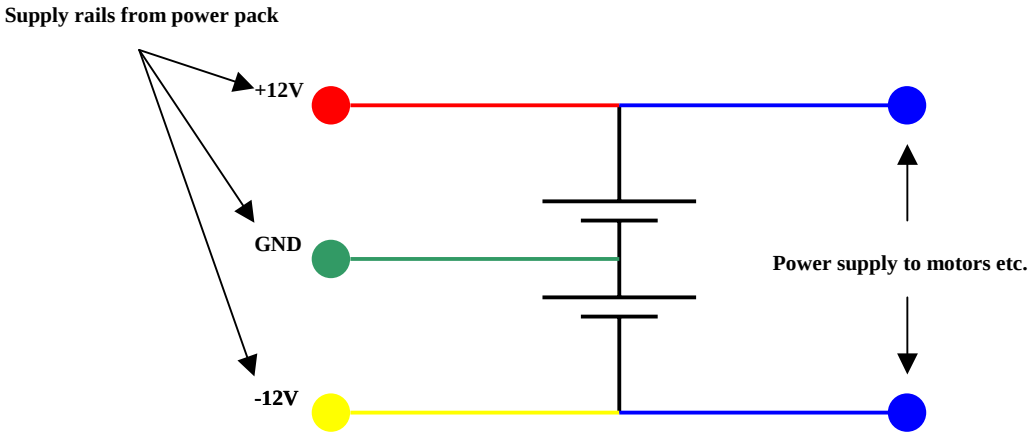

Figure 2-7: Wiring diagram for batteries

The lead in the plates of the batteries contributes significantly to the overall weight of MARVIN. The two driving motors weigh approximately 5.5kg each and the bare chassis weighs 10kg. As the batteries are approximately 20kg each they make up over 60% of the overall weight. The advantage of this weight is that it can be incorporated into the design of the chassis to create a low centre of gravity, increasing stability by counteracting the height of the device.

2.4 CHASSIS DESIGN

MARVIN's chassis needs to be of a suitable size to patrol the corridors of an office block and manoeuvre in the space allowed. The robot has to be large enough to support

the weight of its power supply and any additional payloads that may be added at a later stage. The chassis has been designed to be as flexible as possible to allow for future development whilst not sacrificing the overall strength.

Figure 2-8 shows the chassis of the security device, which has been designed and constructed in two major parts, the base and the frame. The base is designed to act as the backbone of the entire device with the wheels, frame and batteries directly attached to it. This arrangement causes all the stresses of the singular parts to be relayed back through the base, and as such it must be very strong.

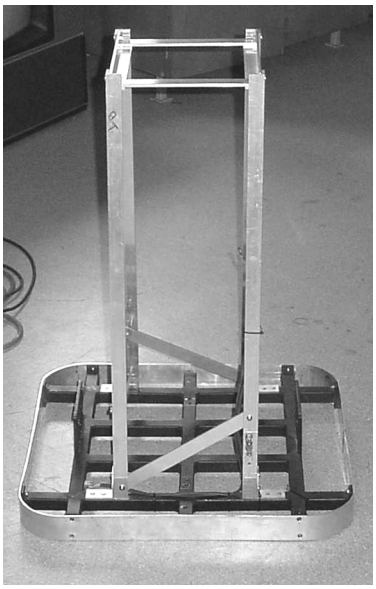

Figure 2-8: Steel chassis base (black) with aluminium frame and bumper

The material chosen for the construction of the base is 3 mm thick square steel tubing, the exterior dimensions of the tubing are 25 mm x 25 mm. The individual sections of steel are fastened together using a Metal Inert Gas welder (MIG). The steel has been welded on all four sides of the joint to produce an extremely strong and unyielding structure from which the remaining parts of the security device can be assembled.

The upper frame of the chassis has been constructed from extruded aluminium in an attempt to reduce excess weight. The frame is assembled using bolts and rivets which, unlike welding, allows the design to be kept modular and can be disassembled without

the destruction of its components. The design also allows for further extensions and modifications to be made easily without major chassis redesign. Due to the height of the framing above the base chassis, it is necessary to cross-brace the structure to increase stability and strength. Attachments such as the laser range-finding assembly and PC motherboard are bolted to the primary framework with the aid of further aluminium railings to ensure that all components are securely held in place.

MARVIN's driving motors are mounted to a section of 5mm steel plate, which is securely welded to the base structure. Three bolts hold each of the motors firmly in place, with the planetary gearheads mounted to their drive shafts. The gearhead mates with the ring gear on the inside of wheel rim. The wheel is bolted to the same plate as the motors to ensure that the gears mesh together in a tight fit to reduce any "slop" in the wheels.

The computer aided design software Solidworks© was used extensively in the design of the chassis to enable an accurate assembly of the components. This software also allows for realistic 3D visualisation of the design without the need for time consuming modelling and can accommodate small changes to different parts in respect to the overall design. The discrete components of each individual part may have their dimensions altered or additional parts can be added to the overall design with ease, without the entire assembly being rebuilt. Figure 2-9 shows an example of the 3D capabilities of the software.

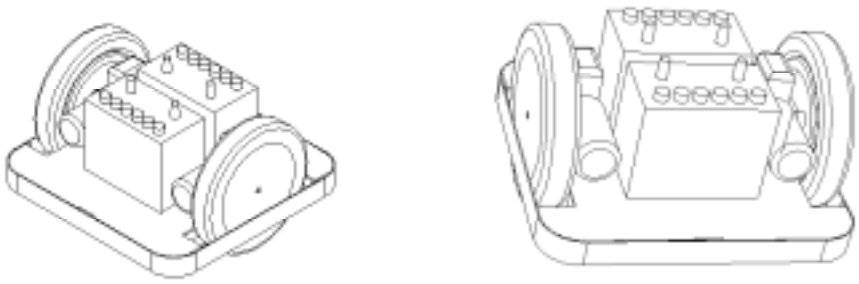

Figure 2-9: Design drawings developed with Solidworks© enabling 3D visualisation of the design before construction.

The rendering abilities of the software allow the user to add colour and texture to the design so that the aesthetics of the device can be considered. Once a design has been finalised, working drawings can easily be extracted complete with dimensions and a bill of materials.

As mentioned, the motors chosen to drive the robot require 24V DC and as such the chassis needs to incorporate the two large lead-acid batteries as the power supply. This, combined with the desire for the overall height of the robot to be approximately one metre, determines the dimensions of the base chassis. The batteries are mounted as low as possible between the motors, producing a low centre of gravity which will stabilise the robot when opening doors or if further appendages are added at a later stage.

3. CONTROL ELECTRONICS

The control of the driving motors is accomplished with the use of a microcontroller, which can be programmed from a PC using the C Programming Language. The microcontroller will deliver commands to the motors of the device via the driver circuitry. The motor driver has been designed to limit the current delivered to the motors and controls the consequent speed of the driving wheels.

3.1 THE MICROCONTROLLER

The microcontroller used to control the drive system is the **Phillips 87C552** (‘552). The device is based on the 8051 architecture and has the following features:

- 8k byte EPROM (one time programmable)
- 256 bytes of internal RAM
- Five 8-bit I/O ports
- One 8-bit input port
- Two 16-bit timers/event counters
- An additional 16-bit timer for capture and compare
- A fifteen source, two priority level, nested interrupt structure
- An 8-input ADC
- A dual DAC PWM interface
- Two serial interfaces (I^2C bus and UART)
- A watchdog timer
- Can be extended using standard TTL memories and logic

3.1.1 Power Supply

The power supply for the microcontroller is drawn from one of the two 12V lead acid batteries. To guard against high voltage and incorrect polarity, a crowbar circuit has been implemented and is illustrated below in Figure 3-1.

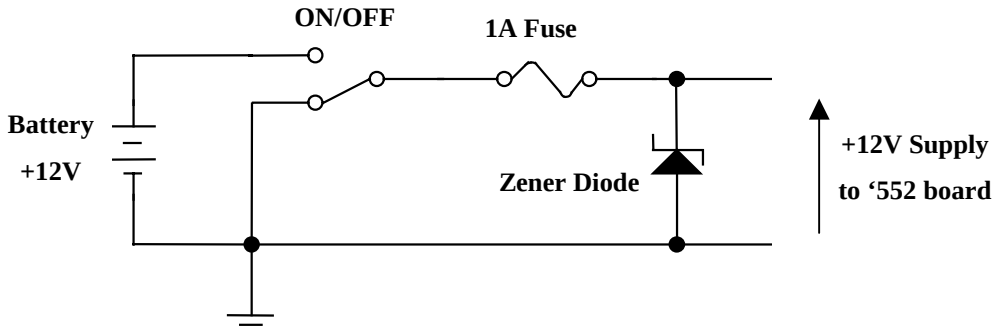

Figure 3-1: Crowbar circuit for the 87C552 power supply

The BZX79C15 Zener diode will prevent current flow up to 350mW, at which point the diode acts as a short circuit. The excess current flow caused by this short is sufficient to blow the 1A fuse and disconnect the power. The MC7805 voltage regulator is used to provide +5V to the discrete components of the motherboard. Two electrolytic capacitors are placed either side of the regulator to increase the stability of the device with additional non-polar capacitors used to prevent voltage spikes on the supply. Diodes are put in place to prevent incorrect current flow and also to ensure V_{out} is never greater than V_{in}. This arrangement is shown in Figure 3-2 below:

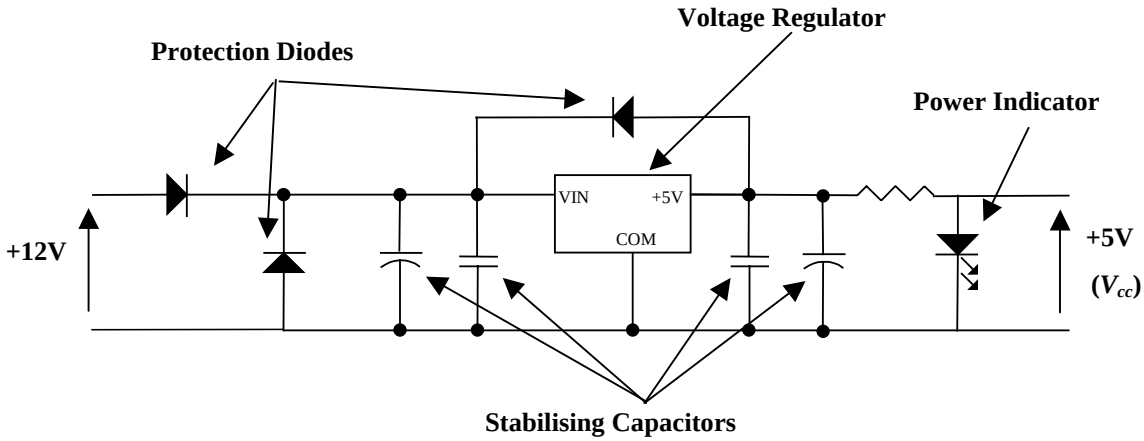

Figure 3-2: The voltage regulating circuit

3.1.2 Reset Circuitry

The reset circuitry on the motherboard allows the user to reset the '552 as required. An internal reset is executed in the second machine cycle in which the *RST* pin of the 87C552 chip is logic high and is repeated every cycle until the pin goes low. To ensure *RST* is held high for long enough to perform a chip reset, a capacitor is placed in parallel with a push button switch so that after the switch has shorted the capacitor, it will slowly charge causing *RST* to drop to logic low. This arrangement is shown in Figure 3-3 below. The value of this capacitor is chosen so that the time for *RST* to drop to logic low is longer than two machine cycles.

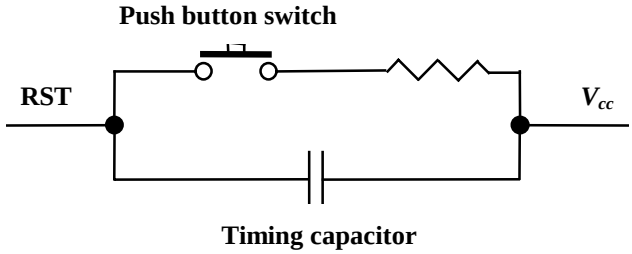

Figure 3-3: Reset circuitry

A resistor is placed in series with the switch to slow the discharge of the capacitor. This prevents the microcontroller from being accidentally reset if the switch is

unintentionally pressed momentarily. Once the ‘552 is reset, I/O Ports 1 to 4 are set high, while Port 5 is undetermined.

3.1.3 Watchdog Timer

The watchdog timer of the 87C552 is designed to reset the chip and reboot the device should a software lockup occur. This function is rarely used as it introduces the chance of the chip being reset accidentally. A three pin jumper has been used to set the *Not Watchdog Enable* pin of the ‘552 either on or off. This method is less invasive of board space than a switch.

3.1.4 Memory Allocations

The 8k byte EPROM of the ‘552 is used to store the download code which outlines how the chip is to store data downloaded from the PC. The microcontroller will run this code when reset with the Run/Download switch in the Download position. When the switch is in the run position all functions are performed from external memory.

The microcontroller’s motherboard incorporates two external 32k 8-bit Static RAM chips (KM62256CL) in a mapped memory configuration, one for storing program data and one as a data memory. Although the onboard EPROM of the ‘552 is sufficient to store the simple control algorithms for MARVIN, the additional external RAM provides ample memory for more complex programs that may be implemented in the future.

The RAM is corruptible during a power down and as such a “Smart Socket” is used for the program memory to provide a battery backup, thus preventing the need to download fresh code whenever the board is switched off. A low power RAM is used in conjunction with the smart socket to draw as little power as possible from the back-up battery when in use. This socket is not required for the data memory, as it is only accessed by the ‘552 to store variables and other parameters when running a program. This data is not vital and does not need to be available at start-up.

There are 15 address lines on each of the RAM chips, which are configured as input only lines. The external memory is accessed by the microcontroller through Ports 0 and 2. Port 0 outputs the low order 8 bits of the external memory address and is also used as a data line for both RAM chips. The 74HCT573 latch is used to control the data being written to the external memory. The latch stores the data until the *Address Latch Enable* line drops low. This ensures the correct address has been set on the RAM when the write instruction is given.

Port 2 outputs the upper 7 bits of the address bus, with the eighth, most significant bit (*A15*) used to select between the two RAM chips through an inverting transistor circuit. This circuit sets *Not Chip Select* of the data memory to be the inverse of whatever logic is present on the gate of the BST70A transistor. A 1kΩ resistor is used to prevent a short circuit when the MOSFET is open. The inverting circuit is shown in Figure 3-4.

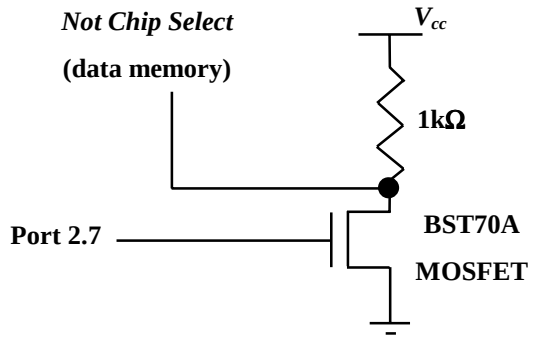

Figure 3-4: Inverter circuit for mapping of external memory

When *A15* is high, the MOSFET is switched on and the *Not Chip Select* pin of the data RAM is set low, selecting the data memory. If *A15* were set low, the MOSFET is switched off and the *Not Chip Select* on the data RAM is set high. The *Not Chip Select* pin of the program RAM is hardwired to *A15* and so its selection is determined directly from P2.7. This will always be the inverse of the control signal for the data memory.

The *Not Program Store Enable* (*NPSEN*) pin of the ‘552 is used as the read strobe to access the external program memory. This strobes the *Output Enable* pin of the RAM low whenever the *Run/Download* switch is set to *Run*. The *Not Write Enable* pin of the program RAM is only set low when data is downloaded from the PC.

3.1.5 Buffer

The multi-channel MAX232 driver/receiver is used to buffer the serial signals received from the PC and those sent by the 87C552 via the serial output port (Port 3.1). The buffer scales the voltage of the incoming signal, from the ±10V sent by the PC, so that the voltage received by the microcontroller is between +5V (V_{cc}) and *GND*. The buffer can also be used as a driver to produce an output swing of up to ±8V.

The serial port of the microcontroller is a Universal Asynchronous Receiver/Transmitter (UART) port and can transmit and receive simultaneously. The data being sent and received between the PC and microcontroller consists of a start bit, 8 data bits (LSB first) and a tenth stop bit.

3.1.6 Run/Download Circuitry

A Double-pole/Double-throw (DPDT) switch is implemented to swap the microcontroller between run and download modes of operation. When in the *Download* position, the *Not External memory Enable* (*NEA*) pin of the ‘552 is set high, causing the microcontroller to run from its internal ROM. In this position the switch also connects the *Receive Data Out* (*RDO*) pin of the MAX232 buffer to Port3.1 on the ‘552, which is the serial input port. If the microcontroller is reset with the switch in this position, it will reboot from the download code stored on the internal ROM and sit idle, waiting to receive data from the PC via the 9-pin D-connector on the motherboard.

The 9-pin D-connector is wired in the format of a standard null-modem cable, with many of the connector’s pins left unused. The relevant connections for the cable are:

- Pin 2: Transmit line
- Pin 3: Receive line
- Pin 5: Earth line

If the DPDT switch is in the *Run* position, *NEA* is set low and the '552 will reboot from external program memory when reset. In this position, the *Receive Serial Data* (*RXD*) pin of the microcontroller is connected to the transmitted serial output of the MAX232, with *Transmit Serial Data* (*TXD*) connected to the transmitted serial input. This enables serial transmission and reception through the buffer attached to the dedicated 10-pin header on the motherboard.

3.1.7 Port Structure

The 87C552 microcontroller has six 8-bit ports, which it uses to communicate with the peripheral components on the motherboard. Port 0 and Port 2 are the address buses for the external Data and Program memories. Ports 1,3,4 and 5 are multifunctional and can be accessed through the 10 pin headers of the motherboard. Their alternate functions are listed in Table 3.1.

Port	**Alternate Function**
P1.0, 1, 2, 3	Capture Timer input signals for Timer 2
P1.4	Timer 2 event input
P1.5	Timer 2 reset signal
P1.6	Serial clock line (I^2C bus)
P1.7	Serial port line (I^2C bus)
P3.0	Serial input port (UART)
P3.1	Serial output port (UART)
P3.2	External interrupt 0
P3.3	External interrupt 1
P3.4	Timer 0 external input
P3.5	Timer 1 external input
P3.6	External data memory write strobe
P3.7	External data memory read strobe
P4.0, 1, 2, 3, 4, 5	Timer 2: compare and set/reset outputs on a match with Timer 2
P4.6, 7	Timer 2 compare and toggle outputs on a match with timer 2
Port 5	Eight analog ADC inputs

Table 3.1: Input/Output ports of the 87C552 microcontroller

3.1.8 The Oscillator

An HC49 oven crystal is used to run the internal clock of the 87C552. This was chosen over a ceramic variation as it produces a more accurate signal. The crystal produces a sinusoidal signal that is input to the *XTAL1* and *XTAL2* pins of the microcontroller. The crystal oscillates at 14.7456 MHz, which determines the speed at that the '552 will operate at.

Figure 3-5 shows the microcontroller and other digital components that placed together on a separate printed circuit board (PCB) measuring 115mm by 125mm.

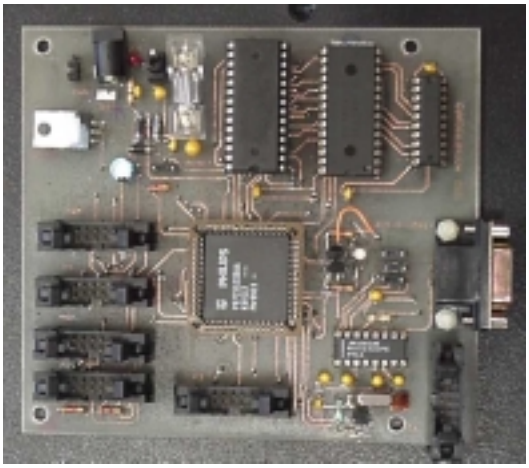

Figure 3-5: The 87C552 motherboard

The signals sent to the driver circuitry and received from the sensors are transmitted via ribbon cable to the 10-pin headers of the digital board which are connected to the I/O ports of the microcontroller in the following manner (Table 3.2):

CONNECTION	**'552 PORT**
Shaft Encoders	Port 3
Driver Shutdown Control	Port 4
PWM Signals	PWM / ADC Port

Table 3.2: Port connections for 87C552 microcontroller

The full schematic of the microcontroller motherboard can be found in Appendix A.1.

3.2 MOTOR DRIVER CIRCUIT

3.2.1 The H-bridge

Each motor is controlled by a full H-bridge arrangement. Four MOSFETs are arranged in such a manner that when two alternate transistors are switched on the motor will run. If the opposite two MOSFETs are opened the motor will run in the other direction, as shown in Figure 3-6.

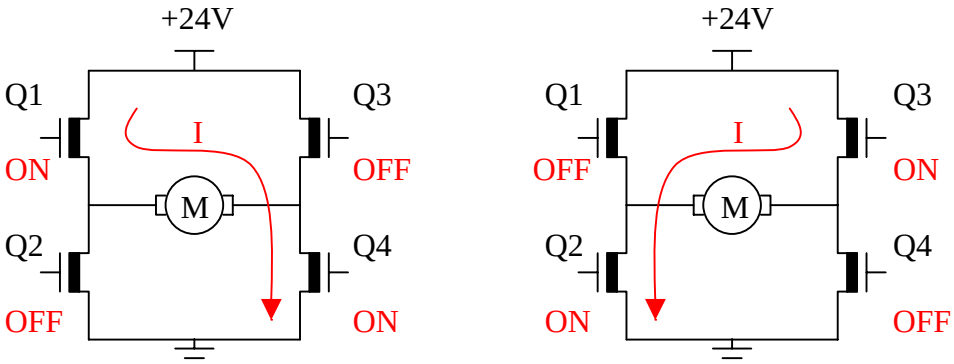

Figure 3-6: Current flow through the H-bridge circuit

Due to the high voltage driving the motors and the large amount of current that is drawn under load, the IRLZ44N power MOSFET is used. This FET has a drain to source current of 47A and is able to cope with voltages up to 55V (the full data sheet is available in Appendix C). In order to produce the required voltage drop between the gate and the source, the MOSFETs must be driven by the IR2110 high and low side MOSFET Gate Driver (MGD). The IR2110 has independent high and low side referenced outputs and so can be used to control either of the current paths, either Q1 and Q4 or Q2 and Q3. It has built in undervoltage lockout to prevent the motor from being activated when the control signal is absent.

3.2.2 Pulse Width Modulation

Pulse Width Modulation (PWM) is a method of controlling the amount of current supplied to driving motors that is much easier to implement with a microcontroller than limiting the supplied voltage. The PWM supplies the motors with a square-wave signal which is either at +24V or *GND*. The resultant speed of the motors is determined by the *Pulse Width Ratio* of the signal, which is calculated by Equation [3-1].

$$Pulse\ Width\ Ratio = \frac{PWM_n}{255} \qquad \textbf{Eqn. [3-1]}$$

where PWM_n = the value of either *PWM0* or *PWM1* (set in software)

Therefore, the *Pulse Width Ratio* has a range of 0 to 255/255 and can be programmed in increments of 1/255. The signals produced are similar to those illustrated below:

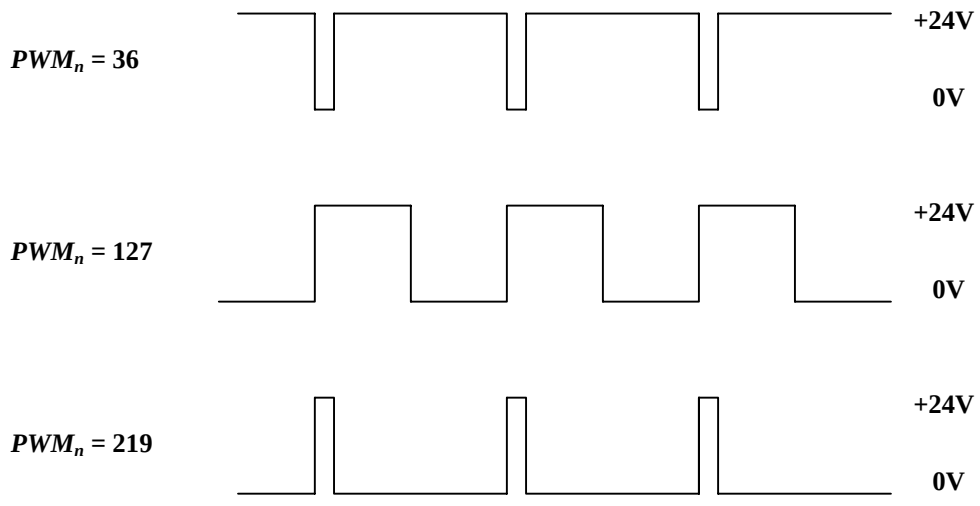

Figure 3-7: PWM motor input examples

It can be seen from Figure 3-7 that the lower the set value of PWM_n, the more current is supplied to the motors and the faster they turn.

PWMP controls the frequency of the PWM signal, f_{PWM}, and has been set to zero so that it has the maximum value as calculated using Equation [2-2] below:

$$f_{PWM} = \frac{f_{OSC}}{2 \times (1 + PWMP) \times 255} \qquad \textbf{Eqn. [3-2]}$$

The frequency of the oscillator f_{OSC} = 14.75MHz, so the value of f_{PWM} = 28.9 kHz. The PWM signal is sent to both the high and low side transistors of the H-bridge. This makes it possible to control the speed of two motors using one microcontroller, as there are only two PWM outputs available on the 87C552

The PWM signal from the 80C552 microcontroller is passed through the MC14504B CMOS level shifter to both inputs of the MOSFET driver. This raises a logic high signal from the '552 from +5V to the required +15V for the MGD input. It is the PWM that determines the speed of the motors by altering the duty cycle of the 24V signal that passes through the motor, the longer the signal is high per cycle, the faster the motor will turn.

3.2.3 Hardware Protection

As the inputs of the MGD are always receiving the PWM signal, it is the shutdown pin (SD) of the IR2110 which is used to control the direction, if any, of the motor. The pair of driver chips are configured in such a way that when the first is on and the other is off, the motor will travel in the reverse direction to that when the first is off and the other is on. Care is required to ensure that both current paths are never open at the same time as this will result in a short circuit between +24V and ground through the transistors. The transistors are not able to cope with such current and would destruct. To prevent this situation from arising accidentally, a Programmable Logic Device (PLD) has been employed as hardware protection. The program in the PLD produces the following truth table:

SD1A	SD1B	OUT1	OUT2	Motor direction
0	0	1	1	Stopped
0	1	1	0	Forward
1	0	0	1	Backward
1	1	1	1	Stopped

Table 3.3: Truth table for programmable logic device

The output of the IR2110 is shutdown when there is a high signal on its SD pin. The PLD is used to invert the signal received from Port 4 so that both channels are never on at the same time and are shutdown at start-up when all Ports of the '552 are set high. A current path is activated in software by selecting the appropriate bit on port 4 of the microcontroller and setting it low. As is shown in Table 3.3, it is impossible to have a low signal on the shutdown pin of both the MOSFET drivers. The output from the PLD is also passed through the CMOS level shifter to raise it to the required logic levels.

3.2.4 Power Supply

The MC7815ACT voltage regulator is used to deliver the 15V power supply to the IR2110 and MC14504B chips from the 24V of the lead-acid batteries. The programmable logic device and buffer also require a 5V supply that is obtained from the microcontroller motherboard. To guard against incorrect polarity or excessive voltage, a crowbar circuit has been implemented by way of the Zener diode, which will begin to conduct when the voltage is greater than 27 volts. Non-polar capacitors are added to prevent any voltage spikes in the supply and a diode is used to ensure V_{out} is never higher than V_{in}.

Decoupling capacitors have been placed over the terminals of the motors and also between +24V and *GND* in the driver circuit in an attempt to reduce noise. The driving motors introduce large voltage spikes in the circuitry when driven by the PWM signal. These spikes can cause excess loading on the MOSFETs of the H-bridge, which may cause them to fail.

Heat sinks are attached to the MOSFETs of the H-bridge purely as a precautionary measure to prevent overheating from occurring. The driver PCB has been symmetrically laid out with an H-bridge on either side for each motor. Figure 3-8 shows the motor driving PCB with the large heat sinks at the top of the photo along with the terminal block used to connect the motors and power supply.

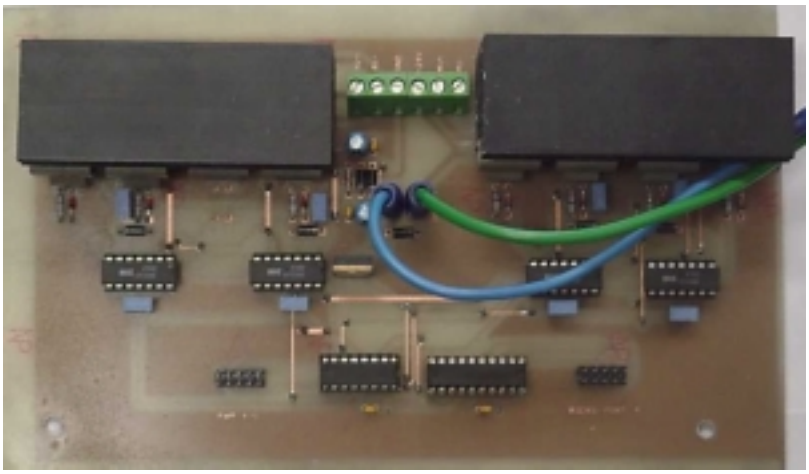

Figure 3-8: The motor driver circuit board

A schematic diagram of the entire driver circuit is located in Appendix A.2

4. SENSING TECHNIQUES

4.1 OVERVIEW

The sensing requirements of a large-scale security device are many. The device must be able to navigate its surroundings accurately, while avoiding any obstacles that are in its path. In the office environment, it is likely that many of the obstacles that MARVIN will encounter will not be fixed, and their position may change from day to day. MARVIN needs to be able to detect these obstacles in time for it to take evasive action and avoid collision.

The device must be able to map its surroundings in order for it to achieve a sense of location. It is possible to perform map-matching on the data received from the sensors, from which the robot will be able to "recognise" its surroundings and therefore calculate its absolute position. For MARVIN to calculate its position, information on the distance and heading that it has travelled is required.

4.2 PROXIMITY SENSORS

Proximity sensors are used to detect the presence (or absence) of an object. MARVIN will require such sensors to prevent collision with obstacles it may encounter in its operating environment. The methods of sensing listed below are some of the more common forms of proximity sensing.

4.2.1 Tactile Sensors

This detection method involves direct physical contact between the sensor and the object detected. This contact may be executed through the use of an antennae or feeler, or by a touch-sensitive bumper. The feeler method is comprised of a flexible feeler

attached to an actuator. The feelers protrude out from the body of the robot with the actuator detecting any contact as shown below:

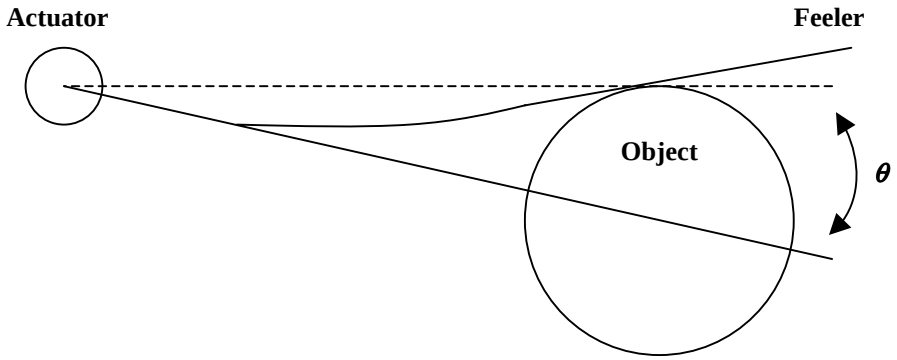

Figure 4-1: Flexible feeler tactile sensor

It is possible to calculate the point of contact along the feeler if the actuator measures the amount of rotation after contact, θ, and the corresponding torque induced.

Tactile bumpers are relatively simple and can only detect the presence or absence of an obstacle. The protective bumper of the device has sensors attached in such a way that if it comes into contact with an object the sensor is activated. This system is often implemented as the last means of obstacle detection on a mobile robot.

4.2.2 Ultrasonic Proximity Sensors

Ultrasonic sensing is an example of reflective sensing. The sensor usually consists of a transmitter and receiver pair and responds to variation in the amount of reflected energy detected by the receiver. The transmitter emits a high frequency sound wave, which reflects off the object and is detected by the receiver, where the Time-of-Flight (TOF) information can be calculated. The range of the object can be determined from the TOF data if the speed of the sound wave is a known constant. These sensors are accurate over distances of several metres, with their accuracy dependant on the span of the transmitted signal.

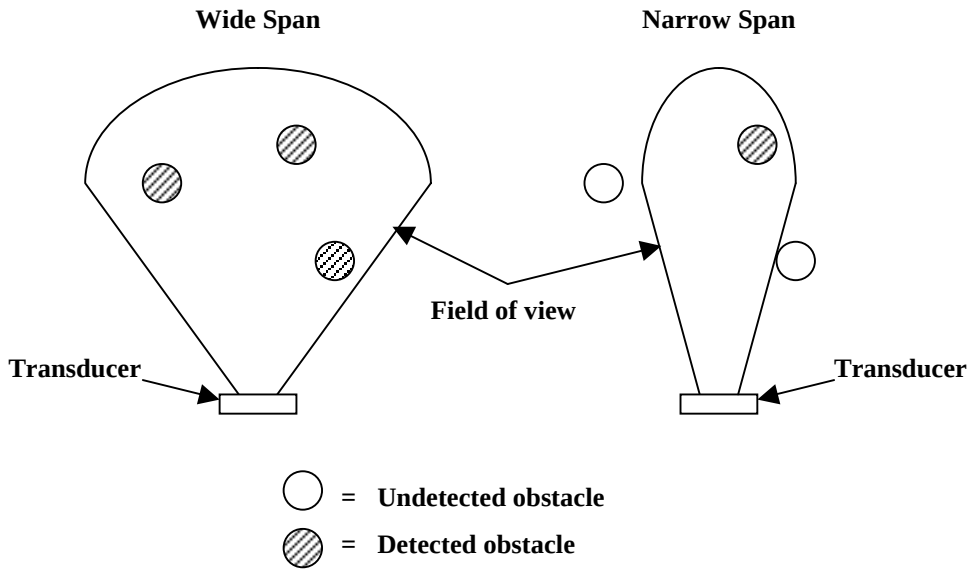

Figure 4-2: Ultrasonic accuracy is dependent on the area covered by the transmitted signal

If the transmitted signal covers a large area, the likelihood of an obstacle being detected is higher than if a narrow span were used. The advantage of the narrow span is that the position of the obstacle relative to the device is known with more accuracy as shown in Figure 4-2.

A disadvantage of ultrasonic sensors is that, as the incident angle, θ, of the ultrasonic beam decreases below a critical value, the reflected energy does not return within the acceptance angle of the receiver.

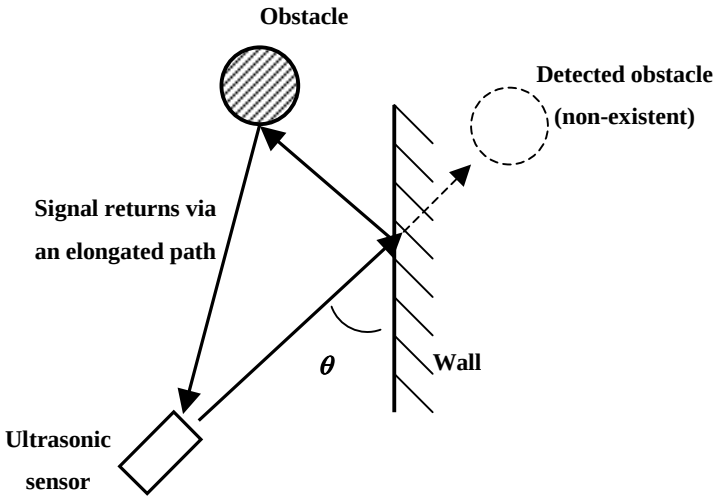

Figure 4-3: Disadvantages of ultrasonic sensors.

The reflected signal can produce a false echo, where the ultrasonic energy returns to the receiver over an elongated path, resulting in the distance to the obstacle being overestimated. This is illustrated in Figure 4-3. If the reflected energy were to reflect off another obstacle, there is a possibility that the receiver will detect the subsequent signal. The TOF calculations from this signal would indicate a single object at a distance equal to half of the total signal path (indicated by the dashed line).

Ultrasonic sensors are more sensitive to such errors than infrared due to the speed of sound being much slower than light, affecting time of flight information, also the critical angle at which the signal is dissipated is larger for the ultrasonic receiver, making the error more likely to occur.

4.2.3 Microwave Proximity Sensors

Microwave sensors operate on a similar principle to the ultrasonic sensor but have a much greater range, from one to thirty metres. An electromagnetic signal is emitted in the microwave spectrum, which is reflected by the object and detected by a receiver. The microwave sensor can also be configured to detect relative motion by analysing the doppler shift in the reflected signal.

4.2.4 Infrared Sensors

Infrared sensors calculate the range of an object by implementing a form of triangulation. A light source is placed at a known distance and angle from a small, Charge Coupled Device (CCD) detector. As the angle between the source and detector, θ, is fixed, there is a direct relation between the distance to the object, x_{OBJECT}, and the position of the object on the CCD array of the detector, x_{CCD}. This method is illustrated in Figure 4-4 in which θ has been exaggerated for clarity.

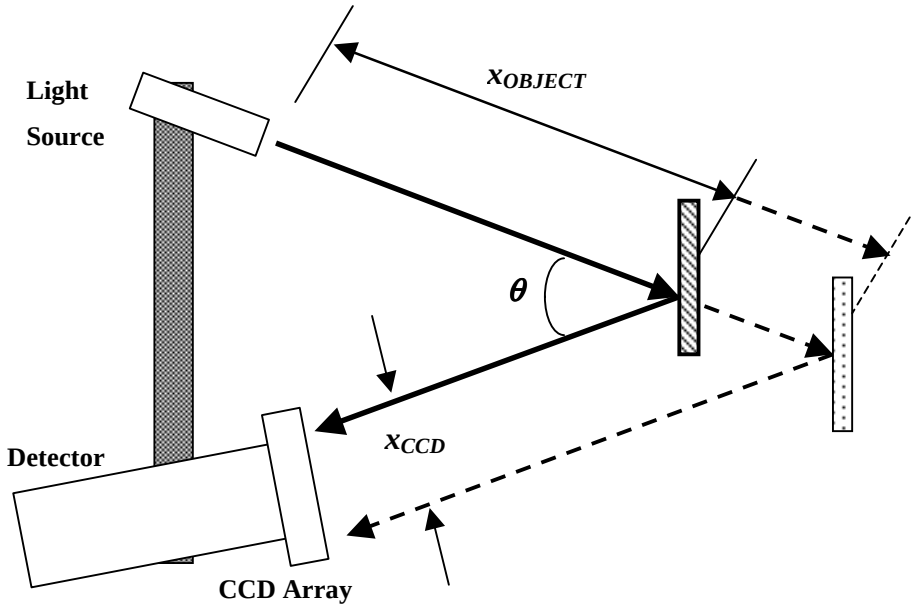

Figure 4-4: Triangulation method of range finding

4.3 MARVIN'S PROXIMITY SENSORS

Infrared sensors were chosen to implement the proximity sensing on MARVIN. They are relatively simple to implement and are more accurate over shorter distances than ultrasonic sensors. They also provide a form of short-range obstacle detection that is less invasive than tactile sensors, which is desirable when the operating environment for MARVIN is considered. Tactile sensors require precise control of the robot's motion to ensure that it can stop as soon as contact is detected. This form of control is not available with the drive system employed on MARVIN.

The infrared emitter/detector (IRED) pair chosen to perform the detection from onboard MARVIN is the Sharp GP2D12 shown in Figure 4-5, which is a Position Sensitive Device (PSD). The emitter and receiver are in a fixed arrangement and are constructed in single package as shown above. A small linear CCD array detector is positioned 18.75mm away from an infrared emitter and is used to compute the intensity of the infrared reflection in the field of view. The specifications for this device state that it is almost immune to interference from ambient light and can accurately detect objects from 0.1m to 0.8m away.

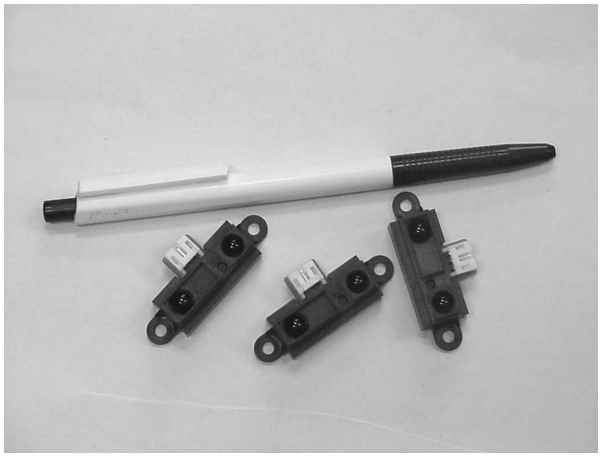

Figure 4-5: The Sharp infrared emitter/detector modules

The receiver outputs a value between 0 and 5V, which is proportional to the distance of the obstacle. The output voltage generated by the sensor is a trigonometric function of the distance to the object, with a relationship similar to that shown in Figure 4-6 below:

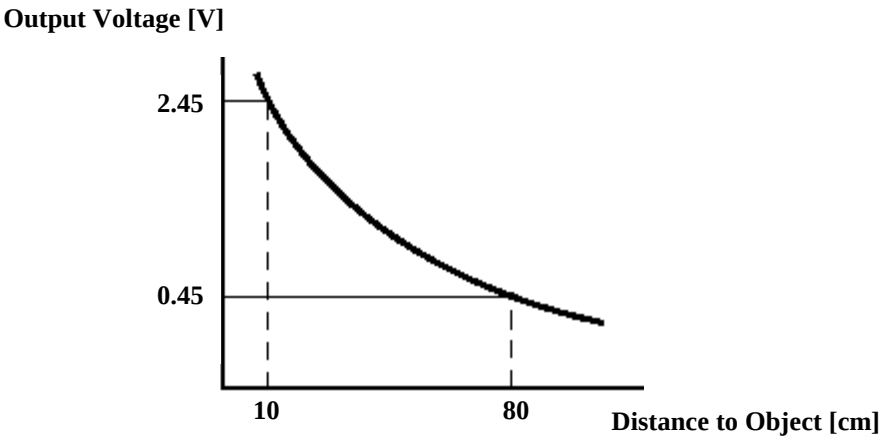

Figure 4-6: Output pattern of IRED sensors

The outputs from the receivers are fed directly to the ADC ports of the ‘552 from which a digital representation of the distance can be computed and used in the control algorithm.

The infrared sensors are mounted in a manner so that there are two sensors mounted either side of the chassis for wall detection, with two mounted at the front for detection of any objects that may be in the path of the device. MARVIN uses the side sensors

before it executes a turn to ensure there is sufficient room to complete the manoeuvre while avoiding collision.

As MARVIN is required to operate in an office environment, the infrared detectors are subject to a large amount of ambient light from the fluorescent lights overhead as well as natural lighting conditions. Although the IRED sensors are largely immune to ambient light, the various surfaces that the infrared signal will encounter will vary in reflective efficiency, with darker surfaces absorbing more of the infrared signal emitted from the sensor than lighter surfaces. This occurrence will only affect the range calculations when the object is more than 35cm from the IRED sensor as shown in Figure 4-7.

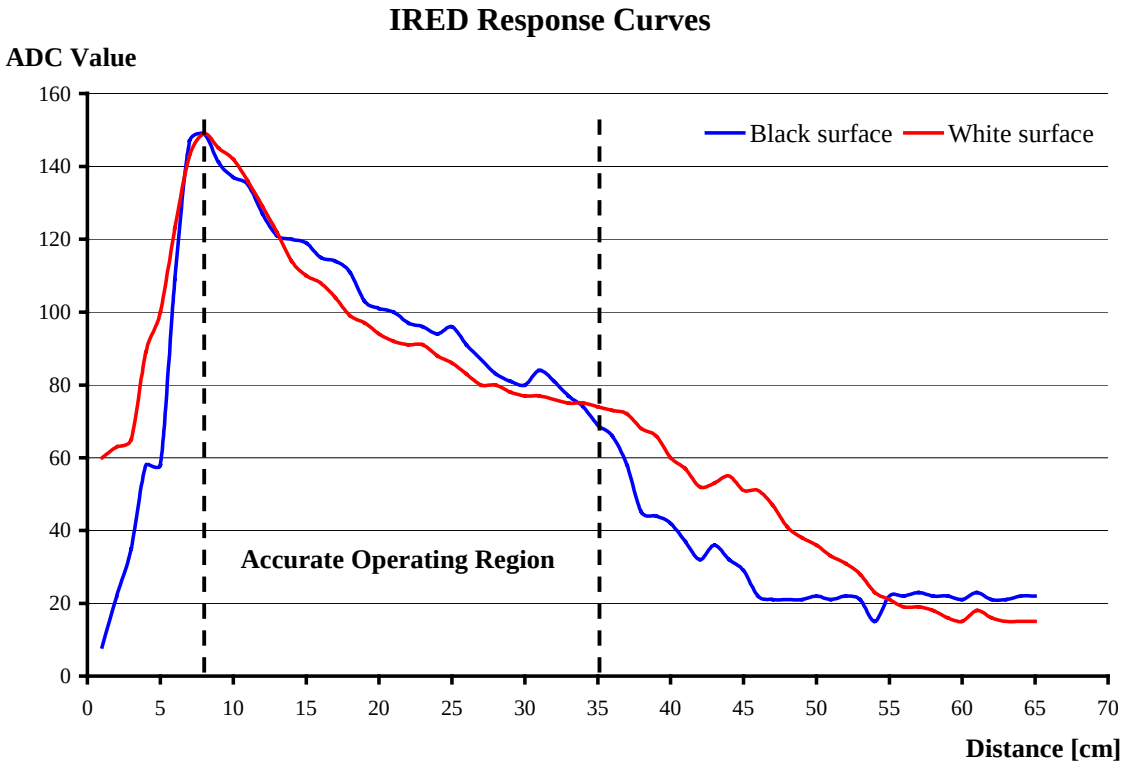

Figure 4-7: IRED response curve (high ambient light)

The above plot shows the two extremes in reflectivity. While operating in the office environment, the sensors will be required to reflect off a range of surfaces, from timber to aluminium, plastic or paint of various colours. The above response curve illustrates that the detectors will give an accurate indication of distance up to approximately 35cm before errors from surface absorption will occur. The curve also highlights an initial

black spot from 0 to 8cm, as the reflected signal is outside the acceptance angle of the detector.

The black spot of the IRED sensors effectively increases the exterior dimensions of MARVIN by 8cm, as any obstacle closer to the sensors than this will not be detected accurately. If an obstacle is allowed to get close enough to enter the black spot, the control system will class it as an impending collision and take evasive action.

4.4 POSITION SENSORS

If a mobile robot can determine its absolute location with respect to an arbitrary start point, it is possible for a map of the environment to be created. The mapping information can then be used by the robot to determine its current position, and the relative position of its target location. Some common methods of position sensing are listed below.

4.4.1 Active Beacon Navigation Systems

These systems provide the mobile robot with information on its position relative to a fixed origin. Transmitters are placed at known positions and emit a signal from which the receiver can identify its position. There are many variations of this system with the robot determining its absolute position relative to the network of transmitters.

The Global Positioning System (GPS**)** uses a network of 24 satellites orbiting the earth in six set orbit patterns and is an example of an active beacon navigation system. A mobile receiver analyses the signal from the satellite and determines the time taken for the signal to arrive. From this information, the distance to the satellite can be computed and, if repeated with at least three satellites, the exact position of the receiver can be triangulated. If four satellites are analysed it is possible to determine the altitude of the receiver also. By continually updating the position of the receiver, the GPS can accurately provide speed and heading information.

GPS acquisition software is readily available and can provide real-time analysis of GPS position, course and velocity. It is possible to construct and store a reference map of the operating environment for the mobile robot, which can then be used to efficiently navigate its surroundings and achieve its target destination.

4.4.2 Landmark Navigation

This form of position sensing employs a network of set features in the operating environment of the robot to guide it toward the target destination. The landmarks used in the navigation of the device can either be distinctive natural features, or artificial landmarks, specifically placed to assist the robot in navigation. These systems can remove an aspect of the robot's autonomy due to the external feedback control it provides.

Landmark navigation is the primary guidance system in Automated Guided Vehicles (AGV), which follow a network of artificial landmarks to their target destination, such as the large mobile robot developed by the University of Canterbury, in Christchurch. As the landmarks are mainly used for obstacle avoidance, this system does not give an accurate representation of the robots' location with respect to its starting point.

4.4.3 Laser Range-Finding

The Laser Range Finder uses a similar method of triangulation to that used in the IRED sensors. A laser line is produced that is analysed by a CCD camera, this takes a "snapshot" of the line against the robot's surroundings. The position of the line on the CCD array determines the distance to the obstacles in the frame as is done with the IRED method.

Laser Range Finding has the advantage of being an independent unit and does not require a system of beacons or landmarks to be constructed in the operating environment. The range finding assembly will not have the additional reception concerns, which can render an active beacon system useless should the signal from the beacons be interrupted. These factors add to the versatility of the range finding system.

4.4.4 Dead Reckoning

If the initial position of the robot is known, it is possible to deduce its current position by "Dead Reckoning". A controller receives information on speed and heading from odometers attached to the drive wheels, from which it is able to calculate its current position within a reasonable error. This system is prone to accumulative errors, as an error in the heading or positional information will compound continually until the sensors are calibrated. Dead reckoning systems are usually implemented in conjunction with some other form of position sensing for this reason. Odometry can, however, provide a simple basis for the calculation of the vehicle's speed and heading.

4.5 MARVIN'S POSITION SENSORS

The position sensing to be implemented on MARVIN is a combination of dead reckoning and Laser Range Finding methods. The determination of speed and heading in odometry is very simple, which allows the control systems for MARVIN to be kept reasonably straightforward. The inherent errors of this system can be corrected when calibrated against the information received from the range finder. This system does not require MARVIN's operating environment to be altered in order for the position sensors to be implemented and will provide the most versatile arrangement for future developments.

4.5.1 Laser Range Finder

The laser range-finding system designed and developed by Shaun Hurd[7] is mounted to the top of the robot's chassis to enable an accurate mapping of its environment. The laser and camera are mounted on a platform, which is driven by a stepper motor to enable the orientation of the camera relative to the robot to be more accurately controlled. This arrangement allows the assembly to rotate about 360 degrees producing a 3D scan of MARVIN's immediate surroundings without the robot needing to turn at all. The position of the camera (with respect to the robot) is moved in multiples of 1.8 degrees, a much more precise control than would be possible if the whole device were to

be moved. The resolution of the stepper motor allows for 200 scans of the robot's environment to be made per revolution of the range finding assembly.

Figure 4-8 illustrates the laser range finding equipment used during experimental testing. A computer screen is used to monitor the image being processed by the range finder, the power supply is used for the stepper motor and laser, with the floppy and CD drives used to move data for further analysis. When the range finder is mounted to the security robot these peripherals are omitted.

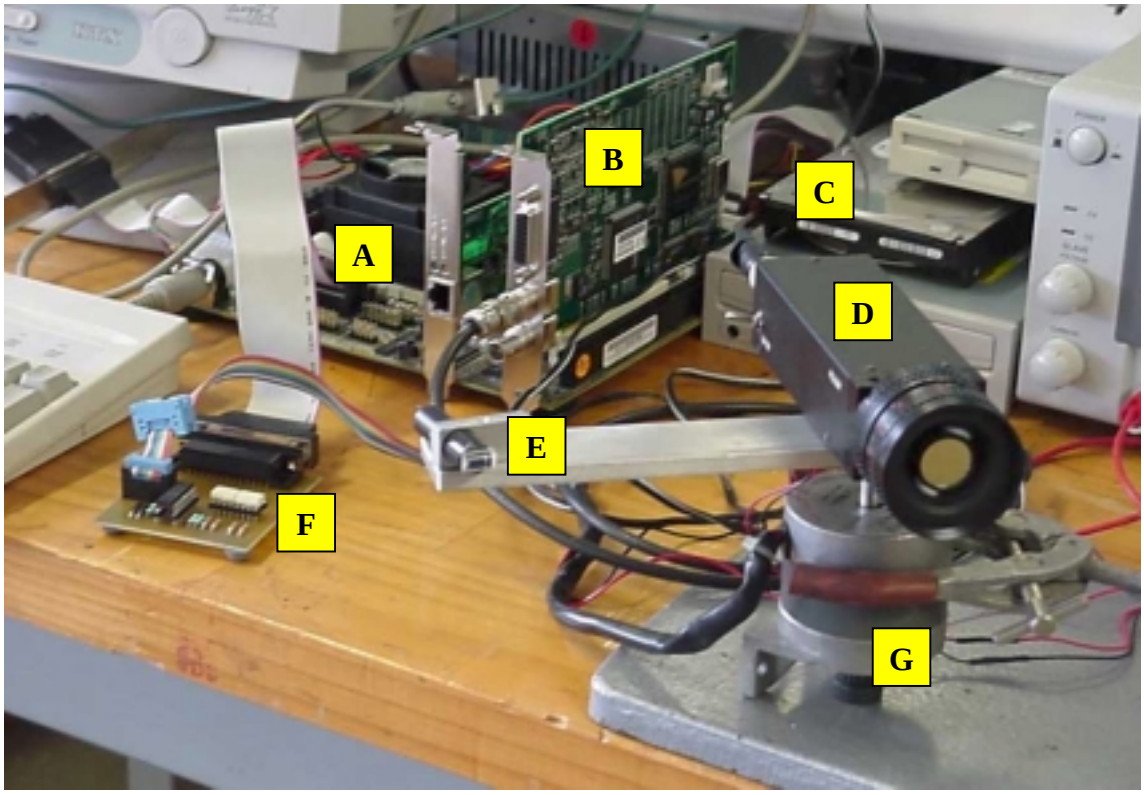

Figure 4-8: The laser range finding assembly

where:
A = Celeron 533MHz processor and motherboard with 64MB of RAM
B = Imagenation PX-610A frame-grabber
C = 8Gb hard-drive
D = Pulnix TM-7645I interlacing CCD Camera
E = Class IIIa 633nm laser with small cylindrical lens
F = Stepper motor driver circuitry
G = 23LM-C304-14 Miniangle Stepper motor

The stepper motor driver circuitry is connected to the parallel port of the PC motherboard, which supplies a control signal to determine the angle through which the motor will turn. The laser and motor require a +5V power supply, which will be drawn from the lead acid batteries. A cylindrical lens is placed in front of the laser beam to produce a vertical line that can be captured by the camera and analysed to determine range data.

The system uses a method of triangulation to determine the distance to an object and is accurate from distances of 0.50m to 10m. The range finder has an accuracy of ±476mm at 9.75m, but as accuracy is inversely proportional to distance it is increased to ±50mm at distances less than 3.2m.

The computer motherboard and hard drive are mounted to the frame of the robot in a modified desktop PC case. The computing power of the Celeron processor is employed to compute the range-finding information and allows for future expansion, for example, the mapping algorithms necessary for MARVIN to navigate around its environment. The PC processor can communicate this information to the drive controller through the MAX232 buffer and serial communications port of the 87C552 microprocessor.

It is possible to conduct a scan of the robot's immediate environment, from which a 3D map can be constructed. This data can be used, not only for collision avoidance, but also to determine the absolute location of the device. As the principle structures of the environment, such as walls and doors, are known in advance and change infrequently, it is possible to compare the mapping data with reference data to determine MARVIN's location. This comparison also allows the device to identify any anomalies in its surroundings[7].

There are some circumstances where the Laser Range Finding assembly may not detect an obstacle. If the object is moving, it is possible that it will not register in the laser mapping, similarly, if the object is not very high it may escape detection by the laser. To ensure that MARVIN does not collide with any such obstacles, infrared sensors are used in conjunction with the laser assembly. The infrared sensors have a much shorter range than the laser, and can more reliably locate nearby objects.

4.5.2 Odometry

The odometry system is implemented with the Hewlett Packard HEDS 9100 incremental optical encoders combined with the HEDS-5120 code wheel. The number of pulses detected over a predefined period of time allows the speed of the driving wheel to be determined. By comparing the information received from the encoders of the left and right wheels, it is also possible to compute the orientation of the robot with respect to the origin. The HEDS 5120 code wheel is a metal wheel with a resolution of 512 slots per revolution. As the drive system has a reduction ratio of 51.56:1 (from Equation [2-1]), the encoder will produce 26400 pulses per revolution of the wheel. The circumference of the driving wheels is $C_{R.L}$ = 1052.4 mm, therefore the resolution provided by the odometers is 25 pulses per millimetre.

The optical encoder module has an emitter/detector pair arranged in a presence sensing arrangement with the code wheel in between the two. Whenever a slot passes between the pair, the photo-detector receives the signal from the emitter and the module will output +5V until the wheel cuts the signal again as illustrated in Figure 4-9.

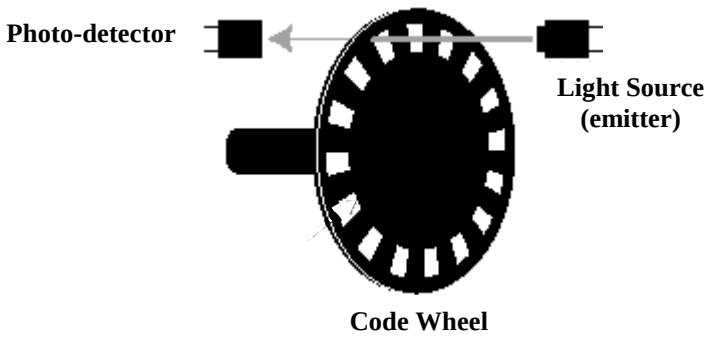

Figure 4-9: Workings of the optical encoder

The HEDS 9100 encoder module produces two signals in quadrature (90 degrees out of phase with each other) to enable the determination of direction. Only one of these channels is implemented on MARVIN as the physical characteristics of the drive system provide that the direction of the driving wheel is set by the microcontroller alone, due to the physical braking system that has been implemented.

The encoder module and code wheel are mounted to the back of the motor as shown in Figure 4-10.

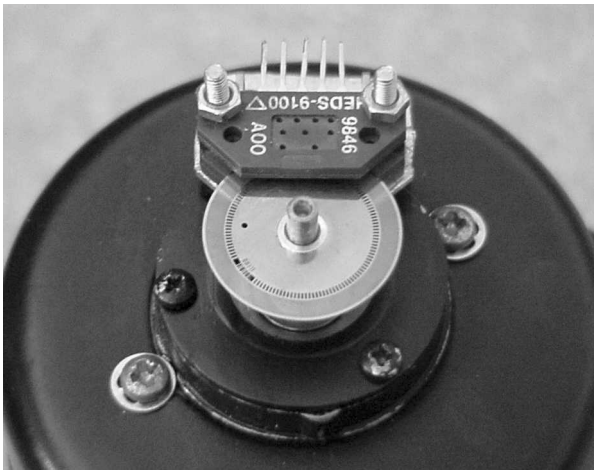

Figure 4-10: Encoder module and code wheel assembly

Dead reckoning systems such as this are susceptible to a variety of odometry errors both systematic and non-systematic. Systematic errors include:

- Unequal wheel diameters
- Discrepancies between nominal and actual wheel diameters
- Discrepancies between nominal and actual wheelbases
- Misaligned wheels

Non-systematic errors include:

- Uneven floor
- Wheel slippage

Systematic errors accumulate constantly and are the major contributor to odometric error. Non-systematic errors are more likely to be a “one-off” unpredictable occurrence and as such they are much more difficult to reduce in the control theory.

4.6 MEASUREMENT OF ODOMETRY ERRORS

Unequal wheel diameters and wheelbase discrepancies cause the two fundamental systematic errors produced by odometry. The former will cause the vehicle to travel in a curved path when the controller intends a straight line, while the latter will cause a heading error whenever the robot executes a turn. The wheelbase of the vehicle determines how far each drive wheel must travel (in opposite directions) in order to achieve a 90 degree turn.

To compensate for the systematic errors induced by odometry sensing it is necessary to calculate the magnitude that each component contributes to the total error. The "Bi-directional Square-path Experiment", also know as the "University of Michigan Benchmark"[4] (UMBmark), highlights the error caused by an inaccurate wheelbase, e_b and unequal wheel diameters, e_d. In this test, the robot is programmed to travel a square path comprising four straight line segments and four 90 degree turns, theoretically returning to its initial position. The path is completed in both clockwise and anticlockwise directions, with the final position of the device in relation to the origin (positional error) recorded for each direction. The experiment is run at least five times in order to generate a sufficient data set for analysis. The error in orientation is not noted as it is directly proportional to the positional errors and so is automatically accounted for.

When the results from the clockwise and anticlockwise paths are plotted they form two distinct groupings as shown in Figure 4-11. These data values are averaged so as to reduce the random effect of non-systematic errors on the trial.

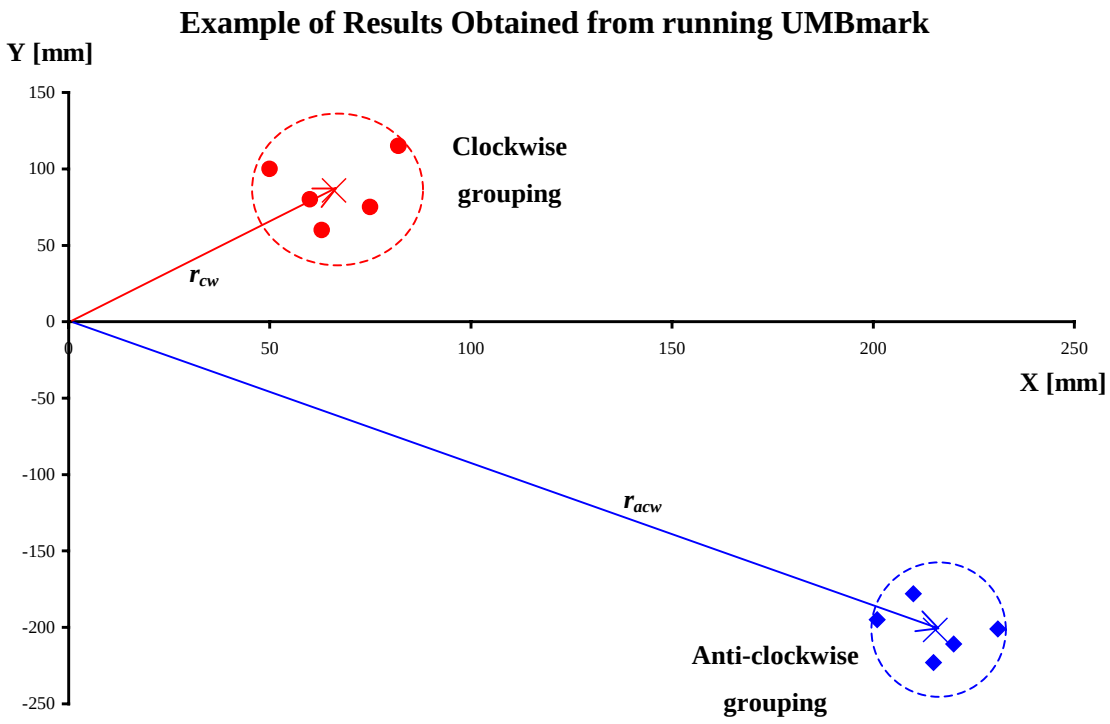

Figure 4-11: Results from running UMBmark

The average for each direction is found as the sum of all the values divided by the number of data points:

$$x_{cw} = \left(\frac{1}{n}\right)\sum_{i=1}^{n} ex_{icw} \qquad \textbf{Eqn. [4-1]}$$

$$y_{cw} = \left(\frac{1}{n}\right)\sum_{i=1}^{n} ey_{icw} \qquad \textbf{Eqn. [4-2]}$$

where x_{cw}, y_{cw} = average value of x and y components for clockwise direction

ex_{icw}, ey_{icw} = ith x and y component of clockwise error

n = total number of data points

A reference vector is generated that defines the average offset from the origin by Equation [4-3]:

$$r_{cw} = \sqrt{x_{cw}^2 + y_{cw}^2} \qquad \textbf{Eqn. [4-3]}$$

where r_{cw} = clockwise reference vector

The above calculations are repeated for the anti-clockwise data, to compute the anti-clockwise reference vector, $r_{acw.}$ The larger of the two reference vectors defined as the **measure of odometric error**, which is used to define the "worst case" scenario.

To reduce these errors, the contribution of each individual systematic error toward the total must be determined. To achieve this, the errors deduced from the UMBmark test are grouped into two categories:

TYPE A: those errors that increase (or decrease) the total amount of rotation by the robot in both the clockwise and anti-clockwise directions.

TYPE B: those errors that increase the amount of rotation in one direction but reduce it in the other.

Intuitively it can be seen that TYPE A are mostly due to the nominal wheelbase error as the orientation of the device is determined from the vehicle wheelbase as explained in Section 5.5.1. TYPE B errors are mostly due to unequal wheel diameters causing the robot to travel in a curve. As both errors occur simultaneously during a test run, the individual contributions must be determined from the overall error.

4.6.1 TYPE A Errors

The wheelbase error, e_b, causes the robot to understeer (or oversteer) by an angle, α, when executing a 90 degree turn as shown in Figure 4-12. The value of α (in degrees) can be determined geometrically

$$\alpha = \left(\frac{x_{cw} + x_{acw}}{-4L} \right) \frac{180^\circ}{\pi} \qquad \textbf{Eqn. [4-4]}$$

where x_{cw} = x component of the clockwise error

x_{acw} = x component of the anti-clockwise error

L = length of a side

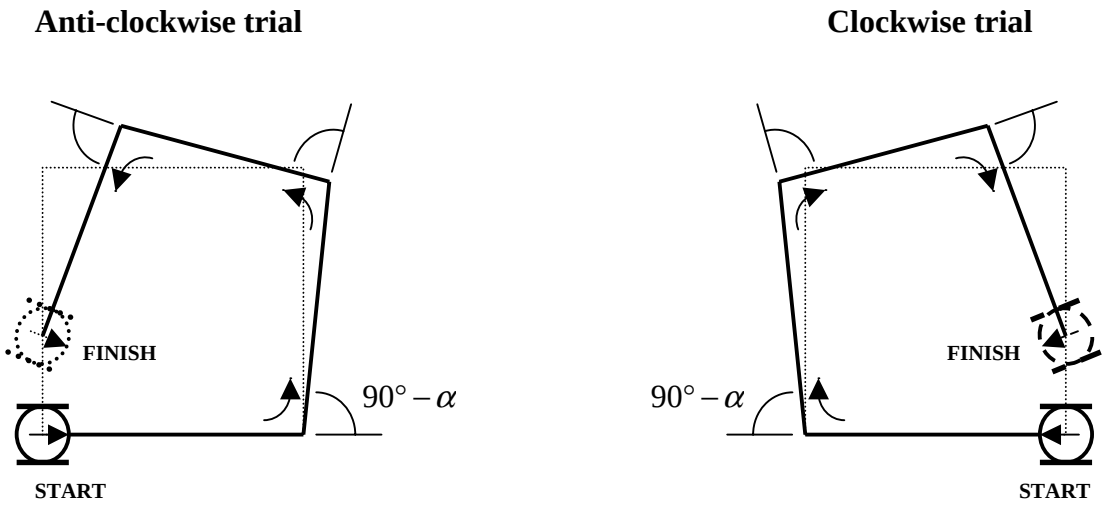

Figure 4-12: TYPE A errors decrease (or increase) the total amount of rotation of the robot in both clockwise and anticlockwise directions

The wheelbase, *b*, is directly proportional to the amount of rotation of the device in each turn, and as such the wheelbase error can be found by considering that e_b is the percentage error of the actual wheelbase to the nominal.

$$\frac{b_{actual}}{90°} = \frac{b_{nominal}}{(90° - \alpha)} \qquad \textbf{Eqn. [4-5]}$$

$$b_{actual} = \left(\frac{90°}{90° - \alpha}\right) b_{nominal}$$

as $$e_b = \frac{b_{actual}}{b_{nominal}},$$

then $$e_b = \left(\frac{90°}{90° - \alpha}\right) \qquad \textbf{Eqn. [4-6]}$$

4.6.2 TYPE B Errors

The difference in wheel diameters contributes significantly to TYPE B errors. If the robot travels in a curve to the left when moving forward, this will cause it to rotate further than intended on the anti-clockwise trial, but not far enough on the clockwise trial as shown in Figure 4-13.

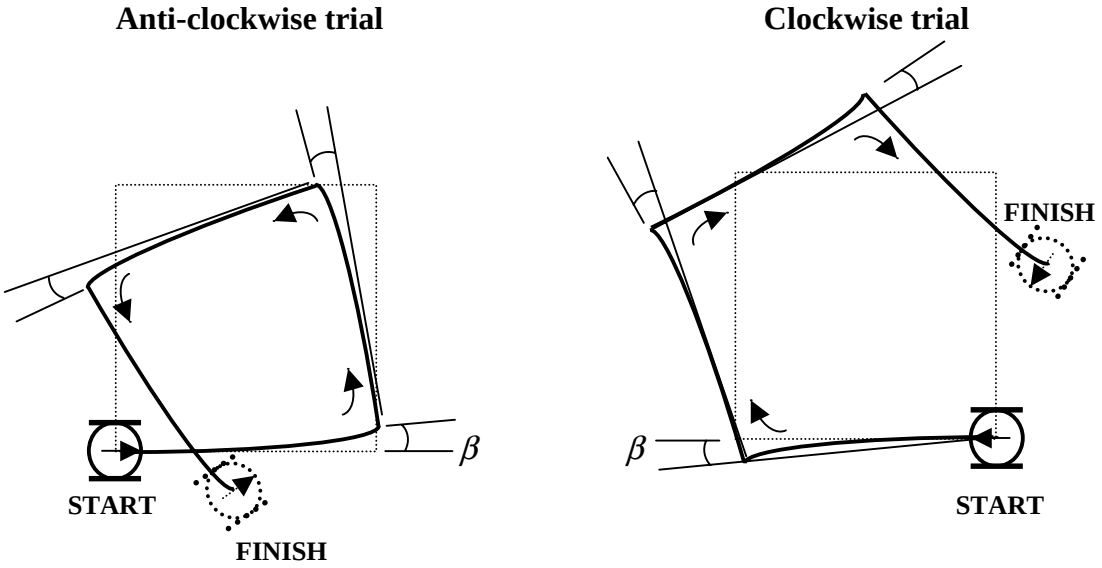

Figure 4-13: TYPE B errors increase the total amount of rotation in one direction, but reduces it in the other

The orientation error, β, can be calculated (in degrees) as follows:

$$\beta = \left(\frac{x_{cw} - x_{acw}}{-4L} \right) \frac{180^\circ}{\pi} \qquad \textbf{Eqn. [4-7]}$$

The radius of curvature, *R*, of the path is:

$$R = \frac{L/2}{\sin(\beta/2)} \qquad \textbf{Eqn. [4-8]}$$

So the ratio between the diameters of the right wheel, D_R, and the left wheel, D_L, is found from *R*:

$$e_d = \frac{D_R}{D_L} = \frac{R + b/2}{R - b/2} \qquad \textbf{Eqn. [4-9]}$$

where e_d = error ratio between right and left wheels

b = wheelbase of robot

Taking these factors into consideration and adjusting for the errors in software, the accuracy of the odometry system can easily be improved ten times or more.

4.7 REDUCTION OF ODOMETRIC ERRORS

There are several factors that influence the accuracy of odometry readings for position sensing. The following are guidelines that should be considered when designing a mobile robot.

- Castors should bear as little weight as possible, especially when the robot is accelerating or decelerating. If the centre of gravity is kept as low as practically possible, the drive wheels are less likely to lose traction under load and cause errors.

- If pneumatic tyres are used, they should be kept with ample pressure, reducing their compressibility and hence the chance of the diameter being reduced or becoming unequal.

- The wheelbase of a differential drive robot should be kept to a minimum. The probability of orientation errors occurring is higher with a large wheelbase than with smaller wheelbases. The smaller the wheelbase, the higher the torque required to execute a turn and as such, the size can be limited by the power of the driving motors.

- If the odometers are mounted to the driving wheels then wheel slippage must be avoided. If the driving motors are powerful enough to cause the wheels to lose traction under acceleration, then the acceleration of the device should be limited to ensure that this does not occur.

- The odometry equipment should be of a suitable accuracy. If the odometers are mounted directly to the driving wheels will the resolution provided be sufficient for accurate control? The odometers on MARVIN are mounted to the driving motors, taking advantage of the reduction ratio of the gear train to increase the resolution.

5. MOTOR THEORY AND CONTROL

The motors used in the drive train of the robot are 24V DC motors, originally intended for use in an electric wheelchair. They are manufactured by Dynamic Mobility in Christchurch and have a single worm gearbox incorporated in the motor housing.

5.1 MODEL OF THE DC MOTOR

A basic model of a DC motor can be considered as a large number of current carrying wire loops in the presence of a magnetic field. The magnetic field generated between the two poles of a permanent magnet and creates a force, *F(t)*, which acts on each of the current loops according to the Lorentz law (Equation [5-1]), in the direction determined by the "Right-hand rule".

$$F(t) = B\, l\, I(t) \qquad \textbf{Eqn. [5-1]}$$

where B = magnetic field flux density

l = length of wire loop

$I(t)$ = current flowing in wire loop

The right-hand rule states that if the fingers of the right hand are pointed in the direction of the magnetic field with the thumb in the direction of current flow, the palm will be facing in the direction of the force. The opposite sides of the wire loop therefore have forces acting on them in opposite directions, inducing a torque as shown in Figure 5-1. The torque generated increases linearly with current by the relationship:

$$T = K_t\, I(t) \qquad \textbf{Eqn. [5-2]}$$

where K_t = the torque constant

T = induced torque

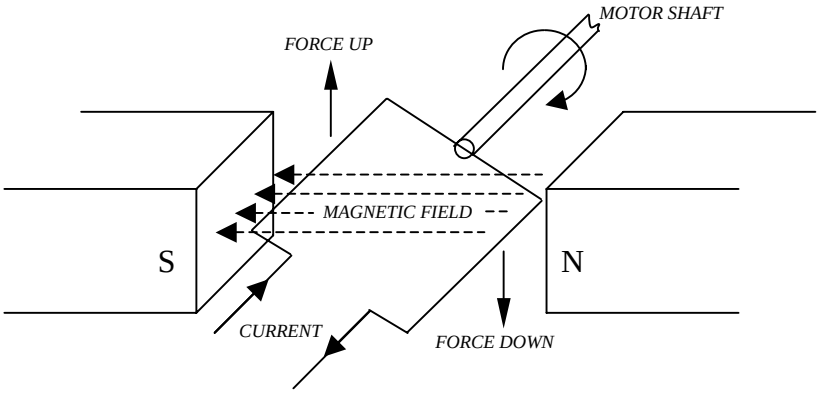

Figure 5-1: An illustration of the torque generated on the motor shaft due to the force acting on the armature

As the motor shaft rotates, the motion of the loop through the magnetic field causes a voltage to be induced which opposes the motor current. This voltage is called the **back emf,** e_b. The multiple coils of the motor result in a smooth back emf voltage, which is dependent only on the speed of the armature.

$$e_b = K_e \, \omega_a \qquad \textbf{Eqn. [5-3]}$$

where K_e = back emf constant

ω_a = angular velocity of armature

K_e is numerically equivalent to the torque constant, K_t, when SI units are used. When the current is kept constant, the armature voltage consists of the back emf and the voltage drop across the armature resistance.

$$e_a = i_a R + e_b \qquad \textbf{Eqn. [5-4]}$$

where e_a = armature voltage

i_a = armature current

R = armature resistance

5.2 ELECTRICAL MODEL OF A DC MOTOR

A permanent magnet DC motor can be represented electrically as the following model:

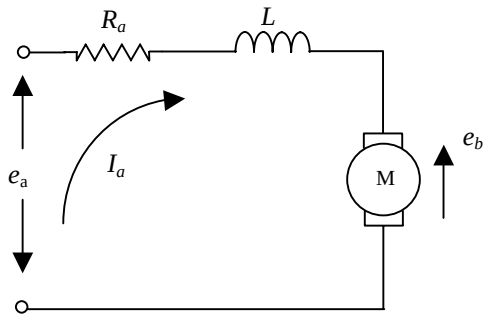

Figure 5-2: Electrical model of a DC motor

Analysis of the above current loop yields the electrical equation of a DC motor:

$$e_{in} = R_a I_a + L\frac{dI_a}{dt} + e_b \qquad \textbf{Eqn. [5-5]}$$

where R_a = armature resistance

I_a = motor current

L = armature winding inductance

e_b = back emf voltage

If we define J_m as the combined moment of inertia for the motor and load, and allowing for the friction torque of the system, then by Newton's second law we can state that:

$$T_m = J_m\frac{d\omega_m}{dt} + T_f \qquad \textbf{Eqn. [5-6]}$$

where T_m = motor torque

ω_m = rotation speed at shaft

T_f = fiction torque

The friction torque component is dependent on angular velocity and can be defined as:

$$T_f = B_m\omega_m \qquad \textbf{Eqn. [5-7]}$$

where B_m = the viscous friction

5.3 MOTOR CONTROL

In order to control the motors of the robot more efficiently it is necessary to calculate their transfer function. To achieve this the equations developed earlier in the chapter must be converted from the time to the frequency domain (*s*-domain). The following equations are produced:

From Eqn [5-2]:

$$T_m(s) = K_t I_a(s) \qquad \textbf{Eqn. [5-8]}$$

From Eqn [5-3]:

$$E_b(s) = K_e \Omega_m(s) \qquad \textbf{Eqn. [5-9]}$$

From Eqn [5-5]:

$$E_a(s) = LsI_a(s) + RI_a(s) + E_b(s)$$

$$I_a(s) = [E_a(s) - E_b(s)]\left(\frac{1}{R + Ls}\right) \qquad \textbf{Eqn. [5-10]}$$

By rearranging these equations and substituting for $I_a(s)$, the following velocity transfer function is found:

$$\frac{\Omega_m(s)}{E_a(s)} = \frac{K_t}{RB_m + K_e K_t + RB_m(\tau_m + \tau_e)s + RB_m \tau_m \tau_e s^2} \qquad \textbf{Eqn. [5-11]}$$

This formula can be further simplified if the armature inductance is small or the motor inertia is large (as is the case with MARVIN), in which case the assumption that $\tau_e = 0$ can be made. The simplified version of the velocity transfer function is:

$$\frac{\Omega_m(s)}{E_a(s)} = \frac{K_s}{1 + \tau_s s} \qquad \textbf{Eqn. [5-12]}$$

where $K_s = \dfrac{K_t}{RB_m + K_e K_t} =$ simplified gain

$\tau_s = \dfrac{RJ_m}{RB_m + K_e K_t} =$ simplified time constant

as $$\tau_m = \frac{J_m}{B_m}$$

The planetary gear head attached to the motor's shaft acts as a speed reducer, increasing the torque of the system. The reducer changes the mechanical resistance of the load so that the motor experiences less friction torque, but the added load on the shaft will slow the motor's response, increasing the mechanical time constant, τ_m. If N_1 is the number of teeth on the gear head, with N_2 the number of teeth on the wheel, then the speed of the load (or wheel) can be computed as:

$$\omega_w = \left(\frac{N_1}{N_2}\right)\omega_m \qquad \textbf{Eqn. [5-13]}$$

Therefore the torque seen at the wheel is:

$$T_w = \left(\frac{N_2}{N_1}\right)T_m \qquad \textbf{Eqn. [5-14]}$$

where ω_w = wheel speed

T_w = wheel torque

The total inertia and friction combine to produce the mechanical time constant for the system:

$$J_T = J_m + \left(\frac{N_1}{N_2}\right)^2 J_L \qquad \textbf{Eqn. [5-15]}$$

$$B_T = B_m + \left(\frac{N_1}{N_2}\right)^2 B_L \qquad \textbf{Eqn. [5-16]}$$

$$\tau_T = \frac{J_T}{B_T} \qquad \textbf{Eqn. [5-17]}$$

where J_T = total inertia

B_T = total friction

τ_T = total torque

J_L = load inertia

B_L = load friction

The block diagram for the motor, gearing and load is illustrated in Figure 5-3 below:

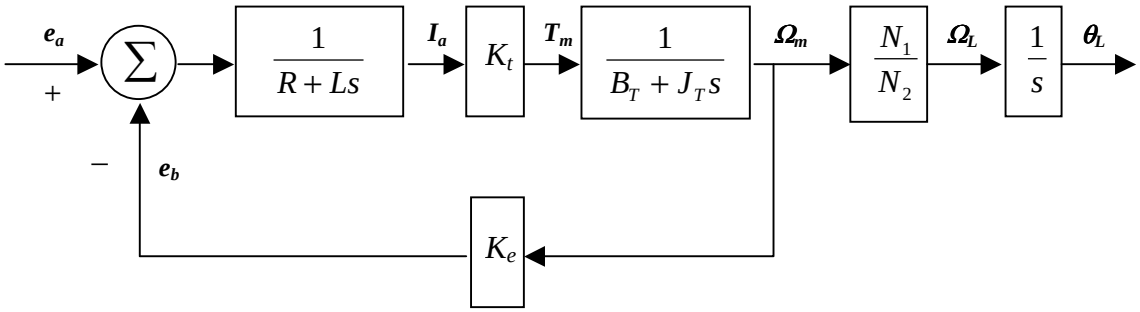

Figure 5-3: Block diagram of the DC motor

where e_a = armature voltage

e_b = back emf

I_a = motor current

T_m = motor torque

Ω_m = shaft speed

Ω_L = load speed

θ_L = load position

The transfer function for the entire system can be derived from Equation [5-11] if B_m is replaced with B_T, J_m with J_T and τ_m with τ_L and the gearing is accounted for by multiplying by N_1/N_2.

$$\frac{\Omega_m(s)}{E_a(s)} = \left(\frac{K_t}{RB_T + K_eK_t + RB_T(\tau_T + \tau_e)s + RB_T\tau_T\tau_e s^2} \right)\left(\frac{N_1}{N_2} \right)$$

Eqn. [5-18]

5.4 MOTOR PARAMETERS

The specifications of the motors used on MARVIN need to be calculated experimentally as the manufacturer's data sheets are not available. The armature resistance of the motor is measured with a multi-meter across the terminals and is R = 1.5 Ω. The inductance, L, of the motor is found to be 0.45 mH.

K_e, the back emf constant, is calculated by running the motor as a generator and measuring the voltage produced relative to the speed. The relation in Equation [5-3] gives a K_e value of 4.34 V/krpm, which is equal to the torque constant, K_t with units of Nm/A or V s/rad.

The mechanical time constant, τ_m, is computed graphically from the step response of the motor. τ_m is defined as the time the motor takes to reach 63.2% of its maximum speed when a step input is applied to the terminals. This is found to be 0.195s from Figure 5-4 where the maximum speed ω_{max} = 4330 rpm.

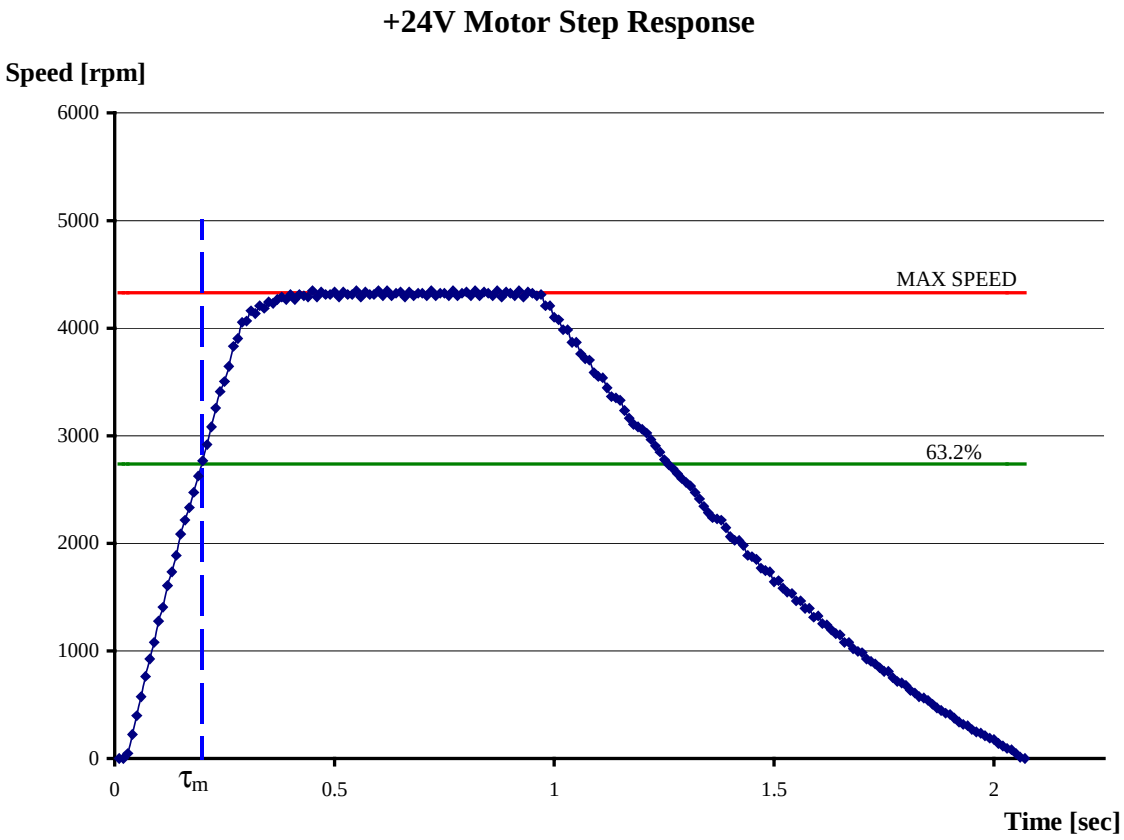

Figure 5-4: Calculation of the mechanical time constant.

The breakaway, or friction torque, is calculated from the starting current, I_{as}, that is, the current required to overcome the torque caused by static friction and the inertia of the system. I_{as} is found experimentally to be 1.2 A. The motor will draw current when there is no load on the shaft due to losses through the bearings, brush friction, eddy currents and air gap flux densities. This no load current can be measured with an ammeter in series, and has the value I_{a0} = 1.75 A at a no load speed, ω_0, of 4330 rpm. The friction

torque of the system, is calculated using Equation [5-2] and has the value T_f = 5.21 Nm, which acts against the armature torque.

The maximum current of the system is 5A, from which the maximum torque of the motors can be calculated by:

$$T_m = K_t I_a - T_f \qquad \textbf{Eqn. [5-19]}$$

Therefore,

$$\begin{aligned} T_{\max} &= K_t I_{\max} - T_f \\ &= (4.34)(5) - 5.21 \\ &= 19.10 \text{ Nm} \end{aligned}$$

Also the power, P, of the motors is computed using:

$$P = \omega T_m \qquad \textbf{Eqn. [5-20]}$$

$$\begin{aligned} P_{\max} &= \omega_{\max} T_{\max} \\ &= (4.330)(19.10) \\ &= 82.68 \text{ W} \end{aligned}$$

where P_{max} = maximum power of the motors

For an accurate analysis of the motors to be performed, the exact loading must be known, as any load on the motors will effect the values of the above parameters. The exact load experienced by each motor is difficult to measure during operation, as such, the parameters calculated above are all taken from the motor under “no-load” conditions. This provides a point of reference for comparison with alternative motors.

5.5 PHYSICAL MOTION OF THE ROBOT

5.5.1 Turning

In the majority of circumstances MARVIN will encounter in its environment, the required turning angle is a multiple of 90°. Once the robot can execute a 90° turn it can then turn left, right and turn to face the direction from which it has come. To achieve the turn, each of the driving wheels must travel a distance equal to one quarter of the circumference of the robot, C_{rob}, in opposite directions as illustrated in Figure 5-5.

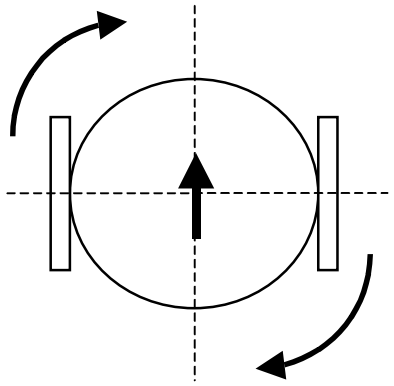

Figure 5-5: Each driving wheel must travel C_{rob} / 4 to turn 90°.

The circumference C_{rob} is calculated from the circle with a diameter equal to the wheelbase of the robot, $b_{nominal}$. To convert this distance into a specific number of motor revolutions, the circumference of the driving wheels must be calculated and used along with the total reduction ratio, N, of the motor gearing, as calculated in Equation [2-1].

The diameter of the driving wheels, $D_{R,L}$ = 335mm, so the circumferences of the wheels, $C_{R,L}$ = 1052.4 mm. Therefore:

$$1\ \text{rev}_{\text{motor}} = C_{R,L} / N \qquad \textbf{Eqn. [5-21]}$$

$$= 20.41\text{mm of travel for the robot}$$

As there are 512 pulses on the encoder module per motor revolution, the resolution of the odometers is 0.04mm per pulse.

5.5.2 Acceleration

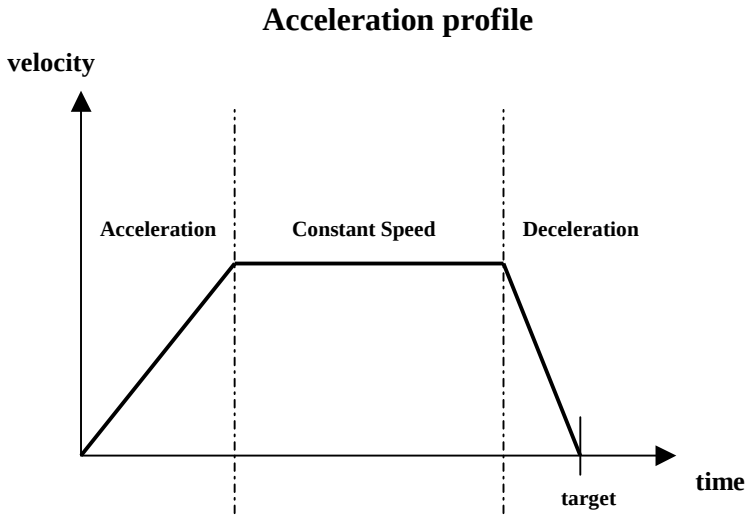

Figure 5-6: Required acceleration profile to reach a target position

In order for MARVIN to travel in a straight line to a target position, it is necessary for it to follow an acceleration profile as illustrated in Figure 5-6 above. The most efficient profile requires the robot to accelerate to a desired speed, maintain that speed for a required distance, and then decelerate to a stop at the specified target position.

The acceleration of the device to a desired speed follows a complex curve, but if the step responses of are analysed some simplifications can be made. The time taken for MARVIN to reach its maximum speed varies from 0.56 to 1.36 seconds depending on the set PWM value. In this time the robot could cover a distance between 20 and 90 cm. Due to the physical characteristics of the device and the maximum power that the driving motors can provide, wheel slippage is not a limiting factor of its acceleration.

Figure 5-7 shows the velocity profiles generated by the mechatron in response to a variety of step inputs. This clearly illustrates the motion of the robot under acceleration, as it reaches a steady-state speed dependant on the input PWM value. The deceleration of the device is purely frictional, achieved by removing power from the driving motors and allowing it to coast to a stop. Irrespective of the set PWM value, the robot decelerates at the same constant rate, A_o.

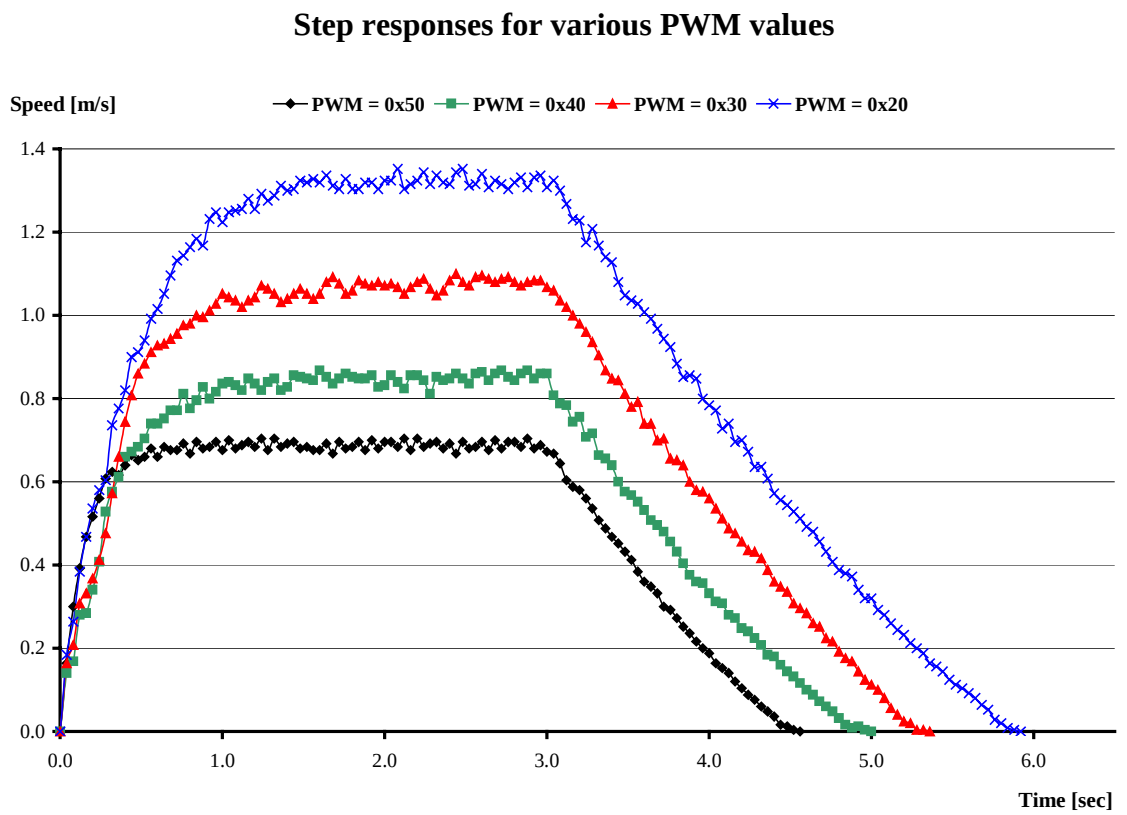

Figure 5-7: Robot step responses for various PWM values

5.5.3 Braking

This deceleration constant is calculated from the above graph to be, A_o = -0.445m/s^2. If MARVIN is travelling in a straight line at the maximum velocity of v_{max} = 1.32m/s and decelerates to a stop, the distance covered in doing so is:

$$t_{dec} = \frac{-v_{\max}}{A_o} \qquad \textbf{Eqn. [5-22]}$$

$$= \text{-1.32 / -0.445}$$

$$= 2.97 \text{ s}$$

$$x_{dec} = v_{\max} t_{dec} + 0.5 A_o t_{dec}^2 \qquad \textbf{Eqn. [5-23]}$$

$$= 1.32(2.97) + 0.5(-0.445)(2.97)^2$$

$$= 1.96 \text{ m}$$

where t_{dec} = time to decelerate to a stop

x_{dec} = distance covered in decelerating to a stop

It is undesirable for the robot to have such a large stopping distance. IRED position sensitive devices (PSD) have been implemented as the sensors used to detect objects that lie in the path of the device. The variation in the reflectivity of the surfaces MARVIN is likely to encounter in its immediate environment, limit the accuracy of these sensors to within 0.35m (the reasons for which are explained in further detail in Section 4.3). As the IRED sensors are used to detect obstacles in the immediate path of the device, it is necessary for MARVIN to be able to stop from full speed within 0.35m in order for it to avoid collision with possible hazards.

To achieve this there are two options, the first is to reduce the maximum speed of the robot thus reducing the distance taken to stop. This method reduces the performance of the device and is also impractical as the required value for v_{max} would be in the region of 0.5m/s, which is far below the required speed in the initial design specifications. The second is to introduce a form of braking to increase the deceleration constant of the robot. This is the more desirable option, as it does not compromise performance to the same extent.

There are many different ways in which the braking of a dynamic system can be implemented:

- Regenerative braking utilises the current generated by the decelerating motor, by feeding it back into the system where it can be used to recharge the batteries if required.
- Dynamic braking also uses the stored mechanical energy of the motor, but instead of returning the current to the system, the energy is dissipated as heat through braking resistors or even through the motor itself, as a decelerating torque is temporarily produced by the generator action of the motor.
- Mechanical friction braking is the simplest of the variations to implement, as it involves a slowing of the motor by physically hampering its rotation. This method can be achieved in a number of ways.

Both the regenerative and dynamic systems can be complicated to implement and may add additional stress to the motors. The system chosen for MARVIN is a slightly

developed version of that present on the original electric wheelchair system and is a form of mechanical friction braking.

The system consists of an electromagnet, which is used to raise the brake pad off the worm drive to release the brake. When the current to the magnet is removed, a strong spring pushes the pad down onto the helical worm and, due to the gear reduction ratio of the entire drive system, produces enough of a decelerating torque to act as an effective brake. This system of braking is illustrated in Figure 5-8.

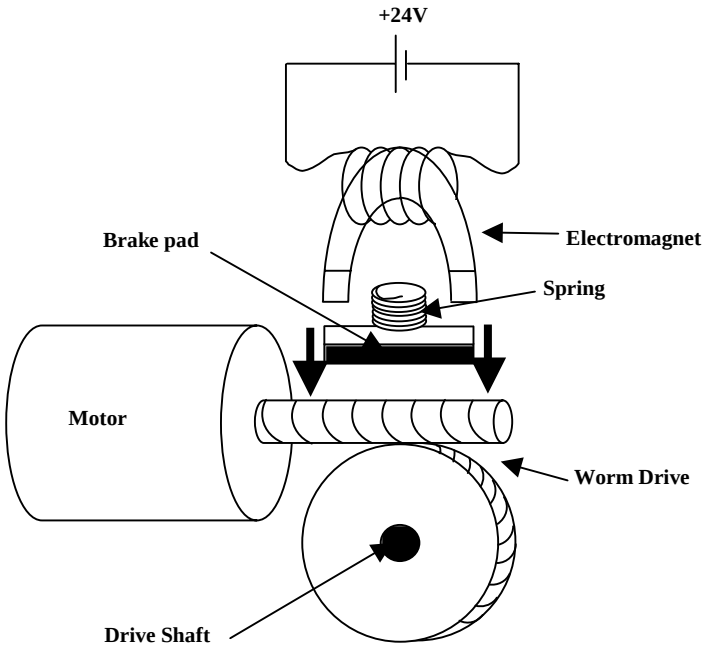

Figure 5-8: Mechanical brake system acting on the worm drive of the motor

In this arrangement, the electromagnet must hold the brake off the helical gear any time the motor is being driven. The force on the brake produced by the spring is so great that there must be at least 20V on the electromagnet's coil before the brake is released and the coil draws a constant current of 1.35A at 24 volts. These values highlight the inefficiencies of this method, but the system produces a very strong brake as shown by the increased deceleration constant, illustrated in Figure 5-11.

The actual components of the braking system are shown in Figures 5-9 and 5-10 below:

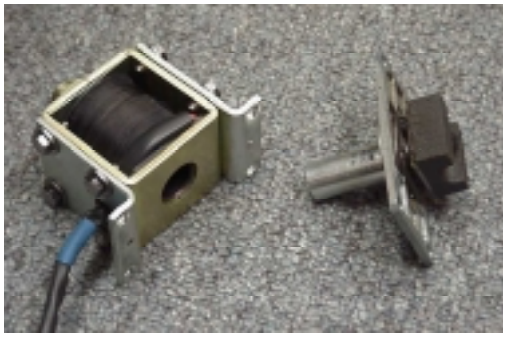

Figure 5-9: Brake assembly with electromagnet, left, and brake pad, right.

Figure 5-10: Brake mounted onto the motor gearbox.

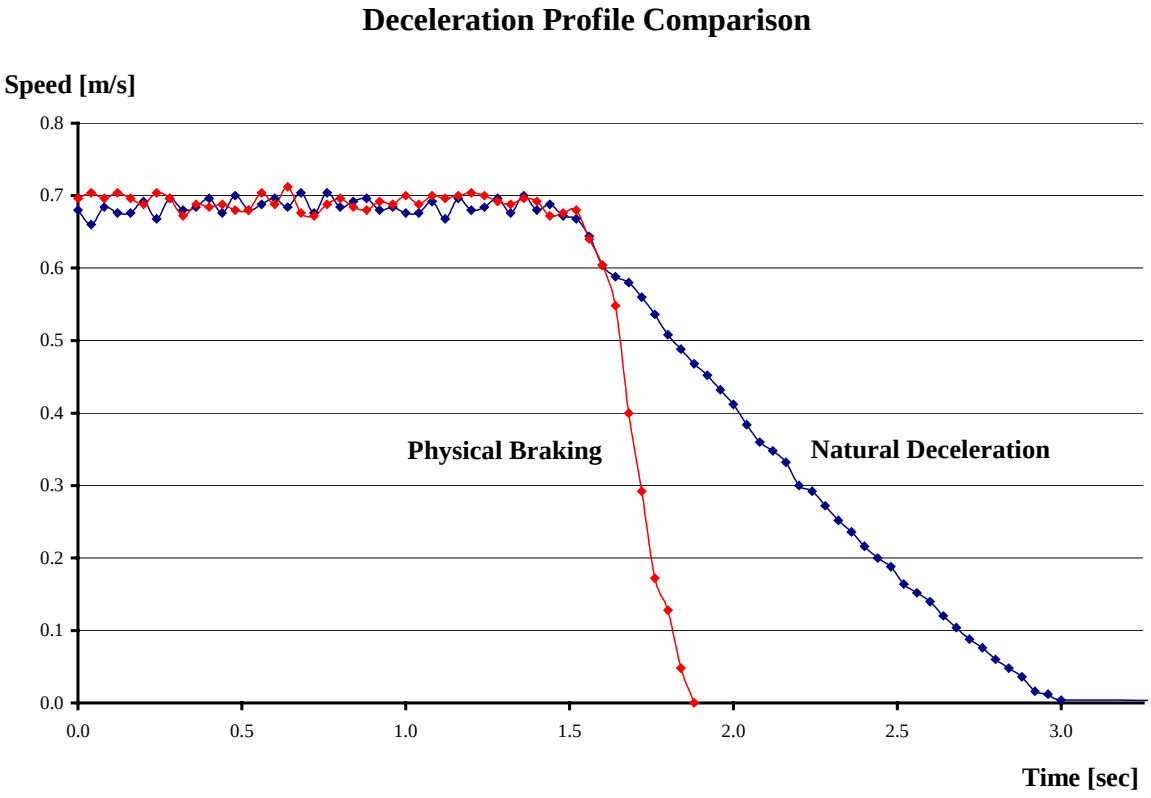

Figure 5-11: Deceleration profile comparison between physical braking and the natural deceleration of the mechatron, illustrating the increase in A_o

The new value for A_o can be calculated from Figure 5-11 and is found to be –2.38m/s^2. With this new value, the distance covered by the robot in decelerating from v_{max} to a stop is calculated as:

$$t_{dec} = 0.555\text{s}$$

$$x_{dec} = 0.366\text{m}$$

The distance taken to stop from v_{max} is still greater than the range of the IRED sensors, but if v_{max} is reduced to 1.25m/s, x_{dec} becomes 0.33m and the specifications for the robot's speed are met.

The electronics to control the brake are very simple. A transistor is placed between the inductor of the electromagnet and ground, as shown in Figure 5-12, this transistor must be able to cope with a continuos drain current of 1.5A.

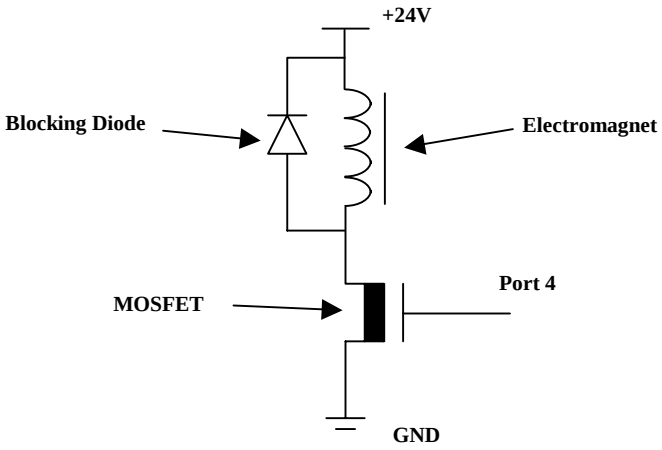

Figure 5-12: Schematic of the brake electronics

As the source of the n-type MOSFET is coupled to ground, the gate only requires a 5V input to achieve a gate-to-source voltage greater than the threshold voltage. This 5V control signal is sourced directly from the 87C552 microcontroller's Port 4. The brake can now be controlled in software, being released before the motors are switched on and applied as soon as they are switched off. A blocking diode is placed over the terminals of the coil to prevent large voltage spikes from occurring when the brake is released.

5.6 CONTROL SOFTWARE

The characteristics of the robot's movement are used to produce equations that will ensure the acceleration curve is followed to its target destination. It is noted that the device can have an inconsistent heading when the motors are started with a high target speed. This problem is overcome by starting the motors at a slower, more controlled speed, then ramping them up to the faster desired speed.

Many of the control functions for MARVIN are similar to those used in the earlier mechatronics projects conducted with the micromouse at the University of Waikato. The initialisation of the microprocessor to enable it to receive odometry information, analyse IRED values and send or receive serial transmissions are all conducted through the use of the *MARVINlib.h* library file. This is a modified version of *Mouselib.h* developed by S H Su [8]. A full listing of *MARVINlib.h* is included in Appendix B.

5.6.1 Interrupt Code

The total distance covered by each driving wheel of the device and the speed at which they are currently travelling is all calculated in one of the Timer 2 compare interrupts of the 87C552. The interrupt is configured in the *timers2_init* function of the *MARVINlib.h* library file, to be triggered every ten milliseconds, and the following code is executed:

```
1    s_rgt = shaft_encoder(1);            //counts since last interrupt
2    s_lft = shaft_encoder(0);
3    count_rgt = count_rgt + s_rgt;       //running count of distance
4    count_lft = count_lft + s_lft;
5    P1b.B5 = FALSE;      P1b.B5 = TRUE;  //reset timer T2
6    CMI2 = FALSE;                        //reset interrupt flag
```

Figure 5-13: Interrupt code for Timer 2 interrupt

The interrupt calls the function *shaft_encoder* from the library file on lines 1 and 2, which returns the number of counts from the shaft encoders since the last interrupt. This can be used as a representation of the motor's speed in units of counts per 10 milliseconds.

count_lft and *count_rgt* are used on lines 3 and 4 to record the total number of counts received from the shaft encoders, which is used as a measure of the total distance traveled since the variables were last reset.

5.6.2 Straight Drive Control

The information from the interrupt routine is used in conjunction with the deceleration constant (calculated from Figure 5-11) to ensure the robot travels in a straight line and stops at the target destination. As the rate of deceleration is the same regardless of the speed the device is travelling, it is possible to calculate the time and distance covered in decelerating to a stop, x_{dec}, using Equations [5-22] and [5-23].

If the distance to stop is subtracted from the desired displacement, the distance required for the motors to drive, x_{drive}, is obtained. This calculation can be performed repeatedly, using the current speed of the robot as it accelerates, thus eliminating the need to linearise the acceleration curve. If the x_{drive} is reached while accelerating, the motors will simply be shut down as if it were travelling at a constant speed.

The following code segment performs this operation using Equations [5-22] and [5-23] given the target distance, *dist*, and required *speed* inputs.

```
1    Ao_straight = 2.38;              //deceleration constant
2    dist = dist * 25086;             //convert from metres to pulses
3    x_drive = dist;                  //initially set x_drive to max
4    while(count < x_drive)
5    {
6       count = (count_lft + count_rgt)/2;  //average dist covered
7       rgt_motor = speed;                  //set motor speeds
8       lft_motor = speed;
9       P4 = 0x35;
10      ave_speed = ((s_lft + s_rgt)/2)/250;//average speed in m/s
11      t_dec = ave_speed/Ao_straight;
12      x_dec = ave_speed*t_dec – 0.5*Ao_straight*(t_dec)^2;
13      x_drive = dist – x_dec;       //update x_drive
14   }
```

```
15    P4 = 0xCF;                        //stop motors and apply brakes
16    rgt_motor = 0xFF; lft_motor = 0xFF;    //reset PWMs
17    time = (t_dec * 110250);          //change seconds to delay units
18    delay(time);                      //allow robot time to stop
19    count_lft = 0; count_rgt = 0;           //reset count variables
```

Figure 5-14: Segment of code from straight drive function

Line 2 converts the target speed from units of metres to counts per second, to enable calculations to be made directly from the odometry data. The "while" loop will repeat the operations between lines 5 and 14 until the device has traveled a distance equal to x_{drive}. The variable *count* keeps a running tally of the total distance covered as an average of the distance each wheel has covered individually by using the variables from the interrupt routine. Once the motors have been set to the desired PWM value, the brakes are released and the driver circuit is sent the command to drive the motors forward via Port 4 of the '552 (line 9).

The average speed of the driving wheels is used to compute t_{dec} and x_{dec} on lines 11 and 12, as calculated in Equations [5-22] and [5-23]. This information is the used in the calculation of the updated value for x_{drive} (line 13), initially set to the target distance, which would be the value if x_{dec} equaled zero.

Once the robot has traveled a distance equal to x_{drive}, the driver circuit is shutdown and the brakes are applied (line 15). The PWM values are reset and the microcontroller sits idle for a time, t_{dec}, to allow the brakes time to bring the robot to a halt. This is accomplished using the *delay* function of the *MARVINlib.h* file, which computes 110250 delays per second (line 18).

For MARVIN to maintain a straight trajectory, both wheels must be travelling at the same speed. Due to irregularities between the motors, bearings, load distribution and tyre pressures, the wheels may travel at different speeds despite the controller applying equal PWM values to both. To monitor the actual motor speed, the odometry information is used as feedback in a closed control loop.

The input voltage applied causes the motor to turn and, as a result, the shaft encoders return a value for the motor speed. The difference between the desired speed and that returned by the encoders is the error. This is used to adjust the input voltage until the set speed is achieved and should conditions change while the robot is in motion, the controller will maintain the speed at the required value. This is an example of simple proportional control as illustrated in Figure 5-15.

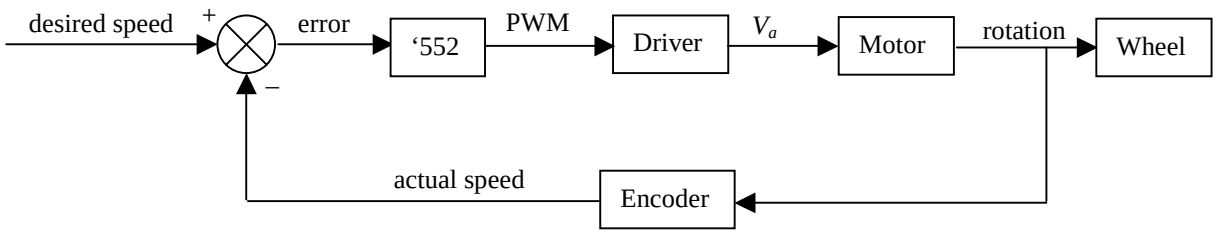

Figure 5-15: Block diagram for the proportional controller

In order for this proportional control to be effective, it is necessary to develop a relationship between the value for speed returned by the odometers and the PWM settings. If the desired speed is different from the actual speed, the error must be translated to a relevant hexadecimal value to be subtracted from the motor's PWM input. By plotting the speed of the device at various PWM settings a trend can be observed, as shown in Figure 5-16.

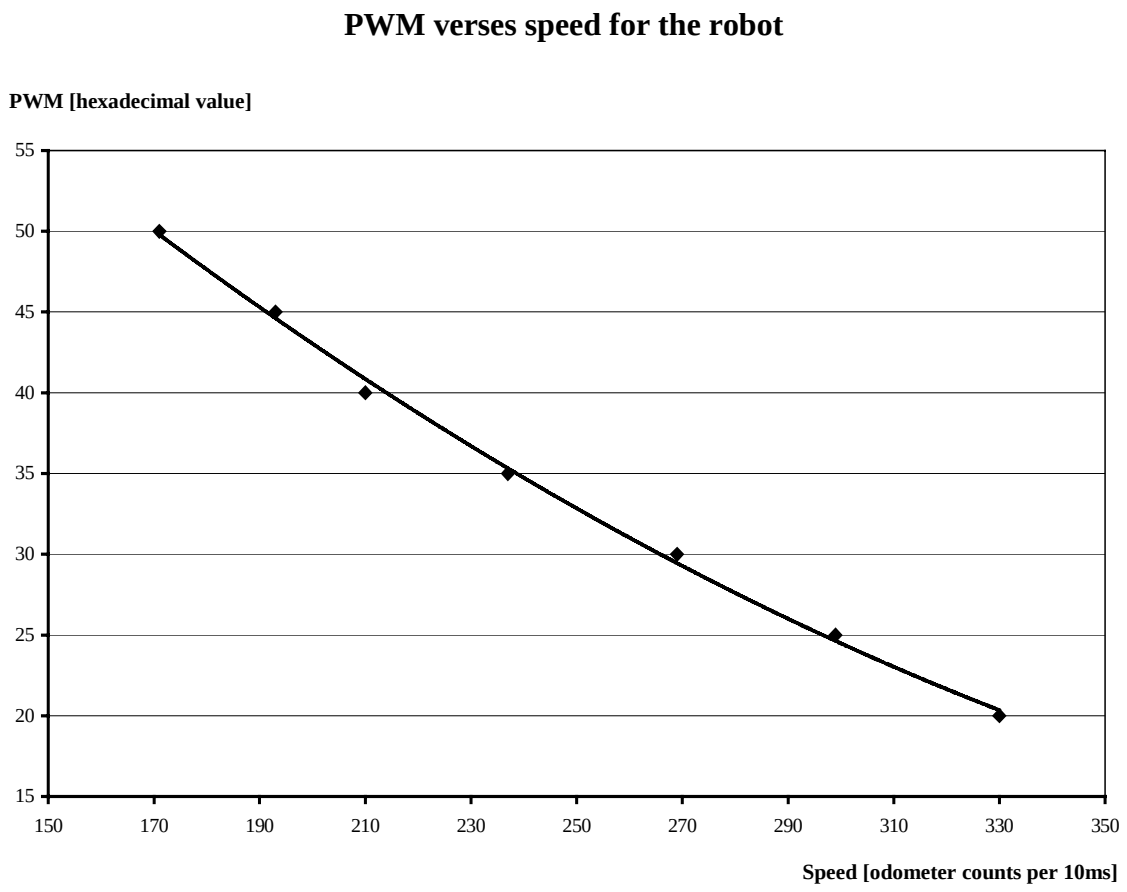

Figure 5-16: Trendline used to produce a hexadecimal PWM representation of motor speed

Microsoft Excel© is used to plot the data and add a polynomial trendline. From the trendline an equation for the relationship between motor speed and the PWM input can be retrieved. This polynomial equation is implemented in the control algorithm to adjust the PWM motor input so that it incorporates an error component. The error value is multiplied by the proportional gain constant, K_p, which can be varied to maximise the performance of the device. This improves the stability of the motor by reducing the effect of the error value on the input, allowing the motor's speed to settle more rapidly.

The equation for this relationship is as follows:

$$y = 0.0004x^2 - 0.369x + 102.18 \qquad \textbf{Eqn. [5-24]}$$

where x = motor speed in counts per 10 milliseconds

y = PWM value input to the motor

Below is a flow diagram for the straight drive function:

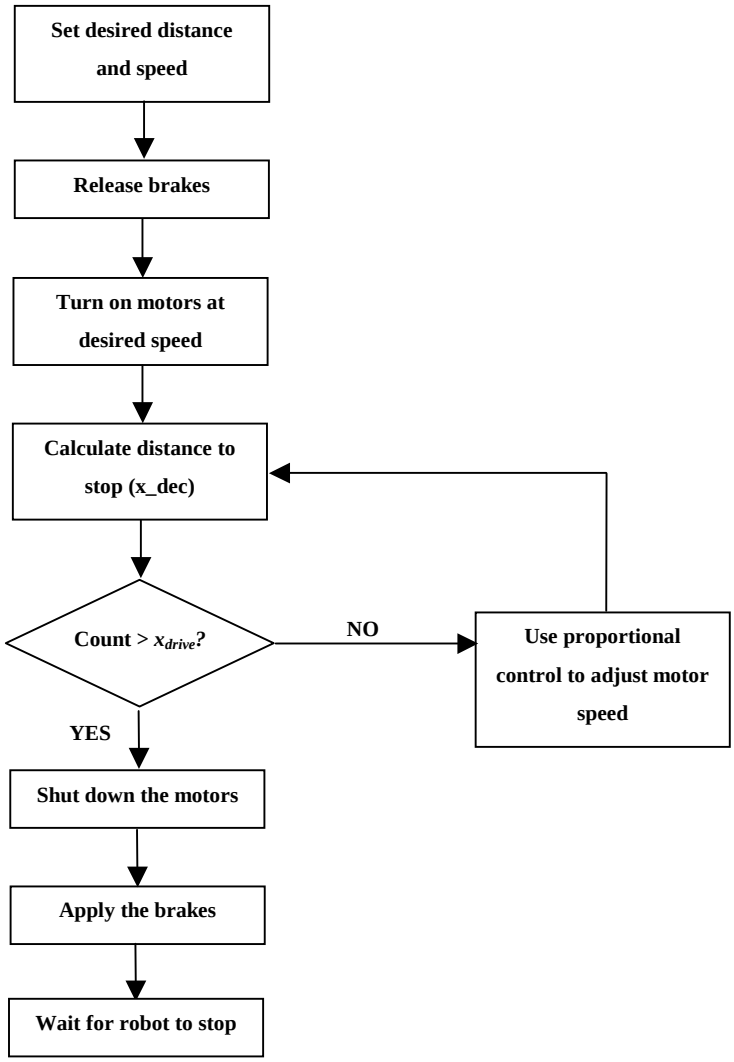

Figure 5-17: Flow diagram for straight drive function

The following code segment can be placed in the "while" loop of the straight drive function in place of lines 7 and 8 of Figure 5-14, to ensure both motors are running at the correct speed:

```
 7    speed_lft = 0.0004*(s_lft)^2 – 0.369*s_lft + 102.18;
 8    speed_rgt = 0.0004*(s_rgt)^2 – 0.369*s_rgt + 102.18;
 9    lft_motor = speed + (speed - speed_lft)*Kp;  //proportional control
10    rgt_motor = speed + (speed - speed_rgt)*Kp;
```

Figure 5-18: Code segment to implement proportional control

Lines 7 and 8 implement the polynomial relationship defined in Equation [5-24], which converts the speed from the odometers to a PWM value. The proportional control is executed in lines 9 and 10, where *(speed - speed_lft)* and *(speed - speed_rgt)* are the error values used to implement the closed loop feedback of Figure 5-15.

5.6.3 Turning the Robot

The function developed to turn MARVIN has two inputs, the speed at which to turn and the angle it is to turn through. This function is similar in many ways to the straight drive function although some of the characteristic values for the robot's motion are different due to the physical nature of the system. The inertia of driving straight from a stationary beginning is greater than that of the stationary robot executing a turn on the spot. This variation is illustrated by the difference in the step responses for the turning and straight drive in Figure 5-19.

Figure 5-19: Turning and straight drive step responses for PWM = 0x50

The differences in the accelerations are not as obvious as the effect on the maximum speed of the robot. The speed is reduced due to the tyres being forced to slip as they rotate, the effect of this additional force is dependent on the surface the device is on at the time. This can make the response of the device unpredictable and so, to reduce the likelihood of errors, the speed at which the device is to complete the turn is set at a PWM value of 0x50 (corresponding to a turning velocity of 0.6m/s). At this speed the motors will reach their top speed in time to complete a 90 degree turn, eliminating the need to allow for the non-linear acceleration profile. This makes the movement of the device more controllable and also simplifies the control algorithm as t_{dec} and x_{dec} do not need to be repeatedly calculated and can be set as constants.

The values for t_{dec} and x_{dec} are calculated using Equations [5-22] and [5-23] as before, and are found to be:

$$t_{dec} = 0.252\text{s}$$
$$x_{dec} = 0.076\text{m}$$

Another consideration is that both wheels will not necessarily complete their turn at the same time. If, for example, one wheel is on carpet at the beginning of the turn while the other is on linoleum, then one wheel will complete the turn before the other. To account for this, the function must ensure that both wheels have completed the turn before it stops. This will involve applying the brakes at different times so that the correct value of A_o is used in the calculations (if the wheel finishing first is left to coast to a stop, a larger value of A_o must be used or it will travel too far). Once both motors have been stopped the turn is completed and the robot can continue on with its task.

Below is a segment of the code from the turning function:

```
1    Ao_turn = 2.38;            //deceleration constant for a turn
2    right = 0;     left = 0;   //flags to signal completion of turn
3    switch (angle)
4    {
5       case 90:  dir = 0x36;   dist = 9850;      break;
6       case 180: dir = 0x36;   dist = 19700;     break;
7       case 270: dir = 0x39;   dist = 9850;      break;
8    }
9    rgt_motor = 0x50;    lft_motor = 0x50; //set speed to turn
10   t_dec = 0.25
11   x_dec = 0.08*25085;        //constant x_dec in # of pulses
12   x_drive = dist – x_dec;
13
```

```
13    /************ drive motors until turn is completed *************/
14    while(flag < 1)
15    {
16       P4 = dir;
17       if(count_rgt > x_drive) //stop right motor when C/4 traveled
18       {     P4 = 0x27;        //stop motor and apply brake
19             if (left > 0)     //check to see if left is finished
20             {     flag = 1; } //break loop if both motors finished
21             right = 1 };
22       if (count_lft = dist)   //stop left when done
23       {     P4 = 0x1D         //stop motor and apply brake;
24             if(right > 0)     //check if right is done
25             {     flag = 1 }; //stop if both motors done
26             left = 1; }
27       }
28    time = (t_dec * 110250);   //convert from seconds to delay units
29    delay(time);               //allow robot time to stop
30    count_lft = 0; count_rgt = 0;//reset count variables
```

Figure 5-20: Code segment from the turning function

This function accepts the angle at which to turn through as an input, either 90 (right turn), 180 or 270 (left turn), in degrees. The input angle determines the direction that each wheel will turn, for example, if MARVIN is to make a left turn, the right wheel will drive forward and the left will drive backward. The selection of distance and direction is achieved with the use of a "switch", between lines 3 and 8. The wheelbase of the robot is 500mm, therefore the circumference, C_{rob} = 1570.80mm. The distance required to execute a 90 degree turn is one quarter of this value, and is achieved by rotating each motor a distance equivalent to 9850 shaft encoder pulses.

The speed that the robot will turn is set at the hexadecimal value of 0x50, with t_{dec} and x_{dec} defined as constants on lines 10 and 11. The "while" loop is used to drive each motor a distance equal to x_{drive} independently to ensure both motors cover their target distance. This is implemented as two separate, nested "if" statements, lines 17 to 21 for the right motor and lines 22 to 26 for the left.

Once both motors have travelled x_{drive}, the microcontroller will sit idle for a time, t_{dec}, to give the wheels time to come to a halt (lines 28 and 29). The *count_lft* and *count_rgt* variables are reset and the microcontroller returns to the main program to complete its set task.

6. CONCLUSION

6.1 CAPABILITIES

MARVIN has been designed to operate as an effective mobile security device for indoor applications. If the robot is to be a suitable platform for such operations, it must meet the requirements as set out in Section 1.3.

The attributes for the device are divided into the following four categories:

6.1.1 Speed

The average walking pace of a human security guard is 1m/s, as such, this is set as the speed at which the device is to travel. At this speed the robot will complete its patrol of the office or warehouse in a reasonable amount of time.

MARVIN's drive train has been developed from that of an electric wheelchair. The 24V motors supply the driving wheels with sufficient torque to allow MARVIN to reach speeds in excess of 1.3m/s. In order to obtain more accurate control of the device, the maximum speed is limited to 1.25m/s, which translates to a PWM value of 0x26. At this speed the braking system can bring the robot to a halt in 0.53 seconds, over a distance of 0.33m. This is within the range of the IRED proximity sensors and consequently allows MARVIN to stop in time to avoid collision with a detected obstacle.

6.1.2 Physical Size

The physical size of the robot is to be suitable for the navigation of an indoor warehouse or office block environment. The chassis and frame are required to stand at the height of one metre, to provide future developments with a suitable base from which to operate. MARVIN stands at a height of 95cm when sitting on the driving wheels, with the Laser Range Finding assembly, which sits on top of the frame, adding further height to the device. The chassis and frame have been designed in such a manner as to permit future expansion, as required.

If the security device is to be the basis for future development, it needs it provide an adequate base from which future developments can operate. The base chassis of MARVIN measures 530mm by 560mm with the batteries of the power supply mounted between the wheels to create a low centre of gravity.

The weight of the device is specified to be at least 30kg to create enough inertia to negotiate fire doors and stabilise the robot once future developments are added. MARVIN weighs 49.6kg with the Laser Range Finder and associated electronics.

6.1.3 Manoeuvrability

MARVIN is manoeuvrable enough to navigate within the confines of an office or corridor, as the differential drive system makes it possible for a turn to be executed "on the spot". This system is simple to control due to the less complex mechanics involved, and the external dimensions of the device allow for a 360 degree turn to be completed within a circle of diameter equal to 771mm, well within the original specification of one metre.

The sealed lead-acid batteries of the power supply allow MARVIN to patrol its operating environment continually without recharging for 110 minutes. This is ample time for the device to complete a large patrol several times before recharging is required.

6.1.4 Flexibility

MARVIN has the capability to carry an additional payload of 50kg should any future developments be attached to the chassis. The driving motors employed in the device are powerful enough to support such loading for extended periods of time.

The chassis and frame have been designed with future development in mind and have been kept modular to a large extent. This allows for future improvements to be made with ease and without compromising the strength of the original design. The final design of the mobile device is shown below:

Figure 6-1: Complete assembly of MARVIN and Laser Range Finder

6.2 FUTURE WORK

MARVIN will be the basis for much research and development at the University of Waikato in the future. Appendages and improvements will be designed to allow the robot to operate a lift, open doors and automatically recharge the power supply as required. Much of this work can be designed and tested independently of the security device, but MARVIN will provide a basis for the implementation of such developments.

There is also some additional work to be performed on the security device before the basic robotic platform is complete:

- As the laser range-finding assembly developed by Shaun Hurd[7] is permanently attached to the frame of the security device, the Celeron PC motherboard requires modification in order for it to be powered by the supply from the robot's batteries.

- At present, the 87C552 Phillips microcontroller and the Celeron motherboard are totally independent of one another. In the future it is hoped that the PC motherboard will perform all of the mapping and control calculations due to its superior processing capability. To implement this the '552 must communicate with the PC either through serial or the more efficient parallel communication lines.

- Once the security device has the use of the laser range finder for primary obstacle detection, it will be possible for it to implement a mapping algorithm on its surroundings. Gary Brightwell[10] has developed the software necessary to construct a topographical map of a Mobile Autonomous Robot's environment with the use of a 360 degree laser range finder. This software can be implemented to allow MARVIN not only to create an accurate mapping of its immediate surroundings and identify its position, but also optimise its trajectory.

Initially this may be achieved primarily with the range finding assembly or with the assistance of active or passive beacons. The use of beacons is desirable when the environment is not very well defined and the immediate environment is subject to regular change. In such cases it is difficult for a reference point, such as a desk or wall, to be identified with the required precision to prevent the device from getting lost.

- The IRED sensors, shaft encoders and laser range finder can be developed so that each verifies and calibrates the others as necessary. The range finder can be used to minimise the effects of cumulative odometry errors by correcting any error in the representation of the distance travelled as calculated by the shaft encoders. The range finding assembly is only accurate from a distance of approximately 50cm and so the IRED sensors will be required to detect any objects that are closer to the device.

- The algorithms used by the robot to drive in a straight line for a specified distance and to execute 90 and 180 degree turns required further development and refinement to improve the performance of the security device. The functions written to perform straight drive and turning manoeuvres could be optimised for speed, as although functional, they could be made more efficient.

  As the Laser Range Finder was added late in the development of the device, little development has been done to incorporate the system into the control of MARVIN. There is scope for the device to exhibit limited intelligence by using the knowledge it has of its surroundings. For example, if there is a long straight ahead of the device, the speed used to travel may be set at a higher value than if it is required to stop and turn after a short distance. The performance of the device would also be improved if it could execute an integrated turn while travelling forward instead of being forced to stop before initiating a turn.

6.3 SUMMARY

Although MARVIN has been primarily designed and developed as a large-scale security device, it has the potential to fulfil a number of alternative job descriptions. There is little difference, for example, between the design specifications for an autonomous security device and those of an autonomous porter or mailman. The operating environments for such devices are comparable (the office block), and many of the required tasks are similar. The ability to negotiate fire doors, manoeuvre in the limited space and navigate the immediate environment are attributes common to many such devices. It is this versatility that will ensure that MARVIN is the basis for a considerable amount of future research and development at the University of Waikato.

The mobile autonomous security device has been designed to meet a number of goals that were set out at the beginning of the project. The size, speed and physical ability of the device are all required to fulfil the specifications as outlined in the introduction. All of the design specifications have been met by the final design configuration of the device, with many of them being exceeded. The enclosed CD includes video footage and an extensive photo gallery of MARVIN in operation. Figure 6-2 shows MARVIN in the intended operating environment.

The security device has been developed to the extent where it can execute simple control algorithms within the confines of an office environment. While these tasks can be performed autonomously, the capabilities of the device's navigation are very limited and more work is required on the control systems implemented by the device. MARVIN has been designed to be a flexible base for future work at the University of Waikato's Physics and Electronic Engineering department.

Figure 6-2: MARVIN in its intended operating environment

APPENDIX A: SCHEMATICS

A.1 87C552 MICROCONTROLLER MOTHERBOARD

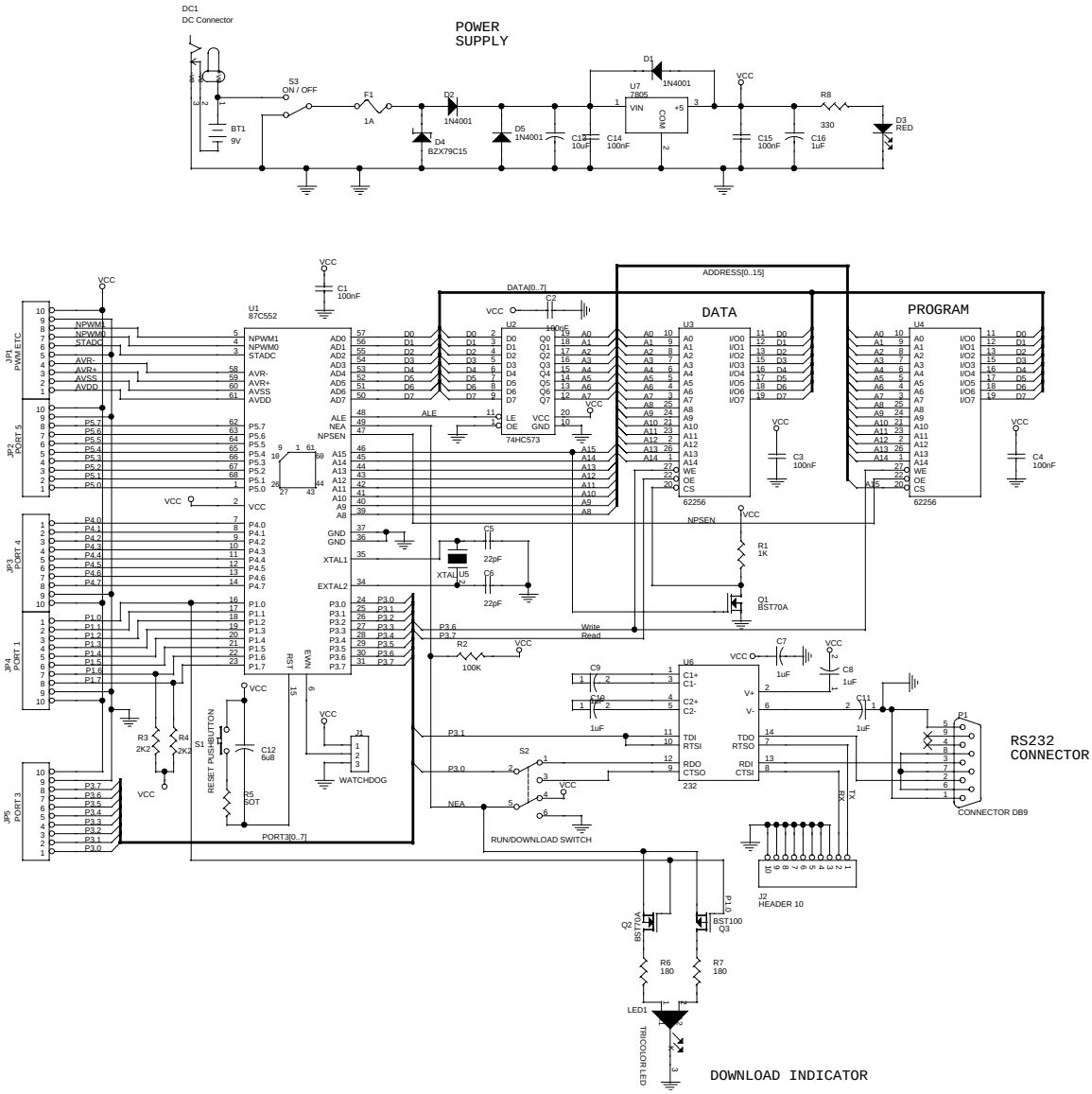

A.2 MOTOR DRIVER SCHEMATIC

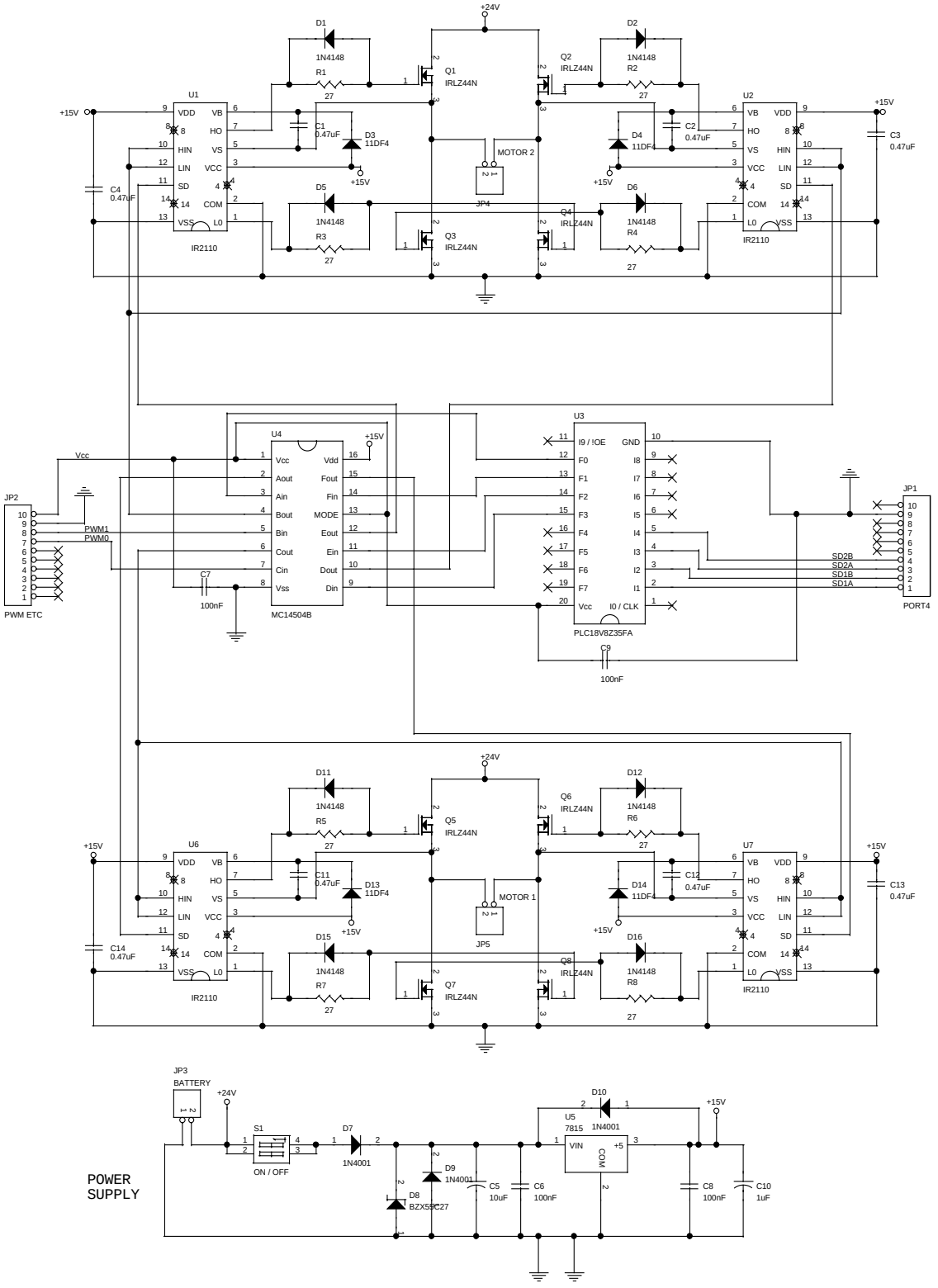

APPENDIX B: MARVINLIB.H

MARVINlib.h

```
#include<intrpt.h>
#include<stdlib.h>
#include<80c552.h>

/*********************************************************This
library file implements the most common functions
*that are be used by the MARVIN
*********************************************************/

/*********************************************************
timers_init2 This function initialises the timer2 interrupt
in the vector table. This initialses the two shaft encoder
capture registers and excutes the interrupt in every 10 ms.
*********************************************************/

void timers_init2()
{
      EA = TRUE;        // Global interrupt enable
      ECM2 = TRUE;
      CMH2 =0x30;       // Control cycle length (10ms)
      CML2 =0x00;
      TM2IR = 0;        // Reset T2 interrupt flags
      TM2CON = 0x21;          // Set rate and start Timer2
      P1b.B5 = FALSE;   // Reset Timer2
      P1b.B5 = TRUE;
      PWMP = 0;           // Set frequency of PWMs

// Timer 0 & 1 (shaft encoders) initialisation

      TMOD = 0x55;            // Set Timer 0 & 1 as counters
      TH0 = 0;    TL0 = 0;    // Clear Timer 0 & 1 registers      TH1
= 0;  TL1 = 0;
      TCON = 0x50;            // Start Timer 0 & Timer 1
}
```

```
/*******************************************************
sensor_reading This is reads the data from the ADC
and returns a unsigned char value.
*******************************************************/

unsigned char sensor_reading(char position)
{
      unsigned char sensor_value;
      ADCON = 10 + position;        // Begin conversion     while
((ADCON & 0x10) != 0x10);//wait for flag
      sensor_value  = ADCH;         // Store value
      ADCON = 0;                    // Reset ADC
      return sensor_value;          // returns decimal value
}

/*******************************************************
shaft_encoder This reads the value out of the capture registers,then
resets it back to zero. This value represents the number of external
interrupt in a giving time (10ms).
*******************************************************/

unsigned short shaft_encoder(char dir)
{
      unsigned char hibyte, lowbyte;
      unsigned short encoder_reading;
      encoder_reading=0;
      if (dir==0)
      {
      TR0 = FALSE;            // Turn off Timer 0
      hibyte = TH0;     lowbyte = TL0;    // Read registers
      TH0 = 0;    TL0 = 0;          // Reset registers
      TR0 = TRUE;       // Restart Timer 0
      encoder_reading= (((unsigned int)hibyte) * 256)
                  + (unsigned int)lowbyte;
      }

      else if (dir==1)
      {
      TR1 = FALSE;                  // Turn off Timer 1
      hibyte = TH1;     lowbyte = TL1;    // Read registers
      TH1 = 0;    TL1 = 0;          // Reset registers
      TR1 = TRUE;             // Restart Timer 1
      encoder_reading= (((unsigned int)hibyte) * 256)
                  + (unsigned int)lowbyte;
      }
      return encoder_reading;       // return the value
}
```

```
/*********************************************************
      delay This wastes the processor's time
*********************************************************/

void delay(unsigned long int time)
{
      unsigned short index;
      for (index=0; index< time;index++);
}

/*********************************************************serial_init
Used for uploading of data to the PC.  configures the serial I/O port
of the '552 to transmit at a baud rate of 9600 using timer1,
transmitting in the format: bit (0) first, followed by 8 data bits
(Lsb first), followed by the stop bit(1);
*********************************************************/

void serial_init()
{
      EA=FALSE;         // disable interrupts
      TM2CON=0;         // stop timer T2
      TCON=0;           // stop timer 0
      PCON=0x80;  // double baud rate
      TMOD=0x20;  // configure timer 1 to count
      TH1= 0;           //initailise register TH1
      TH1 = 248;  TL1=0;      //set baud rate
      TR1=TRUE;   // start timer 1
      S0CON=0x40; // 8 bit UART serial I/O
      REN = TRUE; // enable reception
}

/*********************************************************output_asc
Used in uploading ascii data to the PC. Writes
the byte value to the serial port buffer and waits for confirmation of
transmission.
*********************************************************/

void output_asc(unsigned short byte)
{
      S0BUF=byte;
      while ((S0CON & 0x02) !=0x02);
      {TI = FALSE;}
}
```

```
/*********************************************************
output_dec Used in uploading decimal data to the PC. Writes
the byte value to the serial port buffer and waits for
confirmation of transmission.
*********************************************************/

void output_dec(unsigned long this)
{
      unsigned char a,b,c,d,e,f;
      a=(this/100000)+48;     this%=100000;
      b=(this/10000)+48;      this%=10000;
      c=(this/1000)+48;       this%=1000;
      d=(this/100)+48;        this%=100;
      e=(this/10)+48;
      f=(this%10)+48;

      S0BUF=a;
      while((S0CON&0x02) != 0x02);  {TI =FALSE;}
      S0BUF=b;
      while((S0CON&0x02) != 0x02);  {TI =FALSE;}
      S0BUF=c;
      while((S0CON&0x02) != 0x02);  {TI =FALSE;}
      S0BUF=d;
      while((S0CON&0x02) != 0x02);  {TI =FALSE;}
      S0BUF=e;
      while((S0CON&0x02) != 0x02);  {TI =FALSE;}
      S0BUF=f;
      while((S0CON&0x02) != 0x02);  {TI =FALSE;}
```

APPENDIX C: DATA SHEETS

IR2110 MOSFET GATE DRIVER

International
IOR Rectifier

Data Sheet No. PD-6.011E

IR2110

HIGH AND LOW SIDE DRIVER

Features

- Floating channel designed for bootstrap operation
  Fully operational to +500V
  Tolerant to negative transient voltage
  dV/dt immune
- Gate drive supply range from 10 to 20V
- Undervoltage lockout for both channels
- Separate logic supply range from 5 to 20V
  Logic and power ground ±5V offset
- CMOS Schmitt-triggered inputs with pull-down
- Cycle by cycle edge-triggered shutdown logic
- Matched propagation delay for both channels
- Outputs in phase with inputs

Product Summary

V_{OFFSET}	500V max.
I_O+/-	2A / 2A
V_{OUT}	10 - 20V
$t_{on/off}$ (typ.)	120 & 94 ns
Delay Matching	10 ns

Packages

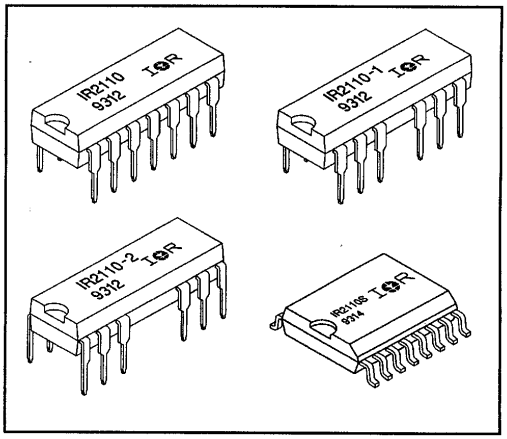

Description

The IR2110 is a high voltage, high speed power MOSFET and IGBT driver with independent high and low side referenced output channels. Proprietary HVIC and latch immune CMOS technologies enable ruggedized monolithic construction. Logic inputs are compatible with standard CMOS or LSTTL outputs. The output drivers feature a high pulse current buffer stage designed for minimum driver cross-conduction. Propagation delays are matched to simplify use in high frequency applications. The floating channel can be used to drive an N-channel power MOSFET or IGBT in the high side configuration which operates up to 500 volts.

Typical Connection

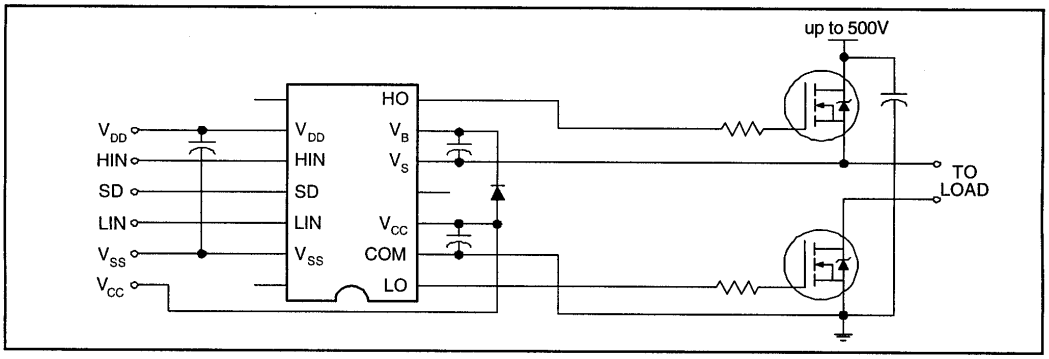

Absolute Maximum Ratings

Absolute Maximum Ratings indicate sustained limits beyond which damage to the device may occur. All voltage parameters are absolute voltages referenced to COM. The Thermal Resistance and Power Dissipation ratings are measured under board mounted and still air conditions. Additional information is shown in Figures 28 through 35.

Parameter		Value		
Symbol	Definition	Min.	Max.	Units
V_B	High Side Floating Supply Voltage	-0.3	525	V
V_S	High Side Floating Supply Offset Voltage	V_B - 25	V_B + 0.3	
V_{HO}	High Side Floating Output Voltage	V_S - 0.3	V_B + 0.3	
V_{CC}	Low Side Fixed Supply Voltage	-0.3	25	
V_{LO}	Low Side Output Voltage	-0.3	V_{CC} + 0.3	
V_{DD}	Logic Supply Voltage	-0.3	V_{SS} + 25	
V_{SS}	Logic Supply Offset Voltage	V_{CC} - 25	V_{CC} + 0.3	
V_{IN}	Logic Input Voltage (HIN, LIN & SD)	V_{SS} - 0.3	V_{DD} + 0.3	
dV_S/dt	Allowable Offset Supply Voltage Transient (Figure 2)	—	50	V/ns
P_D	Package Power Dissipation @ $T_A \leq +25°C$ (14 Lead DIP)	—	1.6	W
	(14 Lead DIP w/o Lead 4)	—	1.5	
	(16 Lead DIP w/o Leads 5 & 6)	—	1.6	
	(16 Lead SOIC)	—	1.25	
$R_{\theta JA}$	Thermal Resistance, Junction to Ambient (14 Lead DIP)	—	75	°C/W
	(14 Lead DIP w/o Lead 4)	—	85	
	(16 Lead DIP w/o Leads 5 & 6)	—	75	
	(16 Lead SOIC)	—	100	
T_J	Junction Temperature	—	150	°C
T_S	Storage Temperature	-55	150	
T_L	Lead Temperature (Soldering, 10 seconds)	—	300	

Recommended Operating Conditions

The Input/Output logic timing diagram is shown in Figure 1. For proper operation the device should be used within the recommended conditions. The V_S and V_{SS} offset ratings are tested with all supplies biased at 15V differential. Typical ratings at other bias conditions are shown in Figures 36 and 37.

Parameter		Value		
Symbol	Definition	Min.	Max.	Units
V_B	High Side Floating Supply Absolute Voltage	V_S + 10	V_S + 20	V
V_S	High Side Floating Supply Offset Voltage	Note 1	500	
V_{HO}	High Side Floating Output Voltage	V_S	V_B	
V_{CC}	Low Side Fixed Supply Voltage	10	20	
V_{LO}	Low Side Output Voltage	0	V_{CC}	
V_{DD}	Logic Supply Voltage	V_{SS} + 5	V_{SS} + 20	
V_{SS}	Logic Supply Offset Voltage	-5	5	
V_{IN}	Logic Input Voltage (HIN, LIN & SD)	V_{SS}	V_{DD}	
T_A	Ambient Temperature	-40	125	°C

Note 1: Logic operational for V_S of -4 to +500V. Logic state held for V_S of -4V to $-V_{BS}$.

Functional Block Diagram

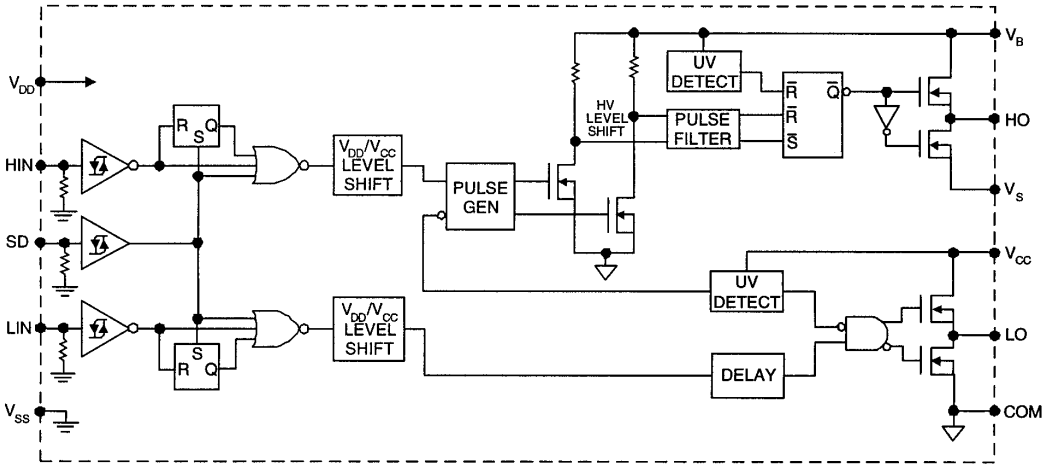

Lead Definitions

Lead Symbol	Description
V_{DD}	Logic supply
HIN	Logic input for high side gate driver output (HO), in phase
SD	Logic input for shutdown
LIN	Logic input for low side gate driver output (LO), in phase
V_{SS}	Logic ground
V_B	High side floating supply
HO	High side gate drive output
V_S	High side floating supply return
V_{CC}	Low side supply
LO	Low side gate drive output
COM	Low side return

Lead Assignments

14 Lead DIP	14 Lead DIP w/o Lead 4	16 Lead DIP w/o Leads 4 & 5	16 Lead SOIC (Wide Body)
IR2110	**IR2110-1**	**IR2110-2**	**IR2110S**
Part Number			

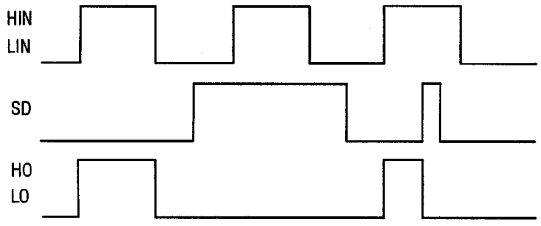

Figure 1. Input/Output Timing Diagram

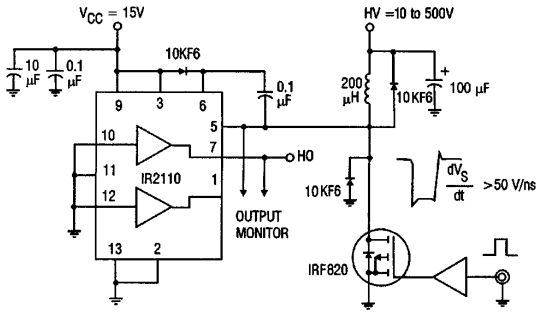

Figure 2. Floating Supply Voltage Transient Test Circuit

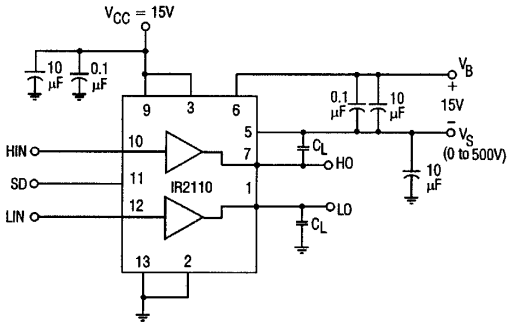

Figure 3. Switching Time Test Circuit

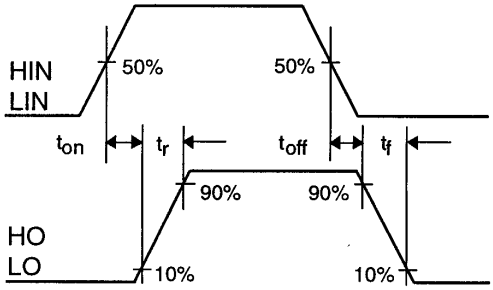

Figure 4. Switching Time Waveform Definition

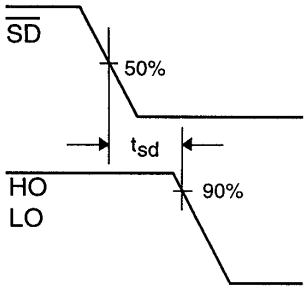

Figure 3. Shutdown Waveform Definitions

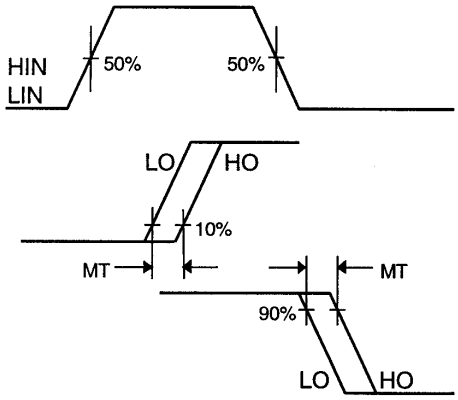

Figure 6. Delay Matching Waveform Definitions

IRLZ44N POWER MOSFET

International
IOR Rectifier

PD - 9.1346B

IRLZ44N

HEXFET® Power MOSFET

- Logic-Level Gate Drive
- Advanced Process Technology
- Dynamic dv/dt Rating
- 175°C Operating Temperature
- Fast Switching
- Fully Avalanche Rated

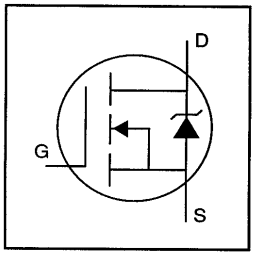

V_{DSS} = 55V

$R_{DS(on)}$ = 0.022Ω

I_D = 47A

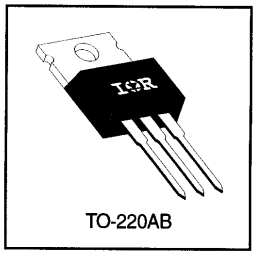

TO-220AB

Description

Fifth Generation HEXFETs from International Rectifier utilize advanced processing techniques to achieve the lowest possible on-resistance per silicon area. This benefit, combined with the fast switching speed and ruggedized device design that HEXFET Power MOSFETs are well known for, provides the designer with an extremely efficient device for use in a wide variety of applications.

The TO-220 package is universally preferred for all commercial-industrial applications at power dissipation levels to approximately 50 watts. The low thermal resistance and low package cost of the TO-220 contribute to its wide acceptance throughout the industry.

Absolute Maximum Ratings

	Parameter	Max.	Units
I_D @ T_C = 25°C	Continuous Drain Current, V_{GS} @ 10V	47	A
I_D @ T_C = 100°C	Continuous Drain Current, V_{GS} @ 10V	33	
I_{DM}	Pulsed Drain Current ①	160	
P_D @T_C = 25°C	Power Dissipation	110	W
	Linear Derating Factor	0.71	W/°C
V_{GS}	Gate-to-Source Voltage	±16	V
E_{AS}	Single Pulse Avalanche Energy ②	210	mJ
I_{AR}	Avalanche Current①	25	A
E_{AR}	Repetitive Avalanche Energy①	11	mJ
dv/dt	Peak Diode Recovery dv/dt ③	5.0	V/ns
T_J T_{STG}	Operating Junction and Storage Temperature Range	-55 to + 175	°C
	Soldering Temperature, for 10 seconds	300 (1.6mm from case)	
	Mounting torque, 6-32 or M3 screw.	10 lbf•in (1.1N•m)	

Thermal Resistance

	Parameter	Min.	Typ.	Max.	Units
$R_{\theta JC}$	Junction-to-Case	—	—	1.4	°C/W
$R_{\theta CS}$	Case-to-Sink, Flat, Greased Surface	—	0.50	—	
$R_{\theta JA}$	Junction-to-Ambient	—	—	62	

8/25/97

IRLZ44N

International
IOR Rectifier

Electrical Characteristics @ T_J = 25°C (unless otherwise specified)

	Parameter	Min.	Typ.	Max.	Units	Conditions
$V_{(BR)DSS}$	Drain-to-Source Breakdown Voltage	55	—	—	V	V_{GS} = 0V, I_D = 250μA
$\Delta V_{(BR)DSS}/\Delta T_J$	Breakdown Voltage Temp. Coefficient	—	0.070	—	V/°C	Reference to 25°C, I_D = 1mA
$R_{DS(on)}$	Static Drain-to-Source On-Resistance	—	—	0.022	Ω	V_{GS} = 10V, I_D = 25A ④
		—	—	0.025		V_{GS} = 5.0V, I_D = 25A ④
		—	—	0.035		V_{GS} = 4.0V, I_D = 21A ④
$V_{GS(th)}$	Gate Threshold Voltage	1.0	—	2.0	V	V_{DS} = V_{GS}, I_D = 250μA
g_{fs}	Forward Transconductance	21	—	—	S	V_{DS} = 25V, I_D = 25A
I_{DSS}	Drain-to-Source Leakage Current	—	—	25	μA	V_{DS} = 55V, V_{GS} = 0V
		—	—	250		V_{DS} = 44V, V_{GS} = 0V, T_J = 150°C
I_{GSS}	Gate-to-Source Forward Leakage	—	—	100	nA	V_{GS} = 16V
	Gate-to-Source Reverse Leakage	—	—	-100		V_{GS} = -16V
Q_g	Total Gate Charge	—	—	48	nC	I_D = 25A
Q_{gs}	Gate-to-Source Charge	—	—	8.6		V_{DS} = 44V
Q_{gd}	Gate-to-Drain ("Miller") Charge	—	—	25		V_{GS} = 5.0V, See Fig. 6 and 13 ④
$t_{d(on)}$	Turn-On Delay Time	—	11	—	ns	V_{DD} = 28V
t_r	Rise Time	—	84	—		I_D = 25A
$t_{d(off)}$	Turn-Off Delay Time	—	26	—		R_G = 3.4Ω, V_{GS} = 5.0V
t_f	Fall Time		15			R_D = 1.1Ω, See Fig. 10 ④
L_D	Internal Drain Inductance	—	4.5	—	nH	Between lead, 6mm (0.25in.) from package and center of die contact
L_S	Internal Source Inductance	—	7.5	—		
C_{iss}	Input Capacitance	—	1700	—	pF	V_{GS} = 0V
C_{oss}	Output Capacitance	—	400	—		V_{DS} = 25V
C_{rss}	Reverse Transfer Capacitance	—	150	—		f = 1.0MHz, See Fig. 5

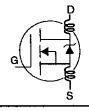

Source-Drain Ratings and Characteristics

	Parameter	Min.	Typ.	Max.	Units	Conditions
I_S	Continuous Source Current (Body Diode)	—	—	47	A	MOSFET symbol showing the integral reverse p-n junction diode.
I_{SM}	Pulsed Source Current (Body Diode) ①	—	—	160		
V_{SD}	Diode Forward Voltage	—	—	1.3	V	T_J = 25°C, I_S = 25A, V_{GS} = 0V ④
t_{rr}	Reverse Recovery Time	—	80	120	ns	T_J = 25°C, I_F = 25A
Q_{rr}	Reverse RecoveryCharge	—	210	320	nC	di/dt = 100A/μs ④
t_{on}	Forward Turn-On Time	Intrinsic turn-on time is negligible (turn-on is dominated by L_S+L_D)				

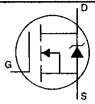

Notes:

① Repetitive rating; pulse width limited by max. junction temperature. (See fig. 11)

② V_{DD} = 25V, starting T_J = 25°C, L = 470μH R_G = 25Ω, I_{AS} = 25A. (See Figure 12)

③ I_{SD} ≤ 25A, di/dt ≤ 270A/μs, V_{DD} ≤ $V_{(BR)DSS}$, T_J ≤ 175°C

④ Pulse width ≤ 300μs; duty cycle ≤ 2%.

GP2D12 IRED SENSORS

SHARP

GP2D12/GP2D15 Distance Measuring Sensors

General Purpose Type Distance Measuring Sensors

■ General Description

SHARP's **GP2D12/GP2D15** are general purpose type distance measuring sensors which consist of PSD* and infrared emitting diode and signal processing circuit.
It enables to detect objects without any influence on the color of reflective objects, reflectivity, the lights of surroundings.

*PSD:Position Sensitive Detector

■ Features

(1) Less influence on the color of reflective objects, reflectivity
(2) Line-up of distance output/distance judgement type
Distance output type(analog voltage) : **GP2D12**
Detecting distance : 10 to 80cm
Distance judgement type : **GP2D15**
Judgement distance : 24cm (Adjustable within the range of 10 to 80cm)
(3) External control circuit is unnecessary.
(4) Low cost

■ Applications

(1) TVs
(2) Personal computers
(3) Cars
(4) Copiers

■ Outline Dimensions (Unit : mm)

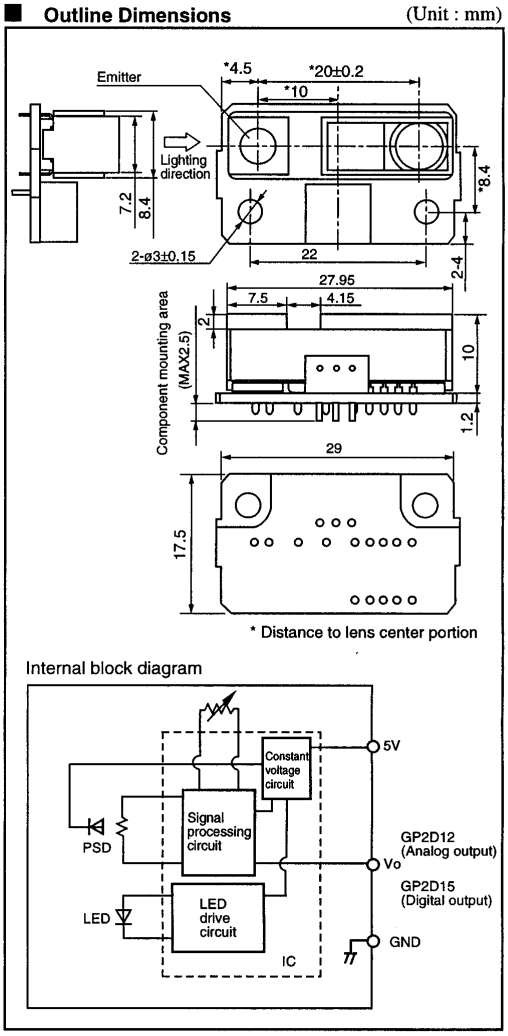

Internal block diagram

SHARP

GP2D12/GP2D15 Distance Measuring Sensors

■ Specifications

GP2D12 (Ta=25°C)

Parameter	Symbol	Rating
Supply voltage	Vcc	4.5 to 5.5V
Dissipation current	Icc	MAX.35mA
Measuring range	L	10 to 80cm
Output type	—	Analog output
Operating temperature	Topr	-10 to +60°C

GP2D15 (Ta=25°C)

Parameter	Symbol	Rating
Supply voltage	Vcc	4.5 to 5.5V
Dissipation current	Icc	MAX.35mA
*Judgement distance	L	TYP.24cm
Output type	—	Digital output
Operating temperature	Topr	-10 to +60°C

* Adjustable within the range of 10 to 80cm.<Custom products>

■ Output pattern

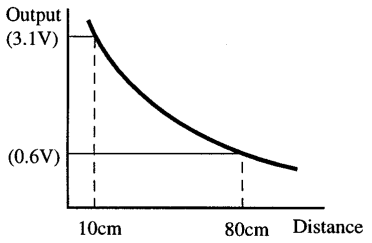

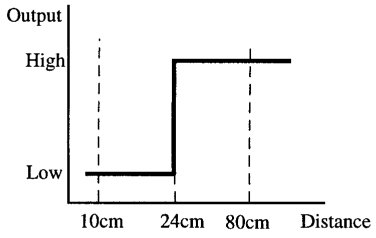

MC14504B LEVEL SHIFTER

MOTOROLA
SEMICONDUCTOR TECHNICAL DATA

MC14504B

Hex Level Shifter for TTL to CMOS or CMOS to CMOS

The MC14504B is a hex non–inverting level shifter using CMOS technology. The level shifter will shift a TTL signal to CMOS logic levels for any CMOS supply voltage between 5 and 15 volts. A control input also allows interface from CMOS to CMOS at one logic level to another logic level: Either up or down level translating is accomplished by selection of power supply levels V_{DD} and V_{CC}. The V_{CC} level sets the input signal levels while V_{DD} selects the output voltage levels.

- UP Translates from a Low to a High Voltage or DOWN Translates from a High to a Low Voltage
- Input Threshold Can Be Shifted for TTL Compatibility
- No Sequencing Required on Power Supplies or Inputs for Power Up or Power Down
- 3 to 18 Vdc Operation for V_{DD} and V_{CC}
- Diode Protected Inputs to V_{SS}
- Capable of Driving Two Low–Power TTL Loads or One Low–Power Schottky TTL Load Over the Rated Temperature Range

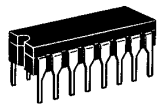

L SUFFIX
CERAMIC
CASE 620

P SUFFIX
PLASTIC
CASE 648

D SUFFIX
SOIC
CASE 751B

ORDERING INFORMATION

MC14XXXBCP	Plastic
MC14XXXBCL	Ceramic
MC14XXXBD	SOIC

T_A = – 55° to 125°C for all packages.

LOGIC DIAGRAM

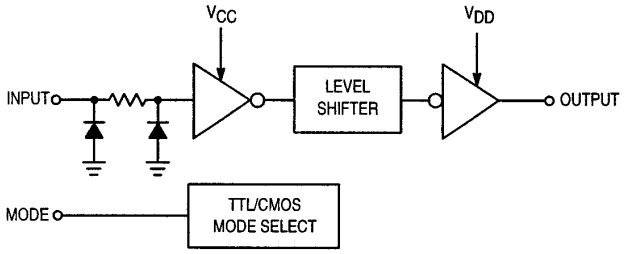

Mode Select	Input Logic Levels	Output Logic Levels
1 (V_{CC})	TTL	CMOS
0 (V_{SS})	CMOS	CMOS

1/6 of package shown.

PIN ASSIGNMENT

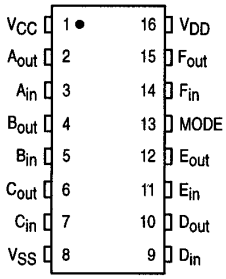

This device contains circuitry to protect the inputs against damage due to high static voltages or electric fields referenced to the V_{SS} pin, only. Extra precautions must be taken to avoid applications of any voltage higher than maximum rated voltages to this high–impedance circuit. For proper operation, the ranges $V_{SS} \le V_{in} \le 18$ V and $V_{SS} \le V_{out} \le V_{DD}$ are recommended.

Unused inputs must always be tied to an appropriate logic voltage level (e.g., either V_{SS} or V_{DD}). Unused outputs must be left open.

REV 3
1/94

MAXIMUM RATINGS* (Voltages Referenced to V_{SS})

Symbol	Parameter	Value	Unit
V_{CC}	DC Supply Voltage	– 0.5 to 18.0	V
V_{DD}	DC Supply Voltage	– 0.5 to + 18.0	V
V_{in}	Input Voltage (DC or Transient)	– 0.5 to + 18.0	V
V_{out}	Output Voltage (DC or Transient)	– 0.5 to V_{DD} + 0.5	V
I_{in}, I_{out}	Input or output Current (DC or Transient), per Pin	± 10	mA
P_D	Power Dissipation, per Package*	500	mW
T_{stg}	Storage Temperature	– 65 to + 150	°C
T_L	Lead Temperature (8–Second Soldering)	260	°C

* Maximum Ratings are those values beyond which damage to the device may occur.
†Temperature Derating:
Plastic "P and D/DW" Packages: – 7.0 mW/°C From 65°C To 125°C
Ceramic "L" Packages: – 12 mW/°C From 100°C To 125°C

ELECTRICAL CHARACTERISTICS (Voltages Referenced to V_{SS})

Characteristic	Symbol	V_{CC} Vdc	V_{DD} Vdc	– 55°C Min	– 55°C Max	25°C Min	25°C Typ #	25°C Max	125°C Min	125°C Max	Unit
Output Voltage "0" Level	V_{OL}	—	5.0	—	0.05	—	0	0.05	—	0.05	Vdc
V_{in} = 0 V		—	10	—	0.05	—	0	0.05	—	0.05	
		—	15	—	0.05	—	0	0.05	—	0.05	
"1" Level	V_{OH}	—	5.0	4.95	—	4.95	5.0	—	4.95	—	Vdc
V_{in} = V_{CC}		—	10	9.95	—	9.95	10	—	9.95	—	
		—	15	14.95	—	14.95	15	—	14.95	—	
Input Voltage "0" Level	V_{IL}										Vdc
(V_{OL} = 1.0 Vdc) TTL–CMOS		5.0	10	—	0.8	—	1.3	0.8	—	0.8	
(V_{OL} = 1.5 Vdc) TTL–CMOS		5.0	15	—	0.8	—	1.3	0.8	—	0.8	
(V_{OL} = 1.0 Vdc) CMOS–CMOS		5.0	10	—	1.5	—	2.25	1.5	—	1.4	
(V_{OL} = 1.5 Vdc) CMOS–CMOS		5.0	15	—	1.5	—	2.25	1.5	—	1.5	
(V_{OL} = 1.5 Vdc) CMOS–CMOS		10	15	—	3.0	—	4.5	3.0	—	2.9	
Input Voltage "1" Level	V_{IH}										Vdc
(V_{OH} = 9.0 Vdc) TTL–CMOS		5.0	10	2.0	—	2.0	1.5	—	2.0	—	
(V_{OH} = 13.5 Vdc) TTL–CMOS		5.0	15	2.0	—	2.0	1.5	—	2.0	—	
(V_{OH} = 9.0 Vdc) CMOS–CMOS		5.0	10	3.6	—	3.5	2.75	—	3.5	—	
(V_{OH} = 13.5 Vdc) CMOS–CMOS		5.0	15	3.6	—	3.5	2.75	—	3.5	—	
(V_{OH} = 13.5 Vdc) CMOS–CMOS		10	15	7.1	—	7.0	5.5	—	7.0	—	
Output Drive Current	I_{OH}										mAdc
(V_{OH} = 2.5 Vdc) Source		—	5.0	– 3.0	—	– 2.4	– 4.2	—	– 1.7	—	
(V_{OH} = 4.6 Vdc)		—	5.0	–0.64	—	–0.51	– 0.88	—	–0.36	—	
(V_{OH} = 9.5 Vdc)		—	10	– 1.6	—	– 1.3	– 2.25	—	– 0.9	—	
(V_{OH} = 13.5 Vdc)		—	15	– 4.2	—	– 3.4	– 8.8	—	– 2.4	—	
(V_{OL} = 0.4 Vdc) Sink	I_{OL}	—	5.0	0.64	—	0.51	0.88	—	0.36	—	mAdc
(V_{OL} = 0.5 Vdc)		—	10	1.6	—	1.3	2.25	—	0.9	—	
(V_{OL} = 1.5 Vdc)		—	15	4.2	—	3.4	8.8	—	2.4	—	
Input Current	I_{in}	—	15	—	± 0.1	—	±0.00001	± 0.1	—	± 1.0	µAdc
Input Capacitance (V_{in} = 0)	C_{in}	—	—	—	—	—	5.0	7.5	—	—	pF
Quiescent Current	I_{DD} or	—	5.0	—	0.05	—	0.0005	0.05	—	1.5	µAdc
(Per Package)	I_{CC}	—	10	—	0.10	—	0.0010	0.10	—	3.0	
CMOS–CMOS Mode		—	15	—	0.20	—	0.0015	0.20	—	6.0	
Quiescent Current	I_{DD}	5.0	5.0	—	0.5	—	0.0005	0.5	—	3.8	µAdc
(Per Package)		5.0	10	—	1.0	—	0.0010	1.0	—	7.5	
TTL–CMOS Mode		5.0	15	—	2.0	—	0.0015	2.0	—	15	
Quiescent Current	I_{CC}	5.0	5.0	—	5.0	—	2.5	5.0	—	6.0	mAdc
(Per Package)		5.0	10	—	5.0	—	2.5	5.0	—	6.0	
TTL–CMOS Mode		5.0	15	—	5.0	—	2.5	5.0	—	6.0	

#Data labelled "Typ" is not to be used for design purposes but is intended as an indication of the IC's potential performance.

TIBPAL16L8-7C PROGRAMMABLE LOGIC DEVICE

TIBPAL16L8-7C, TIBPAL16R4-7C, TIBPAL16R6-7C, TIBPAL16R8-7C
TIBPAL16L8-10M, TIBPAL16R4-10M, TIBPAL16R6-10M, TIBPAL16R8-10M
HIGH-PERFORMANCE *IMPACT-X*™ *PAL*® CIRCUITS

SRPS006D – D3115, MAY 1988 – REVISED MARCH 1992

- **High-Performance Operation:**
  f_{max} (no feedback)
  TIBPAL16R'-7C Series . . . 100 MHz Min
  TIBPAL16R'-10M Series . . . 62.5 MHz Min
  f_{max} (internal feedback)
  TIBPAL16R'-7C Series . . . 100 MHz Min
  TIBPAL16R'-10M Series . . . 62.5 MHz Min
  f_{max} (external feedback)
  TIBPAL16R'-7C Series . . . 74 MHz Min
  TIBPAL16R'-10M Series . . . 52.5 MHz Min
  Propagation Delay
  TIBPAL16L'-7C Series . . . 7 ns Max
  TIBPAL16L'-10M Series . . . 10 ns Max
- **Functionally Equivalent, but Faster than, Existing 20-Pin PLDs**
- **Preload Capability on Output Registers Simplifies Testing**
- **Power-Up Clear on Registered Devices (All Register Outputs are Set Low, but Voltage Levels at the Output Pins Go High)**
- **Package Options Include Both Plastic and Ceramic Chip Carriers in Addition to Plastic and Ceramic DIPs**
- **Security Fuse Prevents Duplication**
- **Dependable Texas Instruments Quality and Reliability**

DEVICE	I INPUTS	3-STATE O OUTPUTS	REGISTERED Q OUTPUTS	I/O PORTS
PAL16L8	10	2	0	6
PAL16R4	8	0	4 (3-state buffers)	4
PAL16R6	8	0	6 (3-state buffers)	2
PAL16R8	8	0	8 (3-state buffers)	0

TIBPAL16L8'
C SUFFIX . . . J OR N PACKAGE
M SUFFIX . . . J PACKAGE
(TOP VIEW)

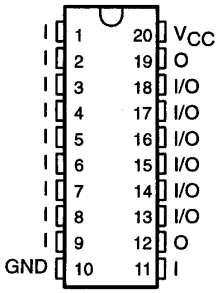

TIBPAL16L8'
C SUFFIX . . . FN PACKAGE
M SUFFIX . . . FK PACKAGE
(TOP VIEW)

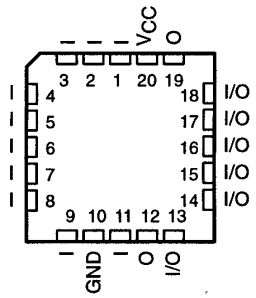

Pin assignments in operating mode

description

These programmable array logic devices feature high speed and functional equivalency when compared with currently available devices. These IMPACT-X™ circuits combine the latest Advanced Low-Power Schottky technology with proven titanium-tungsten fuses to provide reliable, high-performance substitutes for conventional TTL logic. Their easy programmability allows for quick design of custom functions and typically results in a more compact circuit board. In addition, chip carriers are available for futher reduction in board space.

All of the register outputs are set to a low level during power-up. Extra circuitry has been provided to allow loading of each register asynchronously to either a high or low state. This feature simplifies testing because the registers can be set to an initial state prior to executing the test sequence.

The TIBPAL16' C series is characterized from 0°C to 75°C. The TIBPAL16' M series is characterized for operation over the full military temperature range of –55°C to 125°C.

TEXAS INSTRUMENTS
POST OFFICE BOX 655303 • DALLAS, TEXAS 75265

absolute maximum ratings over operating free-air temperature range (unless otherwise noted)

Supply voltage, V_{CC} (see Note 1) ..... 7 V
Input voltage (see Note 1) ..... 5.5 V
Voltage applied to disabled output (see Note 1) ..... 5.5 V
Operating free-air temperature range ..... 0°C to 75°C
Storage temperature range ..... −65°C to 150°C

NOTE 1: These ratings apply except for programming pins during a programming cycle.

recommended operating conditions

			MIN	NOM	MAX	UNIT
V_{CC}	Supply voltage		4.75	5	5.25	V
V_{IH}	High-level input voltage (see Note 2)		2		5.5	V
V_{IL}	Low-level input voltage (see Note 2)				0.8	V
I_{OH}	High-level output current				−3.2	mA
I_{OL}	Low-level output current				24	mA
f_{clock}	Clock frequency		0		100	MHz
t_w	Pulse duration, clock (see Note 2)	High	5			ns
		Low	5			
t_{su}	Setup time, input or feedback before clock↑		7			ns
t_h	Hold time, input or feedback after clock↑		0			ns
T_A	Operating free-air temperature		0	25	75	°C

NOTE 2: These are absolute voltage levels with respect to the ground pin of the device and include all overshoots due to system and/or tester noise. Testing these parameters should not be attempted without suitable equipment.

electrical characteristics over recommended operating free-air temperature range

PARAMETER	TEST CONDITIONS			MIN	TYP†	MAX	UNIT
V_{IK}	V_{CC} = 4.75 V,	I_I = −18 mA			−0.8	−1.5	V
V_{OH}	V_{CC} = 4.75 V,	I_{OH} = −3.2 mA		2.4	3.2		V
V_{OL}	V_{CC} = 4.75 V,	I_{OL} = 24 mA			0.3	0.5	V
I_{OZH}‡	V_{CC} = 5.25 V,	V_O = 2.7 V				100	µA
I_{OZL}‡	V_{CC} = 5.25 V,	V_O = 0.4 V				−100	µA
I_I	V_{CC} = 5.25 V,	V_I = 5.5 V				100	µA
I_{IH}‡	V_{CC} = 5.25 V,	V_I = 2.7 V				25	µA
I_{IL}‡	V_{CC} = 5.25 V,	V_I = 0.4 V			−80	−250	µA
I_{OS}§	V_{CC} = 5.25 V,	V_O = 0.5 V		−30	−70	−130	mA
I_{CC}	V_{CC} = 5.25 V,	V_I = 0,	Outputs open		160	180	mA
C_i	f = 1 MHz,	V_I = 2 V			5		pF
C_o	f = 1 MHz,	V_O = 2 V			6		pF
C_{clk}	f = 1 MHz,	V_{CLK} = 2 V			6		pF

† All typical values are at V_{CC} = 5 V, T_A = 25°C.
‡ I/O leakage is the worst case of I_{OZL} and I_{IL} or I_{OZH} and I_{IH} respectively.
§ Not more than one output should be shorted at a time, and the duration of the short circuit should not exceed one second. V_O is set at 0.5 V to avoid test problems caused by test equipment ground degradation.

GLOSSARY

‘552	Phillips 87C552 microprocessor
ADC	Analogue to Digital Converter
AGV	Automated Guided Vehicle
Bit	Binary Digit – either 0 or 1
Byte	8 bits
CCA	Cold Cranking Amps – a measure of a battery’s capacity [A]
CCD	Charge-Coupled Device
DAC	Digital to Analogue Converter
DC	Direct Current
DPDT	Double Pole / Double Throw switch
Emf	Electro-magnetic field
EPROM	Electronically Programmable Read Only Memory
FLA	Flooded Lead Acid battery
GPS	Global Positioning System – an advanced active beacon system
I^2C	Phillips serial communication protocol
I/O	Input/Output
IC	Integrated Circuit
LSB	Least Significant Bit
MARVIN	Mobile Autonomous Robot for Indoor Navigation
MDARS	Mobile Detection Assessment and Response System
MOSFET	Metal Oxide Semiconductor Field Effect Transistor
MSB	Most Significant Bit of a binary value
NiCd	Nickel Cadmium – material used to manufacture rechargeable batteries
PSD	Position Sensitive Device
PWM	Pulse width modulation – a square wave of constant duty cycle is used as an approximation to a DC voltage
RAM	Random Access Memory

RC	Reserve Capacity - a measure of a battery's capacity [min]
R/F	Radio Frequency - a form of wireless communication
ROBART I	The world's first autonomous security robot
SLA	Sealed Lead Acid battery
TOF	Time Of Flight
TTL	Transistor to Transistor Logic
UART	Universal Asynchronous Receiver/Transmitter
UMBmark	University of Michigan Benchmark experiments

BIBLIOGRAPHY

1. Shepherd, W, Hulley, L.N, Liang, D.T.W, 1995 ***"Power Electronics and Motor Control"***, 2nd Edition, Cambridge University Press.

2. Fowler, K. R, 1996 ***"Electronic Instrument Design - Architecting for the Life Cycle"***, Oxford University Press.

3. Shetty, D, Kolk, R. A, 1997 ***"Mechatronics System Design"***, PWS Publishing Company.

4. Borenstein, J, Everett, H. R, Feng, L, 1996 ***"Navigating Mobile Robots - Systems and Techniques"***, A K Peters.

5. Franklin, G. F, Powell, J. D, Emami-Naeini, A, 1994 ***"Feedback Control of Dynamic Systems"***, 3rd Edition, Addison-Wesley Publishing Company.

6. Phillips Semiconductors, 1996 ***"80C51-Based 8-Bit Microcontrollers"***, Phillips Electronics North America Corporation.

7. Hurd, S. A, 2001 ***"Laser Range Finding for an Autonomous Mobile Security Device"***, MSc Thesis, Department of Physics and Electronic Engineering, University of Waikato.

8. Su, S. H, 2001 ***"Progression from Micromouse to Versatile Mechatron"***, MSc Thesis, Department of Physics and Electronic Engineering, University of Waikato.

9. Borenstein, J. and Feng, L, 1996, ***"Measurement and Correction of Systematic Odometry Errors in Mobile Robots"***, IEEE Transactions on Robotics and Automation, Vol. 12, No. 6.

10. Brightwell, G, 1999 ***"Analysis of Adaptive Reactive Control Systems for Autonomous Mobile Robots"***, DPhil Thesis, Department of Physics and Electronic Engineering, University of Waikato.

11. Brightwell, G, 1993, ***"Design and Construction of a Micromouse"***, MSc Thesis, Department of Physics and Electronic Engineering, University of Waikato.

12. Taberner, A. J, 1994, ***"Design and Construction of a Microcat"***, MSc Thesis, Department of Physics and Electronic Engineering, University of Waikato.

13. Everett, H. R, 1995 ***"Sensors for Mobile Robots: Theory and Application"***, A. K Peters, Ltd.

14. *Exide Batteries,* http://www.exide.co.nz

15. *Farnell Online*, http://www.farnell.com

16. *SPAWAR Systems Centre, San Diego,* http://www.spawar.navy.mil

17. *Chip Centre International,* http://www.chipcenter.com/

18. *IC Masters Online,* http://xilinx.icmaster.com

19. International Rectifier, http://www.irf.com

20. Power Designers, Electrical Engineering and Design Solutions, http://www.powerdesigners.com/